e-ISSN 1308-8459

Official Publication of the Turkish Society of Anatomy and Clinical Anatomy

http://dergipark.org.tr/en/pub/anatomy

anatomy

An International Journal of Experimental and Clinical Anatomy

Volume 19 / Issue 1 / April 2025

Published three times a year

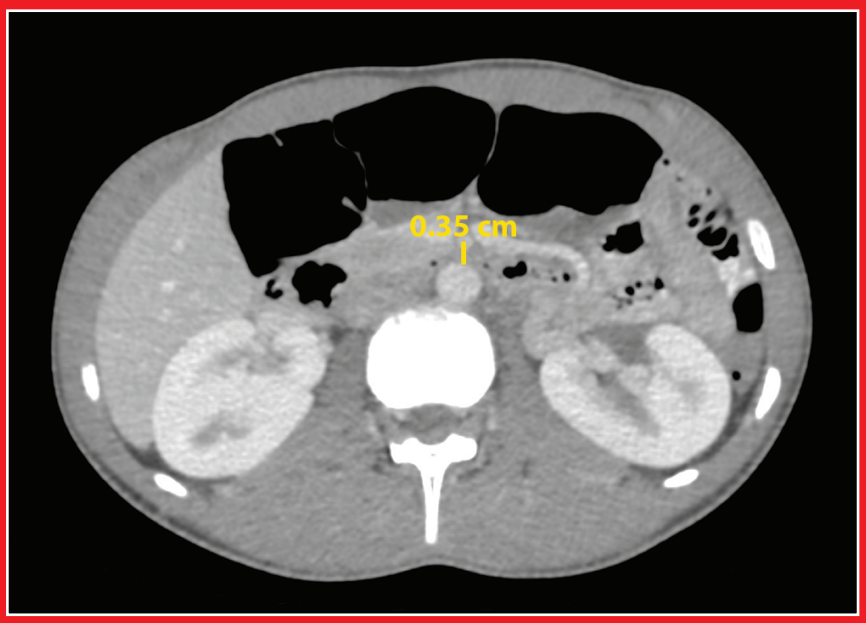

deomed®

https://dergipark.org.tr/tr/pub/anatomy

anatomy

An International Journal of Experimental and Clinical Anatomy

Official Publication of the Turkish Society of Anatomy and Clinical Anatomy

Aim and Scope

Anatomy, an international journal of experimental and clinical anatomy, is a peer-reviewed journal published three times a year with an objective to publish manuscripts with high scientific quality from all areas of anatomy. The journal offers a forum for anatomical investigations involving gross, histologic, developmental, neurological, radiological and clinical anatomy, and anatomy teaching methods and techniques. The journal is open to original papers covering a link between gross anatomy and areas related with clinical anatomy such as experimental and functional anatomy, neuroanatomy, comparative anatomy, modern imaging techniques, molecular biology, cell biology, embryology, morphological studies of veterinary discipline, and teaching anatomy. The journal is currently indexing and abstracting in TUBITAK ULAKBIM Turkish Medical Index, Proquest, EBSCO Host, Index Copernicus and Google Scholar.

Publication Ethics

Anatomy is committed to upholding the highest standards of publication ethics and observes the principles of Journal's Publication Ethics and Malpractice Statement which is based on the recommendations and guidelines for journal editors developed by the Committee on Publication Ethics (COPE), Council of Science Editors (CSE), World Association of Medical Editors (WAME) and International Committee of Medical Journal Editors (ICMJE). Fore detailed information please visit the online version of the journal which is available at https://dergipark.org.tr/tr/pub/anatomy

Authorship

All persons designated as authors should have participated sufficiently in the work to take public responsibility for the content of the manuscript. Authorship credit should be based on substantial contributions to (1) conception and design or analysis and interpretation of data, (2) drafting of the manuscript or revising it for important intellectual content and, (3) final approval of the version to be published. The Editor may require the authors to justify assignment of authorship. In the case of collective authorship, the key persons responsible for the article should be identified and others contributing to the work should be recognized with proper acknowledgment.

Copyright

Publisher

Deomed Publishing
Gür Sok. No:7/B Kadıköy, İstanbul, Türkiye
Phone: +90 216 414 83 43 (Pbx) / Fax: +90 216 414 83 42
www.deomed.com / e-mail: medya@deomed.com

deomed®

Publication Information

Anatomy (e-ISSN 1308-8459) as an open access electronic journal is published by Deomed Publishing, Istanbul, for the Turkish Society of Anatomy and Clinical Anatomy, TSACA. Due the Press Law of Turkish Republic dated as June 26, 2004 and numbered as 5187, this publication is classified as a periodical in English language.

Ownership
On behalf of the Turkish Society of Anatomy and Clinical Anatomy,
Ahmet Kağan Karabulut, MD, PhD; Konya, Türkiye

Editor-in-Chief
Nihal Apaydın, MD
Department of Anatomy,
Faculty of Medicine, Ankara University,
06100, Sıhhıye, Ankara, Türkiye
Phone: 0090 312 595 82 48
e-mail: napaydin@gmail.com; napaydin@medicine.ankara.edu.tr

Administrative Office
Güven Mah. Güvenlik Cad. Onlar Ap. 129/2 Aşağı Ayrancı, Ankara, Türkiye
Phone: +90 312 447 55 52-53

Submission of Manuscripts

Manuscripts should be submitted at our manuscript submission and information portal https://dergipark.org.tr/en/pub/anatomy

Categories of Articles

- ***Original Articles*** describe substantial original research that falls within the scope of the Journal.
- ***Teaching Anatomy*** section contains regular or all formats of papers which are relevant to comparing teaching models or to introducing novel techniques, including especially the own experiences of the authors.
- ***Systematic Reviews and Meta-Analyses:*** Authors are kindly requested to adhere to established reporting standards. Please follow the PRISMA (Preferred Reporting Items for Systematic Reviews and Meta-Analyses) guidelines as well as the general Systematic Reviews and Meta-Analyses Guidelines to ensure clarity, transparency, and methodological rigor in your submissions.
- ***Reviews*** section highlights current development in relevant areas of anatomy. The reviews are generally invited; other prospective authors should consult with the Editor-in-Chief.
- ***Case Reports*** include new, noteworthy or unusual cases which could be of help for basic notions and clinical practice.
- ***Technical Note*** articles cover technical innovations and developments with a specific technique or procedure or a modification of an existing technique. They should be sectioned like an original research article but not exceed 2000 words.
- ***Viewpoint*** articles give opinions on controversial topics or future projections, some of these are invited.
- ***Historical View*** category presents overview articles about historical sections from all areas of anatomy.
- ***Terminology Zone*** category is a platform for the articles which discuss some terminological controversies or opinions.

The categories above are peer-reviewed. They should include abstract and keywords. There are also categories including Letters to the Editor, Book Reviews, Abstracts, Obituary, News and Announcements which do not require a peer review process.

For detailed instructions concerning the submission of manuscripts, please refer to the Instructions to Authors.

Editorial Board

http://dergipark.org.tr/en/pub/anatomy

anatomy
An International Journal of Experimental and Clinical Anatomy

anatomy
http://dergipark.org.tr/en/pub/anatomy
An International Journal of Experimental and Clinical Anatomy

Instructions to Authors

http://dergipark.org.tr/en/pub/anatomy

Anatomy, an international journal of experimental and clinical anatomy, is the official publication of the Turkish Society of Anatomy and Clinical Anatomy, TSACA. It is a peer-reviewed e-journal that publishes scientific articles in English. For a manuscript to be published in the journal, it should not be published previously in another journal or as full text in congress books and should be found relevant by the editorial board. Also, manuscripts submitted to Anatomy must not be under consideration by any other journal. Relevant manuscripts undergo conventional peer review procedure (at least three reviewers). For the publication of accepted manuscripts, author(s) should reveal to the Editor-in-Chief any conflict of interest and transfer the copyright to the Turkish Society of Anatomy and Clinical Anatomy, TSACA.

In the Materials and Methods section of the manuscripts where experimental studies on humans are presented, a statement that informed consent was obtained from each volunteer or patient after explanation of the procedures should be included. This section also should contain a statement that the investigation conforms with the principles outlined in the appropriate version of 1964 Declaration of Helsinki. For studies involving animals, all work must have been conducted according to applicable national and international guidelines. Prior approval must have been obtained for all protocols from the relevant author's institutional or other appropriate ethics committee, and the institution name and permit numbers must be provided at submission.

Anatomical terms used should comply with Terminologia Anatomica by FCAT (1998).

No publication cost is charged for the manuscripts but reprints and color printings are at authors' cost.

Preparation of manuscripts

During the preparation of the manuscripts, uniform requirements of the International Committee of Medical Journal Editors, a part of which is stated below, are valid (*see* ICMJE. Uniform requirements for manuscripts submitted to biomedical journals. Updated content is available at www.icmje.org). The manuscript should be typed double-spaced on one side of a 21×29.7 cm (A4) blank sheet of paper. At the top, bottom and right and left sides of the pages a space of 2.5 cm should be left and all the pages should be numbered except for the title page.

Manuscripts should not exceed 15 pages (except for the title page). They must be accompanied by a cover letter signed by corresponding author and the Conflicts of Interest Disclosure Statement and Copyright Transfer Form signed by all authors. The contents of the manuscript (original articles and articles for Teaching Anatomy category) should include: 1- Title Page, 2- Abstract and Keywords, 3- Introduction, 4- Materials and Methods, 5- Results, 6- Discussion (Conclusion and/or Acknowledgement if necessary), 7- References

Title page

In all manuscripts the title of the manuscript should be written at the top and the full names and surnames and titles of the authors beneath. These should be followed with the affiliation of the author. Manuscripts with long titles are better accompanied underneath by a short version (maximum 80 characters) to be published as running head. In the title page the correspondence address and telephone, fax and e-mail should be written. At the bottom of this page, if present, funding sources supporting the work should be written with full names of all funding organizations and grant numbers. It should also be indicated in a separate line if the study has already been presented in a congress or likewise scientific meeting. Other information such as name and affiliation are not to be indicated in pages other than the title page.

Abstract

Abstract should be written after the title in 100–250 words. In original articles and articles prepared in IMRAD format for Teaching Anatomy category the abstract should be structured under sections Objectives, Methods, Results and Conclusion. Following the abstract at least 3 keywords should be added in alphabetical order separated by semicolumns.

References

Authors should provide direct references to original research sources. References should be numbered consecutively in square brackets, according to the order in which they are first mentioned in the manuscript. They should follow the standards detailed in the NLM's Citing Medicine, 2nd edition (Citing medicine: the NLM style guide for authors, editors, and publishers [Internet]. 2nd edition. Updated content is available at www.ncbi.nlm .nih.gov/books/NBK7256). The names of all contributing authors should be listed, and should be in the order they appear in the original reference. The author is responsible for the accuracy and completeness of references. When necessary, a copy of a referred article can be requested from the author. Journal names should be abbreviated as in *Index Medicus*. Examples of main reference types are shown below:

- **Journal articles:** Author's name(s), article title, journal title (abbreviated), year of publication, volume number, inclusive pages
  - *Standard journal article:* Sargon MF, Celik HH, Aksit MD, Karaagaoglu E. Quantitative analysis of myelinated axons of corpus callosum in the human brain. Int J Neurosci 2007;117:749–55.
  - *Journal article with indication article published electronically before print:* Sengul G, Fu Y, Yu Y, Paxinos G. Spinal cord projections to the cerebellum in the mouse. Brain Struct Funct Epub 2014 Jul 10. DOI 10.1007/s00429-014-0840-7.
- **Books:** Author's name(s), book title, place of publication, publisher, year of publication, total pages (entire book) or inclusive pages (contribution to a book or chapter in a book)
  - *Entire book:*
    - *Standard entire book:* Sengul G, Watson C, Tanaka I, Paxinos G. Atlas of the spinal cord of the rat, mouse, marmoset, rhesus and human. San Diego (CA): Academic Press Elsevier; 2013. 360 p.
    - *Book with organization as author:* Federative Committee of Anatomical Terminology (FCAT). Terminologia anatomica. Stuttgart: Thieme; 1998. 292 p.
    - *Citation to a book on the Internet:* Bergman RA, Afifi AK, Miyauchi R. Illustrated encyclopedia of human anatomic variation. Opus I: muscular system [Internet]. [Revised on March 24, 2015] Available from: http://www.anatomyatlases.org/AnatomicVariants/AnatomyHP.shtml
  - *Contribution to a book:*
    - *Standard reference to a contributed chapter:* Potten CS, Wilson JW. Development of epithelial stem cell concepts. In: Lanza R, Gearhart J, Blau H, Melton D, Moore M, Pedersen R, Thomson J, West M, editors. Handbook of stem cell. Vol. 2, Adult and fetal. Amsterdam: Elsevier; 2004. p. 1–11.
    - *Contributed section with editors:* Johnson D, Ellis H, Collins P, editors. Pectoral girdle and upper limb. In: Standring S, editor. Gray's anatomy: the anatomical basis of clinical practice. 29th ed. Edinburgh (Scotland): Elsevier Churchill Livingstone; 2005. p. 799–942.
  - *Chapter in a book:*
    - *Standard chapter in a book:* Doyle JR, Botte MJ. Surgical anatomy of the hand and upper extremity. Philadelphia (PA): Lippincott Williams and Wilkins; 2003. Chapter 10, Hand, Part 1, Palmar hand; p. 532–641.

Illustrations and tables

Illustrations and tables should be numbered in different categories in the manuscript and Roman numbers should not to be used in numbering. Legends of the illustrations and tables should be added to the end of the manuscript as a separate page. Attention should be paid to the dimensions of the photographs to be proportional with 10x15 cm. Some abbreviations out of standards can be used in related illustrations and tables. In this case, abbreviation used should be explained in the legend. Figures and tables published previously can only be used when necessary for a comparison and only by giving reference after obtaining permission from the author(s) or the publisher (copyright holder).

Author Contribution

Each manuscript should contain a statement about the authors' contribution to the Manuscript. Please note that authorship changes are no longer possible after the final acceptance of an article.

List each author by the initials of names and surnames and describe each of their contributions to the manuscript using the following terms:

- Protocol/project development
- Data collection or management
- Data analysis
- Manuscript writing/editing
- Other (please specify briefly using 1 to 5 words)

For example: NBA: Project development, data collection; AS: Data collection, manuscript writing; STR: Manuscript writing

Funding: information that explains whether and by whom the research was supported.

Conflicts of interest/Competing interests: include appropriate disclosures.

Ethics approval: include appropriate approvals or waivers. Submitting the official ethics approval by whom the research was approved, including the approval date, number or code is necessary.

If the submission uses cadaveric tissue, please acknowledge the donors in an acknowledgement at the end of the paper.

Control list

- Length of the manuscript (max. 15 pages)
- Manuscript format (double space; one space before punctuation marks except for apostrophes)
- Title page (author names and affiliations; running head; correspondence)
- Abstract (100–250 words)
- Keywords (at least three)
- References (relevant to *Index Medicus)*
- Illustrations and tables (numbering; legends)
- Conflicts of Interest Disclosure Statement and Copyright Transfer Form
- Cover letter

All manuscripts must contain the following declaration sections. These should be placed before the reference list at the end of the manuscript.

Original Article

http://dergipark.org.tr/en/pub/anatomy
Received: November 10, 2024; Accepted: February 12, 2025
doi:10.2399/ana.25.1582636

anatomy
An International Journal of Experimental and Clinical Anatomy

Effects of obesity on abdominal wall morphology and diastasis recti abdominis in women

Mehtap Balaban[1], Şeyda Toprak Çelenay[2], Derya Özer Kaya[3]

[1]*Department of Radiology, Faculty of Medicine, Ankara Yıldırım Beyazıt University, Ankara, Türkiye*
[2]*Department of Physiotherapy and Rehabilitation, Faculty of Health Sciences, Ankara Yıldırım Beyazıt University, Ankara, Türkiye*
[3]*Department of Physiotherapy and Rehabilitation, Faculty of Health Sciences, Izmir Katip Celebi University, Izmir, Türkiye*

Abstract

Objectives: Obesity can lead to structural alterations in the abdominal wall, which are important to assess for effective obesity management. This study aimed to investigate the impact of obesity on abdominal wall morphology and the presence of diastasis recti abdominis (DRA) in women, as well as the correlation between body mass index (BMI) and abdominal wall parameters.

Methods: Women were divided into two groups based on BMI: non-obese (BMI<30 kg/m², n=37) and obese (BMI≥30 kg/m², n=36). Using ultrasound, measurements were taken for umbilical subcutaneous adipose tissue (SCAT) thickness, abdominal muscle thickness, linea alba (LA) distortion (using a distortion index formula) and width (using inter-rectus distance, IRD), and presence of DRA.

Results: The obese group showed significantly greater umbilical SCAT thickness, distortion index scores, and IRD measured 2 cm above the umbilicus compared to the non-obese group ($p<0.05$). No significant differences were observed in abdominal muscle thickness between the groups ($p>0.05$). The prevalence of DRA was higher in the obese group (33.3%) than in the non-obese group (10.8%) ($p<0.05$). Significant positive correlations were found between BMI and umbilical SCAT thickness ($p=0.610$), distortion index scores ($p=0.489$), and IRD measured 2 cm above ($p=0.359$) and below the umbilicus ($p=0.304$) ($p<0.05$).

Conclusion: Women with obesity exhibited increased umbilical SCAT thickness, greater linea alba distortion and width, and a higher prevalence of DRA compared to non-obese women. These findings suggest that elevated BMI may negatively influence abdominal wall morphology. Considering these morphological changes may be important in the clinical evaluation and management of obesity.

Keywords: abdominal muscles; diastasis recti abdominis; obesity; ultrasonography

Anatomy 2025;19(1):1–7

Introduction

Globally, obesity is a major public health concern, with its prevalence rising in both developed and developing countries.[1] It is a condition linked to the development of numerous chronic and metabolic diseases, as well as musculoskeletal disorders involving both inflammatory and mechanical components.[2] Musculoskeletal issues, particularly abdominal and lumbopelvic dysfunctions, are strongly associated with increased body mass index (BMI) and accumulation of adipose tissue, especially in the abdominal region.[3,4] Several studies have also reported a higher incidence of postural abnormalities in individuals with elevated BMI and obesity.[5] Furthermore, increased BMI has been associated with reduced trunk stability and decreased endurance of the trunk musculature.[6] Notably, obesity-related factors such as visceral adiposity, chronic systemic inflammation, increased adipokine production, vascular alterations, and elevated intra-abdominal pressure may negatively impact the structural integrity of the abdominal wall.[7]

Anatomically, the abdominal wall is composed of the skin, superficial fascia, muscles and their fascia, fascia transversalis, extraperitoneal fascia and peritoneum.[8] It performs multiple functions, including support for internal organs, facilitation of breathing, coughing, vomiting,

labor, micturition, and defecation, and contributes to trunk stability, mobility, and motor control of both trunk and extremities.[9] Age and gender related differences in the abdominal wall structure have also been documented.[10] Morphological changes in the abdominal wall, reductions in muscle strength, and the presence of conditions such as diastasis recti abdominis (DRA) can impair lumbopelvic stability, postural control, and abdominal organ support.[11] Optimal performance of these functions depends on the coordinated and functional integrity of the abdominal muscles, fasciae, and the linea alba (LA).[9]

Given the complexity of the abdominal wall, detailed examination of its structure is crucial.[12,13] Ultrasound imaging has gained popularity in both clinical assessment and rehabilitation of the abdominal muscles due to its ability to evaluate deep muscle morphology and DRA in a non-invasive manner.[14,15] It also offers valuable information regarding the structure of the LA and the thickness of subcutaneous adipose tissue (SCAT), a key indicator of total body fat.[16,17]

This study aimed to investigate the effects of obesity on abdominal wall morphology and the presence of DRA in women, as well as the correlation between BMI and abdominal wall structural parameters. The underlying hypothesis was that increasing BMI negatively affects the structural integrity of the abdominal wall in women.

Materials and Methods

A case-control study design was employed and all procedures were conducted in accordance with the Declaration of Helsinki. The research was carried out in the Department of Radiology of Bilkent City Hospital. Written informed consent was obtained from all participants.

Initially, 82 individuals were enrolled (non-obese group: n=42; obese group: n=40). In the non-obese group, five individuals were excluded due to unwillingness to participate (n=2), neurological disorders (n=2), and spinal deformity (n=1), resulting in 37 participants (BMI=22.58 [18.71–24.77] kg/m²). In the obese group, four participants were excluded (unwillingness to participate: n=2; abdominal surgery: n=2), resulting in 36 participants (BMI=30.70 [30.00–38.67] kg/m²). Demographic data, surgical history, chronic conditions, and pain status were collected through face-to-face interviews.

All measurements were performed in the morning, following a fasting period of at least 8 hours and avoidance of excessive fluid intake or physical activity. Height was measured using a portable stadiometer (in cm) while participants stood barefoot. Weight was measured using a digital scale (precision: 0.01 kg) with participants in light clothing and barefoot. BMI was calculated as weight divided by height squared (kg/m²). Participants were classified into two groups based on BMI: non-obese (BMI<30 kg/m², n=37) and obese (BMI≥30 kg/m², n=36).[18]

Ultrasound assessments were performed using a Logiq S7 Expert device (General Electric, Canada) with a 9–11 MHz linear transducer in B-mode by a radiologist experienced in musculoskeletal imaging. All scans were conducted with participants in the supine hook-lying position, with pillows under their knees.

SCAT was measured 5 cm above the umbilicus along the midline (**Figure 1a**). The transducer was positioned transversely, and the anteroposterior thickness from the skin to the LA was recorded.[17]

Transverse images of the right and left rectus abdominis (RA) were obtained by placing the transducer lateral to the umbilicus until the RA was centered on the screen. Anteroposterior thickness was measured (**Figure 1b**). For the anterolateral abdominal muscles (external oblique [EO], internal oblique [IO], transversus abdominis [TrA]), the transducer was placed 10 cm lateral to the umbilicus and held perpendicular to the muscle layers (**Figure 1c**). Images were acquired at the end of quiet expiration to standardize measurements and minimize respiratory influence.[19]

The measurement was performed at the midpoint between the umbilicus and the xiphoid process. The shortest linear distance between the medial edges of the RA was calculated. The actual curved path of the LA was then traced, and the area between this path and the shortest distance was computed. The distortion index was calculated as the area divided by the shortest distance (distortion index=bounded area/shortest path).[16]

Inter-rectus distance (IRD) measurements were evaluated for the DRA. To standardize the measurement points, the skin marks were made on 2 cm above and below the umbilicus.[15,20] The transducer was placed transversely on each mark. Images were taken 2 cm above and below the umbilicus at rest and during curl-up.[20] The resting IRD was recorded as the LA width. The occurrence of DRA was determined with a cut-off point of IRD>25 mm at 2 cm above or 2 cm below the umbilicus.[11]

Sample size was calculated using G*Power (v3.0.10, Germany). Based on a pilot study of 10 participants, an effect size of 0.733 was determined from the SCAT measurement. To achieve 80% statistical power at α=0.05, at

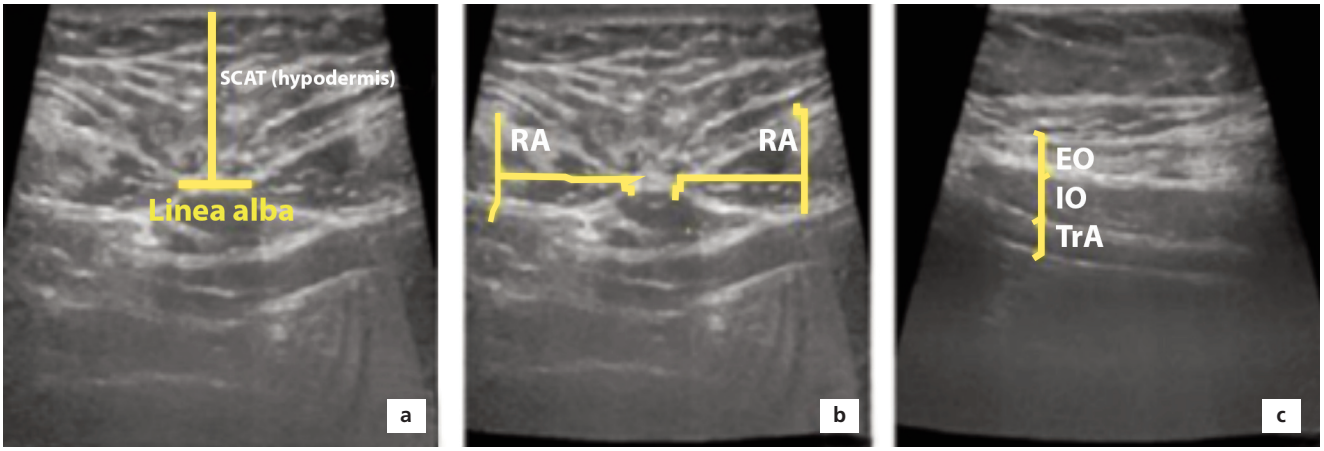

Figure 1. Ultrasound imaging showing measurements. (**a**) Umbilical SCAT measurement; (**b**) RA muscle thickness; (**c**) EO, IO and TrA muscle thickness. **EO:** external oblique; **IO:** internal oblique; **RA:** rectus abdominis; **SCAT:** subcutaneous adipose tissue; **TrA:** transversus abdominis.

least 62 participants (31 per group) were required. Considering potential data loss (≥10%), a total sample size of at least 69 participants was targeted.

Normality of distribution was assessed using visual and analytical methods. Data were presented as mean ± standard deviation ($\bar{X}$± SD), median (min–max), and frequency (n, %) for normally distributed, non-normally distributed, and categorical variables, respectively. Between-group comparisons were performed using the t-test or Mann–Whitney U test for numerical variables, and Chi-square test for categorical data. The Spearman correlation test was applied to evaluate relationships between BMI and abdominal wall parameters. Correlation strength was categorized as: very weak (<0.2), weak (0.3–0.5), moderate (0.6–0.7), strong (0.8–0.9), and very strong (=1).[21] Statistical analyses were conducted using IBM SPSS Statistics (v22.0, Armonk, NY, USA). A p-value <0.05 was considered statistically significant.

Results

The age distribution between the obese and non-obese groups was comparable, with no statistically significant difference observed (p>0.05), except for BMI (**Table 1**). As presented in **Table 2**, significant differences were observed in specific abdominal wall parameters between the groups. Umbilical SCAT thickness, distortion index scores, and IRD measured at 2 cm above the umbilicus were significantly higher in the obese group compared to the non-obese group (p<0.05). However, no significant differences were found between the groups regarding the thickness measurements of the RA, EO, IO, and TrA muscles (p>0.05). The prevalence of DRA was also higher in the obese group. Specifically, DRA was observed in 33.3% (n=12) of women in the obese group and in 10.8% (n=4) of women in the non-obese group, representing a statistically significant difference in DRA occurrence between the two groups (p<0.05).

Correlation analysis revealed a positive weak to moderate association between BMI and several abdominal wall parameters. Specifically, BMI was positively correlated with umbilical SCAT thickness (rho=0.610, p<0.001), the distortion index scores (rho=0.489; p<0.001) and the IRD, measuring at 2 cm above (rho=0.359; p=0.002) and below the umbilicus (rho=0.304; p=0.009). No significant correlations were found between BMI and the thickness values

Table 1
The features of the groups.

Features	Non-obese group (n=37)	Obese group (n=36)	p-value
Age (years, X±SD)	35.11±9.22	38.81±10.76	0.122
BMI (kg/m^2, median (min-max))	22.58 (18.71–24.77)	30.70 (30.00–38.67)	<0.001*

*p<0.05. **SD:** standard deviation; **max:** maximum; **min:** minimum; **X:** mean.

Table 2
The abdominal wall structure parameters of the groups.

Abdominal wall structures	Non-obese group X±SD Median (min-max) n (%) (n=37)	Obese group X±SD Median (min-max) n (%) (n=36)	p-value
Subcutaneous adipose tissue (mm)			
Umblical SCAT	15.20±5.28	20.02±5.21	<0.001*
Abdominal muscle thickness (mm)			
RA_R	6.28±1.32	6.61±1.56	0.338
RA_L	6.02±1.35	6.40±1.47	0.250
EO_R	2.70 (1.30–6.40)	2.65 (1.70–8.50)	0.934
EO_L	3.00 (1.10–4.50)	2.85 (1.90–5.60)	0.331
IO_R	5.10 (3.50–9.30)	5.10 (3.20–8.50)	0.320
IO_L	5.04±1.26	5.41±1.56	0.270
TrA_R	2.60 (2.00–4.50)	2.80 (2.00–4.70)	0.158
TrA_L	2.50 (1.50–4.30)	2.55 (2.00–4.10)	0.332
Linea alba distortion and width (mm)			
Distortion index	0.053 (0.025–0.487)	0.077 (0.028–0.875)	0.005*
IRD_2 cm above umbilicus	12.20 (3.70–34.20)	17.00 (3.20–47.40)	0.032*
IRD_2 cm below umbilicus	4.60 (1.80–20.20)	5.10 (1.30–32.30)	0.200
DRA			
Absent	33 (89.2)	24 (66.7)	0.020*
Presence	4 (10.8)	12 (33.3)	

*p<0.05. **DRA:**diastasis recti abdominis; **EO:** external oblique; **IRD:** inter-rectus distance; **IO:** internal oblique; **L:** left, **R:** right; **RA:** rectus abdominis; **SCAT:** subcutaneous adipose tissue; **TrA:** transversus abdominis.

of the abdominal muscles, including RA (Right (R)= 0.399, Left (L)=0.264), EO (R=0.877, L=0.095), IO (R=0.506, L=0.110), and TrA muscles (R=0.178, L=0.260) was found.

Discussion

Obesity, which may alter the structural integrity of the abdominal wall, remains a major public health concern. In the current study, obese women demonstrated significantly greater umbilical SCAT, IRD, LA distortion and width, as well as a higher occurrence of DRA compared to non-obese women. These findings were further supported by weak-to-moderate positive correlations between body mass index (BMI) and umbilical SCAT thickness, LA distortion, and IRD measurements. In contrast, no significant differences or correlations were observed in the thickness of abdominal muscles between the groups.

Abdominal fat comprises subcutaneous, pre-peritoneal, and visceral components, with visceral fat being particularly implicated in cardiometabolic risk.[22] Various techniques, such as skinfold calipers, computed tomography (CT), magnetic resonance imaging (MRI), and ultrasound, have been employed to quantify abdominal fat.[17,23,24] Few studies, however, have examined umbilical SCAT thickness in relation to BMI. Kim et al.[25] using CT, reported a positive correlation between BMI and SCAT thickness, independent of age or surgical history. Similarly, Torun et al.[17] also found that there was a positive correlation between BMI and umbilical SCAT thickness, measured with ultrasound. In our study, it was seen that women in the obese group had high umbilical SCAT and also there was a positive correlation between BMI and umbilical SCAT thickness. Our findings are in agreement, suggesting that BMI can serve as a reliable proxy for umbilical SCAT thickness.

Assessing abdominal muscle thickness provides insight into potential morphological adaptations of muscle tissue.[26] However, previous studies have yielded inconsistent results regarding the relationship between BMI and abdominal muscle thickness. Tahan et al.[27] evaluated the correlation between BMI and abdominal muscle thicknesses in healthy individuals (age range of 18–44 years) with ultrasound imaging. It was reported

that although a positive correlation was found between the BMI and the thickness of EO and RA muscles, no correlation was seen between the BMI and the thickness of TrA and IO muscles. Springer et al.[10] similarly noted a positive correlation between the BMI and the thickness of lateral abdominal muscle, measured by ultrasound imaging, in healthy individuals (age range of 18–45 years). Saranteas et al.[7] found reduced abdominal muscle thickness in elderly obese individuals, compared to younger non-obese subjects (age=75 (70–83) years) was lower than that of young non-obese people (age=35 (28–38) years). Our study revealed no significant differences or correlations in muscle thickness between groups, potentially attributable to variations in age distribution. Previous research by Khan et al.[28] suggested that abdominal muscle thickness may increase with obesity until the fourth decade of life, followed by a decline. Additionally, as in prior studies, we assessed raw muscle thickness values without normalizing for body mass, which may have confounded results. Future studies should consider allometric scaling[29] to better interpret muscle adaptations.

The LA is formed by the aponeuroses of the EO, IO and TrA. The structural characteristic of LA ensures core stability under abdominal muscle tension and contributes transmit loads between the sides of the abdominal wall.[8] LA dysfunction is associated with pathologies such as hernias, low back pain, and reduced quality of life.[30] The tension, width and thickness of LA may change with increased intra-abdominal pressure (obesity etc.), pregnancy or abdominal surgery. In addition, the LA structure is related to the abdominal muscles activation.[30] In the study of Fan et al.,[31] it was observed that the LA thickness did not change compared to nulliparous women in different birth types (vaginal and cesarean section) and the LA width is increased in women who had cesarean section compared to nulliparous women. Fredon et al.[32] found that there was a positive correlation between the LA width and the BMI in both men and women. Grossi et al.[33] investigated the amount of collagen in the LA of obese people and comparing with non-obese cadavers. It was seen that the amount of collagen in the LA above the umbilical region in the morbidly obese people was smaller than in the non-obese cadavers. According to the authors' knowledge, no study was found examining the correlation between BMI and LA distortion related to tension or stiffness. In our study, it was also found that women in obese group had higher LA width and distortion than women in non-obese group. As a results of our study, it was seen that as the BMI increased, the LA width increased and the LA tension decreased. These findings may be due to increases in intra-abdominal pressure with obesity. In obesity rehabilitation, the LA width and distortion, important in the stability of the abdominal wall, should be evaluated and supported by different treatment approaches such as exercises.

DRA is prevalent among adult women and is influenced by factors such as obesity, pregnancy, and metabolic disease. Wu et al.[34] and Doubkova et al.[35] both identified a significant association between higher BMI and increased DRA risk. Our findings align with these results, as a higher prevalence of DRA was observed among obese women. It is plausible that clinical subtypes of obesity (e.g., sarcopenic obesity or visceral adiposity) exacerbate LA separation by compromising muscular support or increasing intra-abdominal tension. Therefore, obesity prevention may serve as a means of reducing DRA prevalence, though further investigation into these obesity subtypes is warranted.However, more detailed studies are needed on these issues.

This study has several limitations. First, obesity was defined solely by BMI, which may not reflect clinical subtypes such as sarcopenic or metabolically healthy obesity.[18] Second, subgroup analyses based on obesity severity were not performed, though such stratification may yield further insights into the structural changes observed. Third, only women were included to ensure a homogeneous sample; hence, the findings may not be generalizable to men. Lastly, as this was a single-center study, future multi-center investigations with broader demographics are recommended.

Conclusion

This study demonstrates that obese women exhibit significantly greater umbilical SCAT thickness, LA distortion, and DRA occurrence compared to non-obese women, while abdominal muscle thickness remains unaffected. These findings suggest that elevated BMI may negatively impact the structural integrity of the abdominal wall. Therefore, comprehensive obesity management should incorporate not only weight reduction strategies but also physiotherapy interventions—such as exercise and taping—to improve LA function and reduce DRA risk.

Conflict of Interest

The authors declare that they have no conflict of interest.

Author Contributions

MB: protocol/project development, data collection, data analysis, manuscript writing/editing; ŞTÇ: protocol/project development, data analysis, manuscript writing/editing; DÖK: protocol/project development, manuscript writing/editing.

Ethics Approval

The study was approved by the Non-Interventional Clinical Studies Institutional Review Board of Izmir Katip Celebi University (Approval date/number: 23.02.2023/0061).

Funding

The funding source had no role in the design, practice or analysis of this study.

References

1. Bhurosy T, Jeewon R. Overweight and obesity epidemic in developing countries: a problem with diet, physical activity, or socioeconomic status? ScientificWorldJournal 2014;2014:964236.
2. De Heredia FP, Gómez-Martínez S, Marcos A. Obesity, inflammation and the immune system. Proc Nutr Soc 2012;71:332–8.
3. Aune D, Mahamat-Saleh Y, Norat T, Riboli E. Body mass index, abdominal fatness, weight gain and the risk of urinary incontinence: a systematic review and dose-response meta-analysis of prospective studies. BJOG 2019;126:1424–33.
4. Chowdhury D, Sarkar S, Rashid MH, Rahaman A, Sarkar SK, Roy R. Influence of body mass index on low back pain. Mymensingh Med J 2014;23:125–9.
5. Smith AJ, O'Sullivan PB, Beales DJ, de Klerk N, Straker LM. Trajectories of childhood body mass index are associated with adolescent sagittal standing posture. Int J Pediatr Obes 2011;6:e97–106.
6. AlAbdulwahab SS, Kachanathu SJ. Effects of body mass index on foot posture alignment and core stability in a healthy adult population. J Exerc Rehabil 2016;12:182–7.
7. Saranteas T, Anagnostis G, Lappas T, Christodoulopoulou T, Kostopanagiotou G. Feasibility of ultrasound imaging of the abdominal wall in elderly obese volunteers. Br J Anaesth 2010;105:549–50.
8. Flament JB, Avisse C, Delattre JF. Anatomy of the abdominal wall. In: Bendavid R, Abrahamson J, Arregui ME, Flament JB, Phillips EH, editors. Abdominal wall hernias. New York: Springer; 2001. p. 39–63.
9. Lee DG, Lee LJ, McLaughlin L. Stability, continence and breathing: the role of fascia following pregnancy and delivery. J Bodyw Mov Ther 2008;12:333–48.
10. Springer BA, Mielcarek BJ, Nesfield TK, Teyhen DS. Relationships among lateral abdominal muscles, gender, body mass ındex, and hand dominance. J Orthop Sports Phys Ther 2006;36:289–97.
11. Candido G, Lo T, Janssen PA. Risk factors for diastasis of the recti abdominis. Journal of the Association Chartered Physiotherapists in Women's Health 2005;97:49–54.
12. Pachera P, Pavan PG, Todros S, Cavinato C, Fontanella CG, Natali AN. A numerical investigation of the healthy abdominal wall structures. J Biomech 2016;49:1818–23.
13. Pirri C, Todros S, Fede C, Pianigiani S, Fan C, Foti C, Stecco C, Pavan P. Inter-rater reliability and variability of ultrasound measurements of abdominal muscles and fasciae thickness. Clin Anat 2019;32:948–60.
14. Teyhen DS. Rehabilitative ultrasound imaging symposium San Antonio, TX, May 8–10, 2006. J Orthop Sport Phys Ther 2006;36:A1–3.
15. Mota P, Pascoal AG, Sancho F, Bø K. Test-retest and intrarater reliability of 2-dimensional ultrasound measurements of distance between rectus abdominis in women. J Orthop Sport Phys Ther 2012;42:940–6.
16. Lee D, Hodges PW. Behavior of the linea alba during a curl-up task in diastasis rectus abdominis: an observational study. J Orthop Sport Phys Ther 2016;46:580–9.
17. Torun BI, Balaban M, Geneci F, Hatipoglu SC. The relationship between the body mass index and the subcutaneous adipose tissue. Anatomy 2022;16:7–12.
18. Vecchié A, Dallegri F, Carbone F, Bonaventura A, Liberale L, Portincasa P, Fruhbeck G, Montecucco F. Obesity phenotypes and their paradoxical association with cardiovascular diseases. Eur J Intern Med 2018;48:6–17
19. Karakus A, Balaban M, Kaya DO, Celenay ST. Lumbopelvic muscle endurance, morphology, alignment, and mobility in women with primary dysmenorrhea: a case-control study. Clin Biomech (Bristol) 2022;92:105582.
20. Mota P, Pascoal AG, Carita AI, Bø K. The ımmediate effects on inter-rectus distance of abdominal crunch and drawing-in exercises during pregnancy and the postpartum period. J Orthop Sport Phys Ther 2015;45:781–8.
21. Akoglu H. User's guide to correlation coefficients. Turk J Emerg Med 2018;18:91–3.
22. Busetto L, Baggio MB, Zurlo F, Carraro R, Digito M, Enzi G. Assessment of abdominal fat distribution in obese patients: anthropometry versus computerized tomography. Int J Obes Relat Metab Disord 1992;16:731–6.
23. Gradmark AMI, Rydh A, Renström F, De Lucia-Rolfe E, Sleigh A, Nordström P, Brage S, Franks PW. Computed tomography-based validation of abdominal adiposity measurements from ultrasonography, dual-energy X-ray absorptiometry and anthropometry. Br J Nutr 2010;104:582–8.
24. Hastuti J, Rahmawati N, Suriyanto R, Wibowo T, Nurani N, Julia M. Patterns of body mass index, percentage body fat, and skinfold thicknesses in 7- to 18-year-old children and adolescents from Indonesia. Int J Prev Med 2020;11:129.
25. Kim J, Lim H, Lee SI, Kim YJ. Thickness of rectus abdominis muscle and abdominal subcutaneous fat tissue in adult women: correlation with age, pregnancy, laparotomy, and body mass index. Arch Plast Surg 2012;39:528–33.
26. Hildenbrand K, Noble L. Abdominal muscle activity while performing trunk-flexion exercises using the ab roller, abslide, fitball, and conventionally performed trunk curls. J Athl Train 2004;39:37–43.

27. Tahan N, Khademi-Kalantari K, Mohseni-Bandpei MA, Mikaili S, Baghban AA, Jaberzadeh S. Measurement of superficial and deep abdominal muscle thickness: an ultrasonography study. J Physiol Anthropol 2016;35:17.
28. Khan MA, Qureshi K, Rehman Z. Effect of age and obesity on human male anterior abdominal wall muscles: an ultrasonographic anthropometric analysis. Pakistan Journal of Medical & Health Sciences 2012;6:406–12.
29. Linek P. The importance of body mass normalisation for ultrasound measurement of the transversus abdominis muscle: the effect of age, gender and sport practice. Musculoskelet Sci Pract 2017;28:65–70.
30. Benjamin DR, Frawley HC, Shields N, van de Water ATM, Taylor NF. Relationship between diastasis of the rectus abdominis muscle (DRAM) and musculoskeletal dysfunctions, pain and quality of life: a systematic review. Physiotherapy 2019;105:24–34.
31. Fan C, Guidolin D, Ragazzo S, Fede C, Pirri C, Gaudreault N, Porzionato A, Macchi V, De Caro R, Stecco C. Effects of cesarean section and vaginal delivery on abdominal muscles and fasciae. Medicina (Kaunas) 2020;56:260.
32. Fredon F, Hardy J, Germain M, Vincent-Viry E, Taïbi A, Monteil J, Mabit C, Valleix D, Durand-Fontanier S. Correlations of the rectus abdominis muscle anatomy with anthropometric measurements. Surg Radiol Anat 2021;43:589–93.
33. Grossi JV, Nicola FF, Zepeda IA, Becker M, Trindade EN, Diemen VV, Cavazzola LT, Trindade MR. Linea alba collagen assessment in morbidly obese patients. Arq Bras Cir Dig 2016; 29(suppl 1):8–11.
34. Wu L, Gu Y, Gu Y, Wang Y, Lu X, Zhu C, Lu Z, Xu H. Diastasis recti abdominis in adult women based on abdominal computed tomography imaging: prevalence, risk factors and its impact on life. J Clin Nurs 2021;30:518–27.
35. Doubkova L, Andel R, Palascakova-Springrova I, Kolar P, Kriz J, Kobesova A. Diastasis of rectus abdominis muscles in low back pain patients. J Back Musculoskelet Rehabil 2018;31:107–12.

ORCID ID:
M. Balaban 0000-0002-6752-6838;
Ş. Toprak Çelenay 0000-0001-6720-4452;
D. Özer Kaya 0000-0002-6899-852X

Correspondence to: Şeyda Toprak Çelenay, MD
Department of Physiotherapy and Rehabilitation, Faculty of Health Sciences, Ankara Yıldırım Beyazıt University, Ankara, Türkiye
Phone: +90 312 906 19 96
e-mail: sydtoprak@hotmail.com

Conflict of interest statement: No conflicts declared.

 How to cite this article: Balaban M, Toprak Çelenay Ş, Özer Kaya D. Effects of obesity on abdominal wall morphology and diastasis recti abdominis in women. Anatomy 2025;19(1):1–7.

anatomy
http://dergipark.org.tr/en/pub/anatomy
An International Journal of Experimental and Clinical Anatomy

Original Article

http://dergipark.org.tr/en/pub/anatomy
Received: October 15, 2024; Accepted: February 12, 2025
doi:10.2399/ana.25.1567529

Human bicipital groove: a morphometric study on dry humerus

Mehmet Ülkir[1], Mehmet Yılmaz[2], Aybegüm Balcı[2], Burcu Erçakmak Güneş[1], Ceren Günenç Beşer[1]

[1]*Department of Anatomy, Faculty of Medicine, Hacettepe University, Ankara, Türkiye*
[2]*Department of Anatomy, Faculty of Medicine, Ankara University, Ankara, Türkiye*

Abstract

Objectives: The aim of this study is to evaluate the morphometry of the bicipital groove on dry humeri, which is closely associated with the long head of the biceps tendon, a key component in shoulder biomechanics.

Methods: This study involved 109 adult human dry humeri (56 right, 53 left). The humerus length (HL), bicipital groove length (BGL), bicipital groove width (BGW), bicipital groove depth (BGD), opening angle (OA) and medial wall angle (MWA) were measured.

Results: The mean value of HL was measured 30.97±2.01 cm and the mean value of BGL was 89.70±8.09 mm. The mean value of BGW was 10.31±1.51 mm and BGD was 3.98±0.79 mm. The mean value of OA was 99.85±14.53° and MWA was 42.31±8.25°. No significant differences were observed between the right and left sides in the measured parameters. Positive correlations were found between BGW and BGD, BGW and OA, MWA and BGD, and HL and BGL. Negative correlations were observed between BGL and BGD, OA and BGD, and MWA and BGW.

Conclusion: We believe the detailed morphometric evaluation of the bicipital groove presented in this study provides valuable insights into the pathologies of the long head of the biceps tendon and its implications for shoulder arthroplasty.

Keywords: anatomy, bicipital groove, long head of biceps, morphometry

Anatomy 2025;19(1):8–15

Introduction

The bicipital groove (BG), also referred to as the intertubercular sulcus, is a depression that extends distally and is situated between the greater and lesser tubercles on the anterior surface of the proximal humerus.[1,2] The lesser and greater tubercles are connected by a wide transverse humeral ligament, which turns this groove into a tunnel.[3] The long head of biceps tendon (LHBT) passes through this groove before inserting to the supraglenoid tubercle, crossing the capsule of shoulder joint.[4] This tunnel also provides passage for the synovial sheath of the LHBT and the anterior circumflex humeral artery.[5] The medial and lateral lips of the BG serve as attachment points for the tendons of the teres major and pectoralis major muscles, respectively, while the floor of the BG provides attachment for the latissimus dorsi tendon. Also, the muscle fibers of pectoralis major, supraspinatus and subscapularis form the superior border of the BG. Along with the transverse humeral ligament and surrounding muscle fibers, the BG helps stabilize the LHBT, ensuring proper muscle function and preventing dislocation during arm movements.[6]

Anterior shoulder pain is a common condition that affects a significant number of individuals, including the elderly population. Injuries involving the LHBT have been proposed as one of the most common reasons for shoulder disability and pain.[7] Shoulder pain associated with LHBT injuries is believed to be due to impingement, pre-rupture, inflammation, or tendon instability at the point of entry into the BG.[6] The morphometric characteristics of the BG may significantly affect the functionality of the adjacent structures in the shoulder joint[4] and some authors stated that injuries of LHBT caused by the significant anatomical variabilities of the

BG, were the primary reasons for shoulder pain and dysfunction.[8] Bicipital groove width, depth and angulations are crucial parameters in the prevention of subluxation or impingement of the LHBT which can lead to shoulder pain.[4] Understanding the morphometry of BG is extremely beneficial for prosthetic design, sizing and placement and it is a crucial landmark for replacing the humeral head in proximal end fractures and for positioning the lateral fin of the prosthesis during shoulder arthroplasty.[9]

The aim of this study was to evaluate the BG morphometry on the dry humeri, which is important in shoulder biomechanics and has a significant relationship with LHBT.

Materials and Methods

This study involved 109 adult human dry humeri (56 right, 53 left) which were obtained from the Department of Anatomy, Faculty of Medicine, Hacettepe University. The age and sex of the specimens were not identified. Humeri with cortical deformity and fracture were excluded. Ethical approval was obtained from Hacettepe University Health Sciences Research Ethics Committee (30.07.2024, decision number: 2024/13-01).

The following parameters were assessed:

1. **The humerus length (HL):** the distance from the most proximal point of head of humerus to the most distal point of trochlea of humerus (**A–B**) (**Figure 1**).
2. **The bicipital groove length (BGL):** the distance from the point between the lesser and greater tubercles to the end of the bicipital groove depression on the shaft (**C–D**) (**Figure 2**).
3. **The bicipital groove width (BGW):** the distance between the top of the lesser tubercle and top of the greater tubercle (**E–F**) (**Figure 3**).
4. **The bicipital groove depth (BGD):** the distance from the line connects the top of the lesser tubercle and top of the greater tubercle to the deepest point of bicipital groove (**EF–G**) (**Figure 3**).
5. **Opening angle (OA):** the angle between the line connects the deepest point of bicipital groove and top of lesser tubercle and the line connects the deepest point of bicipital groove and top of greater tubercle (**EG-FG**) (**Figure 4**).
6. **Medial wall angle (MWA):** the angle between the line passes from the deepest point of bicipital groove which is parallel to the line connects the top of lesser

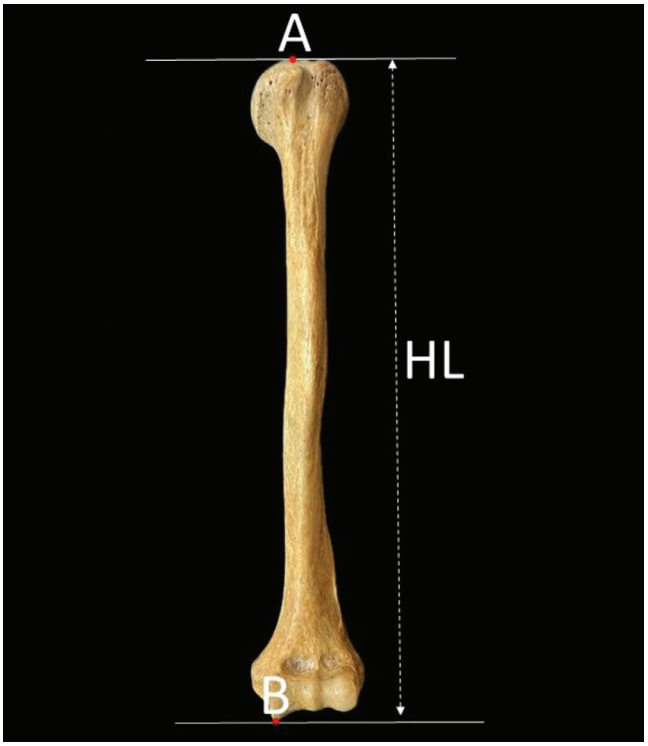

Figure 1. Demonstration of humerus length (**HL**) measurement. **A:** the most proximal point of head of humerus, **B:** the most distal point of trochlea of humerus.

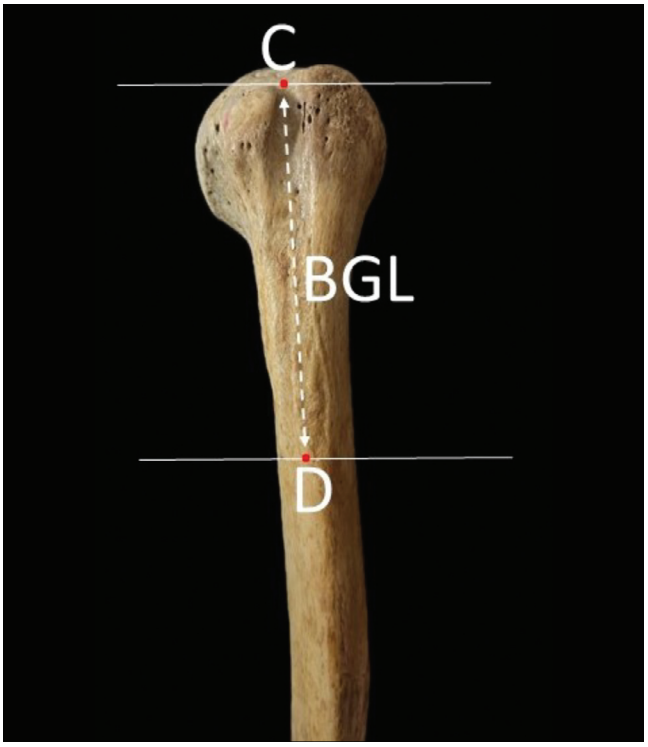

Figure 2. Demonstration of bicipital groove length (**BGL**) measurement. **C:** the point between the lesser and greater tubercles, **D:** end of the bicipital groove depression on the shaft.

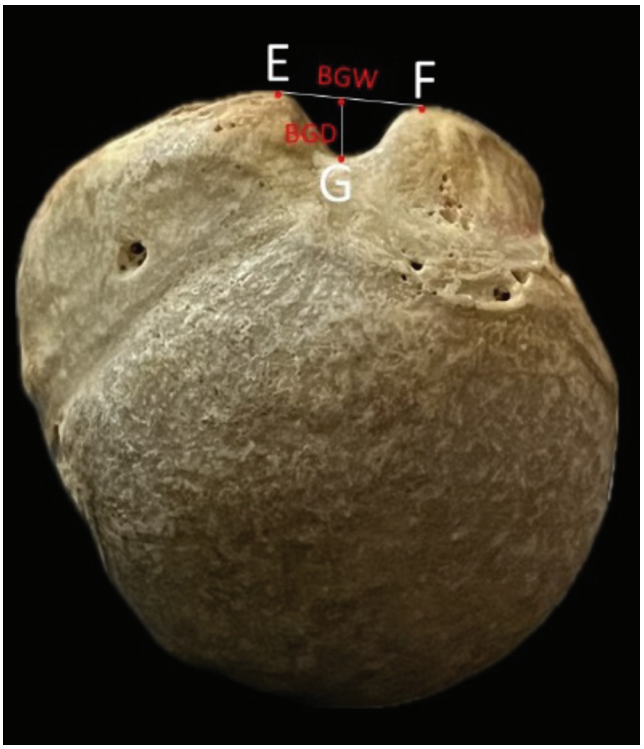

Figure 3. Demonstration of bicipital groove width (**BGW**) and bicipital groove depth (**BGD**) measurements. **E:** top of the greater tubercle, **F:** top of the lesser tubercle, **G:** deepest point of bicipital groove.

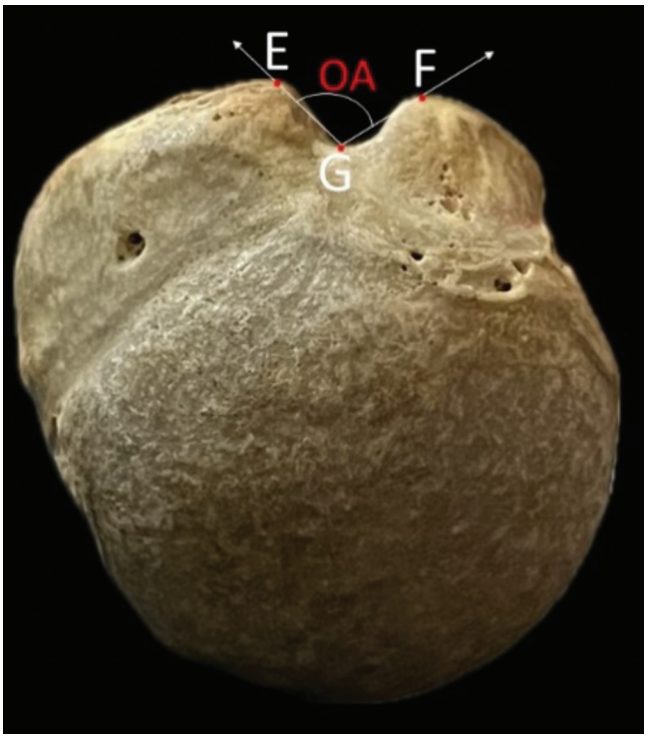

Figure 4. Demonstration of opening angle (**OA**) measurement. **E:** top of the greater tubercle, **F:** top of the lesser tubercle, **G:** deepest point of bicipital groove.

tubercle and top of greater tubercle and the line connects the deepest point of bicipital groove and top of lesser tubercle (**Figure 5**).

The HL was measured with tape measure (150 cm). The BGL, BGW and BGD was measured with 0.01 mm accuracy digital Vernier caliper (150 mm). OA and MWA was measured by angle meter application. For minimizing intra observer error, measurements was performed 3 times with a one-week interval and average values were calculated.

Data analysis was conducted using the Statistical Package for the Social Sciences (SPSS), version 19 (Chicago, IL, USA). The measurements were presented as mean values and standard deviations. The Kolmogorov-Smirnov test was used to analyze the distribution of the data set. Pearson correlation test was used for normally distributed data and the Spearman correlation test for non-normally distributed data. The student's t-test and Mann-Whitney U test were used for comparison of right and left side measurements. For correlation analysis, Pearson correlation test was used. A p-value less than 0.05 was accepted as statistically significant. Sample size was

Figure 5. Demonstration of medial wall angle (**MWA**) measurement. **F:** top of the lesser tubercle, **G:** deepest point of bicipital groove.

calculated using GPower 3.1 program. The study will find a statistical difference of medium effect size (d=0.50, Cohen, J) among the effect sizes recommended in the literature between the means of the two groups (right and left side) with 90% power at 95% confidence level, when samples with a size of at least 100 (50 right, 50 left) are selected from each group.

Results

A total of 109 human dry humeri (56 right, 53 left) from the bone collection of Hacettepe University were examined in this study. The mean value of HL was 30.81±1.72 cm on the right side, 31.21±2.24 cm on the left side, and 30.97±2.01 cm in total. The mean value of BGL was 88.47±6.84 mm on the right side, 91.04±9.14 mm on the left side, and 89.70±8.09 mm in total. The mean value of BGW was 10.10±1.21 mm on the right side, 10.57±1.76 mm on the left side, and 10.31±1.51 mm in total. The mean value of BGD was 3.93±0.69 mm on the right side, 4.01±0.88 mm on the left side, and 3.98±0.79 mm in total. The mean value of OA was 101.70±14.14° on the right side, 98.20±14.86° on the left side, and 99.85±14.53° in total. The mean value of MWA was 41.43±7.90° on the right side, 42.97±8.46° on the left side, and 42.31±8.25° in total (**Table 1**).

There were no statistically significant differences observed between the right and left sides in any of the measured parameters. Positive correlations were observed between BGW and BGD (r=0.232, p=0.15), BGW and OA (r=0.474, p<0.01), MWA and BGD (r=0.533, p<0.01), and HL and BGL (r_s=0.598, r=0). The negative correlations were detected between the BGL and BGD (r=-0.260, p=0.006), OA and BGD (r=-0.682, p=0.0), MWA and BGW (r=-0.370, p=0.0).

Discussion

Anatomical variations in the BG that involve the LHBT were predisposing factors for common sources of shoulder pain, resulting in shoulder joint disability.[8] It is quite common for individuals with a shallow BG to experience subluxation of the long head of the biceps, especially in the medial region. Lateral dislocation or subluxation is relatively uncommon. Besides subluxation and dislocation, a narrow and deep BG can often be the main reason for compressing the long head of the biceps tendon within it, resulting in impingement syndrome, a prevalent functional impairment of the shoulder joint.[4] BGW was measured 10.1 mm by Wafae et al.[1] in Brazil, 8±2 mm by Rajani and Man[6] in India , 9.12±2.18 mm by Kumar et al.[4] in India, 6.79±0.53 mm on the right side and 7.56±1.05 mm on the left side by Karmali and Modi[3] in India, 8.53±1.56 mm on the right side and 7.96±1.39 mm on the left side by Ashwini and Venkateshu[10] in India, 8.42±0.85 mm on the right side and 7.7±0.50 mm on the left side by Srimani et al.[5] in India, 8.99±1.51 mm by Venkatesan et al.[11] in India, 10.3±2.5 mm by Cardoso et al.[12] in Portugal, 12.3±2.1 mm by Tang et al.[13] in China, 11.8±1.7 mm in <55 years old group and 10.9±1.6 mm in >55 years old group by Song and Kim[14] in Korea. In our study BGW was 10.31±1.51 mm, which was higher than majority of previous studies and lower than the studies of Tang et al. and Song and Kim.[1,3–6,10–14] BGD was measured 4.0 mm by Wafae et al.,[1] 6±1 mm by Rajani and Man,[6] 5.49±1.56 mm by Kumar et al.,[4] 4.17±0.56 mm on the right side, 5.01±1.02 mm on the left side by Karmali and Modi,[3] 5.06±0.54 mm in males and 4.51±0.54 mm in females by Duran et al.,[15] 6.48± 1.13 mm on the right side and 6.14±1.04 mm on the left side by Ashwini and

Table 1
Morphometric properties of bicipital groove.

Measurement	Right	Left	Total	p-value
HL (cm)	30.81±1.72	31.21±2.24	30.97±2.01	0.241
BGL (mm)	88.47±6.84	91.04±9.14	89.70±8.09	0.092
BGW (mm)	10.10±1.21	10.57±1.76	10.31±1.51	0.089
BGD (mm)	3.93±0.69	4.01±0.88	3.98±0.79	0.673
OA (°)	101.70±14.14	98.20±14.86	99.85±14.53	0.248
MWA (°)	41.43±7.90	42.97±8.46	42.31±8.25	0.196

BGD: bicipital groove depth; **BGL:** bicipital groove length; **BGW:** bicipital groove width; **HL:** humerus length; **MWA:** medial wall angle; **OA:** opening angle.

Venkateshu,[10] 5.1 mm by Abboud et al.,[7] 4.63±0.38 mm on the right side and 4.45±0.30 mm on the left side by Srimani et al.,[5] 4.6±1.09 mm by Venkatesan et al.,[11] 4.1±1.5 mm by Cardoso et al.,[12] 4.9±1.4 mm by Tang et al.,[13] 4.6±0.7 mm in <55 years old group and 4.6±0.8 mm in >55 years old group by Song and Kim.[14] BGD was measured 3.98±0.79 mm in our study, which was lower than previous studies. Ulucakoy et al. evaluated 200 magnetic resonance imagines and they measured BGD as 5.6 ± 0.8 mm in stable LHBT patients and 5.7 ± 0.9 mm in unstable LHBT patients. No significant difference was detected between the stable and unstable LHBT patients for BGD measurement in their study.[16] Also, no correlation was detected between the BGW and BGD measurements and LHBT pathologies in the studies of Cardoso et al.[12] and Tang et al.[13] Song and Kim[14] compared the BGW and BGD values between the <55 years old group and >55 years old group and statistically significant difference was detected between these groups for BGW measurement. We measured HL and BGL as 30.97±2.01 cm and 89.70±8.09 mm, respectively, which were consistent with previous studies. Measurement differences may result from geographical variations and differing measurement techniques, such as dry bone assessment versus magnetic resonance imaging, radiography and computed tomography imaginations. Radiological imaging techniques are developing and measurements can be done on radiological images in 3D, but we think that measurements done on dry bones are still the most valuable materials since measurements done by touching the hand. Moreover, it is known that morphometric values may differ between populations. We can conclude from **Table 2** that the measurement differences in studies performed with dry bones may be due to the studies being performed in various geographical regions or the studies performed with various measurement techniques.

The LHBT is greatly influenced by the size and dimensions of the bicipital groove (BG). Multiple authors have documented a higher occurrence of dislocation and subluxation of the LHBT when the BG is shallow. The LHBT instability could be caused by the dimension of MWA that vary based on the depth and width leading to a shallow bicipital groove.[10] While it is not known if there is a specific critical MWA value for LHBT instability, Ahovuo[17] demonstrated that 22% of patients with LHBT instability had a MWA below 30° and Hitchcock and Bechtol[8] found that a smaller than 35° MWA was seen in 8% of patients with LHBT instability. In a study of Venkatesan, no bone had MWA lower than 30°.[11] Ashwini and Venkateshu[10] detected humeri with MWA lower than 30° in 6 of 87 humeri which were left sided. In a study of Cardoso et al.[12] MWA lower than 30° was detected in 4 patients (9.1%) and similar to the study by Tang et al.,[13] they did not find a significant difference between MWA and LHTB pathologies. Also, Song and Kim detected no significant difference between the age groups (<55 years old group and >55 years old group) for MWA parameter.[14] In our study MWA was measured 42.31±8.25°, which was lower than majority of previous studies and 4 of 109 bones had MWA below 30° and 22 of 109 bones were between 30–35°. This finding shows us that individuals in the Turkish population may be more prone to LHBT instability due to their lower MWA. Duran et al.[15] measured MWA as 50.01±5.55° in males and 47.91±5.70° in females and no significant difference was detected between sex for MWA measurement. Also, there was no significant difference between the stable LHBT (51.0±8.6°) and unstable LHBT (49.9±8.4°) patients for MWA measurement in a study of Ulucakoy et al.[16]

Pfahler et al.[18] detected a noticeable increasing of damaged LHBT in the presence of a flat groove angle. Several authors have stated that dislocation and subluxation of the biceps tendon are more frequent when the BG is not deep enough. It is also indicated that a shallow BG can make the tendon more prone to chronic injury from being compressed by the coracoacromial arch, rotator cuff and acromion during shoulder movements.[19] Smith[20] categorized different types of BG based on their mean OA being less than 66°, 94°, and 118° into narrow, normal, and shallow classifications. In a study of Abboud et al.,[7] majority of BG had normal OA (38/75) and 20 of 75 were shallow and 17 of 75 were narrow. Cardoso et al.[12] detected majority of BG as normal OA 26 (59.1%). Unlike these studies we detected majority of BG as shallow OA (68 of 109), 1 of 109 was narrow and 40 of 109 were normal. Since individuals in Turkish population have a higher opening angle, they may be exposed to more pressure from the structures around the LHBT, which may cause chronic damage. No significant difference was detected between the LHBT pathologies and OA parameter in the studies of Cardoso et al. and Tang et al.[12,13] The comparison of morphometric properties of BG was summarized in **Table 2**.

Table 2
Comparison of the morphometric properties of the bicipital groove.

Study (year)	Population	N	Method	HL (cm)	BGL (mm)	BGW (mm)	BGD (mm)	OA (°)	MWA (°)
Wafae et al. (2010)[1]	Brazil	50 (25 R, 25 L)	DB	-	81	10.1	4.0	106	-
Rajani and Man (2013)[6]	India	101 (56 R, 45 L)	DB	-	R: 85±0.9 L: 83±10.1	8±2	6±1	82.20±20.62	48.91±10.31
Kumar et al. (2021)[4]	India	100 (57 R, 43 L)	DB	-	72.98±7.54	9.12±2.18	5.49±1.56	72.27±18.12	65.27±10.71
Karmali and Modi (2019)[3]	India	86 (49 R, 37 L)	DB	31.14±2.41	R: 83.93±5.68 L: 86.59±6.28	R: 6.79±0.53 L: 7.56±1.05	R: 4.17±0.56 L: 5.01±1.02	-	-
Duran et al. (2023)[15]	Turkey	110 (50 M, 60 F)	MRI	-	-	-	M: 5.06±0.54 F: 4.51±0.54	M: 78.73±7.90 F: 80.53±8.71	M: 50.01±5.55 F: 47.91±5.70
Ulucakoy et al. (2021)[16]	Turkey	200	MRI	-	-	-	SLHBT: 5.6±0.8 ULHBT: 5.7±0.9	SLHBT: 83.3±12.5 ULHBT: 82.3±12.6	SLHBT: 51.0±8.6 ULHBT:49.9±8.4
Ashwini and Venkateshu (2017)[10]	India	87 (39 R, 48 L)	DB	R: 32.49±1.83 L: 31.72±2.03	R: 89.94±6.35 L: 88.88±8.11	R: 8.53±1.56 L: 7.96±1.39	R: 6.48± 1.13 L: 6.14±1.04	-	R: 66.15±13.20 L: 64.37±18.81
Abboud et al. (2010)[7]	USA	75	MRI	-	-	-	5.1	81	47
Srimani et al. (2016)[5]	India	107 (59 R, 48 L)	DB	R: 30.37±2.12 L: 29.46±2.43	R: 71.59±3.78 L: 70.78±5.04	R: 8.42±0.85 L: 7.7±0.50	R: 4.63±0.38 L: 4.45±0.30	R: 81.41±10.90 L: 79.31±11.32	R: 50.22±5.35 L: 53.83±6.80
Venkatesan et al. (2017)[11]	India	200 (106 R, 94 L)	DB	29.74±2.19	81.8±9.77	8.99±1.51	4.6±1.09	-	56.46±4.32
Cardoso et al. (2023)[12]	Portugal	60	RG	-	-	10.3±2.5	4.1±1.5	80±26	53±15
Tang et al. (2023)[13]	China	126	CT	-	-	12.3±2.1	4.9±1.4	89.8±18.4	40.6±7.9
Song and Kim (2024)[14]	Korea	111	CT	-	-	<55 years old: 11.8±1.7 >55 years old: 10.9±1.6	<55 years old: 4.6±0.7 >55 years old: 4.6±0.8	-	<55 years old: 58.9±11.3 >55 years old: 62.2±10.1
This study (2024)	Turkey	109 (56 R, 53 L)	DB	30.97±2.01	89.70±8.09	10.31±1.51	3.98±0.79	99.85±14.53	42.31±8.25

BGD: bicipital groove depth; **BGL:** bicipital groove length; **BGW:** bicipital groove width; **CT:** computed tomography; **DB:** dry bone; **F:** female; **HL:** humerus length; **L:** left; **M:** male; **MRI:** magnetic resonance image: **MWA:** medial wall angle, **N:** sample size, **OA:** opening angle; **R:** right; **RG:** radiography; **SLHBT:** stable long head of biceps tendon; **ULHBT:** unstable long head of biceps tendon.

In a study of Duran et al.,[15] they detected negative correlation between BGD and OA and positive correlation between BGD and MWA which was accordance with our study. It means that, If BGD increases, OA decreases and MWA increases, this condition results in a deeper and narrower groove. Also, we found positive correlation between the HL and BGL and negative correlation between BGL and BGD. Our findings suggest that individuals who are taller tend to have a groove that is longer and shallower, along with a larger OA, which could lead to a higher risk of subluxation and dislocation of the LHBT.

Moreover, BG serves as a key landmark for guiding retroversion during shoulder prosthesis implantation. In cases of osteoarthritis, the proximal portion of the groove is utilized, while the distal portion is preferred for

fractures. There is considerable variation in the orientation of the groove, so caution is advised regarding the reliance on the bicipital groove as a consistent reference in shoulder replacements for fractures.[21] Angular and morphometric properties of BG was evaluated in our study and we believe that findings of our study will be beneficial in shoulder prosthesis implications for understanding the morphometric properties of BG.

There are certain limitations in this study. One of the primary limitations in this research is the lack of data on the sex and age of the humeri. Therefore, the effects of these parameters on the BG morphometry was not assessed. An additional limitation is that this study was conducted using 109 humeri. In further studies, it is important to analyze the morphometry of the BG on CT or MRI scans using larger sample sizes with patients of known sex and age.

Conclusion

Knowing the morphometric properties of BG is essential for pathologies of LHBT. In our study, we evaluated BG morphometry in detail. The positive correlations were detected between the BGW and BGD, BGW and OA, MWA and BGD, HL and BGL. The negative correlations were detected between the BGL and BGD, OA and BGD, MWA and BGW. No significant differences were detected between the right and left side for measured parameters. We believe our findings are valuable for understanding LHBT pathologies and their relevance to shoulder arthroplasty.

Conflict of Interest

There are no conflict of interest.

Author Contributions

MÜ: Project development, data collection, data analysis, manuscript writing and editing; MY: data collection, data analysis, manuscript writing and editing; AB: data collection, manuscript writing and editing; BEG: data collection, manuscript writing and editing; CGB: data collection, manuscript writing and editing.

Ethics Approval

Ethical approval was obtained from Hacettepe University Health Sciences Research Ethics Committee (30.07.2024, decision number: 2024/13-01).

Funding

No funding was received for this study.

References

1. Wafae N, Santamaría LEA, Vitor L, Pereira LA, Ruiz CR, Wafae GC. Morphometry of the human bicipital groove (sulcus intertubercularis). J Shoulder Elbow Surg 2010;19:65–8.
2. Standring S, editor. Gray's Anatomy. The anatomical basis of clinical practice. 41st ed. London, UK: Elsevier; 2016. p. 804–807.
3. Karmali NK, Modi S. Morphological and morphometric study on bicipital groove of humerus in eastern Indian population. Internatinal Journal of Medical and Health Research 2019;5:25–7.
4. Kumar P, Saha S, Arora G, Aneja PS. Detailed morphometry and morphology of bicipital groove of humerus among North Indian population. Journal of Clinical and Diagnostic Research 2021;15: AC01–AC5.
5. Srimani P, Saha R, Goswami B, Mazumdar S. Morphometric analysis of bicipital groove of humerus with clinical implications: a study in West Bengal. International Journal of Anatomy and Research 2016;4:3009–15.
6. Rajani S, Man S. Review of bicipital groove morphology and its analysis in north Indian population. ISRN Anat 2013;2013: 243780.
7. Abboud JA, Bartolozzi AR, Widmer BJ, DeMola PM. Bicipital groove morphology on MRI has no correlation to intra-articular biceps tendon pathology. J Shoulder Elbow Surg 2010;19:790–4.
8. Hitchcock HH, Bechtol CO. Painful shoulder: observations on the role of the tendon of the long head of the biceps brachii in its causation. J Bone Joint Surg Am 1948;30:263–73.
9. Sethi N, Wright R, Yamaguchi K. Disorders of the long head of the biceps tendon. J Shoulder Elbow Surg 1999;8:644–54.
10. Ashwini N, Venkateshu K. Morphometric analysis of bicipital groove of upper end of humerus in South Indian population. International Journal of Anatomy and Research 2017;5:3870–75.
11. Venkatesan R, Gnanadeepam JC, Rajavel ATS, Eswaran S, Radhakrishnan M, Lakshmanan B, Mathavan H. Morphometry and morphology of the human bicipital groove with its clinical significance. Indian Journal of Basic and Applied Medical Research 2017;6:99–107.
12. Cardoso A, Ferreira J, Viegas R, Amaro P, Gamelas P, Alonso R, Pires L. Radiographic evaluation of the bicipital groove morphology does not predict intraarticular changes in the long head of biceps tendon. Radiología (Engl Ed) 2023;65:S3–9.
13. Tang X, Zhang J, Zhang J, He Y. Correlation between the morphological features of the biceps groove and injuries to the biceps pulley and the long head tendon of the biceps. BMC Musculoskelet Disord 2023;24:377.
14. Song HS, Kim H. Anatomical analysis of bicipital groove and its spur formation using 3D-CT: a retrospective observational study. Life (Basel) 2024;14:1529.
15. Duran S, Çayhan V, Günaydın E. Correlation of the depth, medial wall and opening angle of the bicipital groove and the dimensions of long head of the biceps tendon. Anatomy 2023;17:49–54.
16. Ulucakoy C, Kaptan AY, Yapar A, Orhan O, Ozer M, Kanatli U. The effect of bicipital groove morphology on the stability of the biceps long head tendon. Arch Orthop Trauma Surg 2021;141: 1325–30.
17. Ahovuo J. Radiographic anatomy of the intertubercular groove of the humerus. Eur J Radiol 1985;5:83–6.

18. Pfahler M, Branner S, Refior H. The role of the bicipital groove in tendopathy of the long biceps tendon. J Shoulder Elbow Surg 1999;8:419–24.
19. DePalma AF. Surgical anatomy of the rotator cuff and the natural history of degenerative periarthritis. Surg Clin North Am 1963;43: 1507–20.
20. Smith A. Morphologic classification of the bicipital groove. Proceedings of the Annual Meeting of the American Academy of Orthopaedic Surgeons (AAOS'07) SanDiego, CA, USA, 2007.
21. Balg F, Boulianne M, Boileau P. Bicipital groove orientation: considerations for the retroversion of a prosthesis in fractures of the proximal humerus. J Shoulder Elbow Surg 2006;15:195–8.

ORCID ID:
M. Ülkir 0000-0001-5615-8913; M. Yılmaz 0000-0001-8395-4675;
A. Balcı 0000-0002-6345-1082; B. Erçakmak Güneş 0000-0001-6936-0766;
C. Günenç Beşer: 0000-0002-8230-3974

Correspondence to: Mehmet Ülkir, MD, PhD
Department of Anatomy, Faculty of Medicine,
Hacettepe University, Ankara, Türkiye
Phone: +90 312 310 71 69
e-mail: mehmet.ulkir@hotmail.com

Conflict of interest statement: No conflicts declared.

 How to cite this article: Ülkir M, Yılmaz M, Balcı A, Erçakmak Güneş B, Günenç Beşer C. Human bicipital groove: a morphometric study on dry humerus. Anatomy 2025;19(1):8–15.

anatomy
http://dergipark.org.tr/en/pub/anatomy
An International Journal of Experimental and Clinical Anatomy

Original Article

http://dergipark.org.tr/en/pub/anatomy
Received: January 14, 2025; Accepted: April 9, 2025
doi:10.2399/ana.25.1619768

Anthropometric measurements of human faces generated by artificial intelligence

Ziya Yıldız[1], **Ahmet Ali Süzen**[2], **Osman Ceylan**[3]

[1]*Department of Therapy and Rehabilitation, Isparta University of Applied Sciences, Isparta, Türkiye*
[2]*Department of Computer Engineering, Isparta University of Applied Sciences, Isparta, Türkiye*
[3]*Department of Computer Technologies, Isparta University of Applied Sciences, Isparta, Türkiye*

Abstract

Objectives: Artificial intelligence (AI) systems are capable of detecting human faces from two-dimensional images and generating highly realistic facial representations that do not correspond to any real individuals. This study aims to quantitatively assess the anthropometric features of AI-generated virtual faces and compare these measurements with established facial anthropometric data across different human populations.

Methods: A total of 150 virtual faces (75 male, 75 female) were generated by an artificial intelligence system trained on the CelebAMask-HQ dataset, which consists of 30,000 high-resolution facial images of celebrities. Anthropometric distances between defined facial landmarks were measured using custom-developed software. The obtained measurements were statistically compared with anthropometric reference data from various populations reported in the literature. Statistical analysis was performed using the One-Sample t-test to assess deviations from known population means, and the Chi-square Goodness-of-Fit (χ^2) test to evaluate distribution conformity. A significance level of $p<0.05$ was used for all analyses.

Results: Several periorbital measurements of the AI-generated male virtual faces demonstrated greater similarity to anthropometric data from East Asian populations. Additionally, morphologic face height and nasal height values in male virtual faces were most closely aligned with those reported for Thai, Azeri, and Bulgarian populations. In female virtual faces, the circumference around the eyes was found to be comparable to that of Turkish females. Although certain facial features—particularly nasal and ocular parameters—showed resemblance to those of specific ethnic groups, the overall facial composition of both male and female virtual faces did not consistently correspond to any single racial or ethnic population.

Conclusion: AI-generated virtual faces offer a novel and efficient alternative for establishing standardized anthropometric datasets representative of various ethnic groups. Instead of collecting data from large populations, artificial intelligence can generate virtual facial models based on existing datasets, from which reliable anthropometric measurements can be obtained. These virtual datasets can enhance diversity representation while minimizing racial bias and ethical concerns. Consequently, the anthropometric data derived from AI-generated faces may serve as a standardized reference across populations, supporting applications in forensic science, aesthetic surgery, ergonomics, and facial recognition technologies.

Keywords: aesthetic plastic surgery; artificial intelligence in health; facial anthropometry; generative adversarial networks; photogrammetry

Anatomy 2025;19(1):16–23

Introduction

Artificial intelligence (AI) refers to computational systems designed to mimic human intelligence and enhance their performance through data-driven learning processes.[1] These systems encompass a wide range of capabilities, including behavioral simulation, numerical reasoning, motion analysis, logical deduction, and sound recognition.[2] Subfields of AI, such as machine learning (ML) and deep learning (DL), form the technological backbone of numerous modern applications across various domains.[3] Among these domains, healthcare has emerged as one of the most impactful areas for AI integration.[4] The field is characterized by vast and complex datasets, including patient records, surgical procedures, clinical errors, diagnostic information, and rare disease registries.[5] Leveraging these data sources, AI-driven

systems support clinicians in decision-making processes related to diagnosis, treatment planning, drug discovery, and surgical precision.[6] Furthermore, the integration of AI technologies is projected to enhance the efficiency and cost-effectiveness of healthcare delivery, leading to significant systemic savings.[7]

The human face is a complex anatomical region composed of both hard and soft tissues, and it plays a critical role in individual recognition, emotional expression, and interaction with the external environment.[8,9] Facial morphology varies significantly among individuals based on factors such as sex, age, and ethnic background.

Anthropometry is the scientific discipline concerned with the measurement and proportion of the human body.[10] In facial anthropometry, specific anatomical landmarks are used to measure distances, angles, and proportions that define facial structure.[11] To ensure consistency and reproducibility across studies and clinical applications, internationally recognized reference points and standardized protocols have been established.[12–14] These standardized facial measurements are widely used in clinical disciplines including plastic and reconstructive surgery, orthodontics, craniofacial surgery, and forensic science. They are also applied in the evaluation and treatment of conditions such as cleft lip and palate, and in artistic anatomy.[12,15,16] In plastic surgery, especially aesthetic procedures, knowledge of normal facial proportions is essential for restoring anatomical harmony and achieving desirable cosmetic outcomes. Surgeons frequently reference ethnic and racial characteristics when planning procedures, often using broad categories such as Caucasian, African, or Asian, even though these classifications are not anatomically exhaustive.[17] Facial anthropometric data can serve as a foundation for creating reference models or "average faces" for specific populations, thereby informing surgical planning, enhancing symmetry, and maintaining cultural sensitivity in aesthetic procedures.

Facial morphology often exhibits notable differences across races and ethnicities; however, significant variation can also be observed within individuals of the same ethnic group residing in different geographical regions.[17,18] Understanding these variations is essential for fields such as plastic surgery, forensic science, and facial recognition technologies. This study presents a quantitative evaluation of anthropometric facial data obtained from virtual facial models generated by an AI-based web platform. Using standardized horizontal and vertical reference points from the anterior facial view, a dataset of anthropometric measurements was created. These measurements were then systematically compared with published normative data representing various racial and ethnic groups. The primary aim of the study is to investigate whether the facial anthropometric parameters of AI-generated virtual faces resemble any specific racial group or present a composite that does not correspond to any one ethnicity. The central hypothesis posits that the facial metrics of AI-generated models do not fully align with the facial characteristics of any single racial or ethnic group. This approach may provide new insights into the potential of AI in generating representative or hybrid facial morphologies that transcend traditional racial classifications.

Materials and Methods

The dataset required for this study was obtained from a web-based platform developed by NVIDIA researchers, known as "thispersondoesnotexist".[19] This platform utilizes a type of deep learning algorithm known as Generative Adversarial Networks (GANs) to generate high-resolution, photorealistic images of non-existent human faces. Specifically, the GAN model was trained using the CelebAMask-HQ dataset, which comprises 30,000 high-quality facial images of celebrities. Following model training, the system can generate synthetic facial images at a resolution of 1024 × 1024 pixels with each iteration. These AI-generated facial images are entirely virtual and do not correspond to any real individual, thus providing an unbiased and ethically sound dataset for anthropometric analysis. The use of GAN-generated facial imagery allows for the creation of large, standardized sample sets that are free from personal identification concerns and racial bias inherent in real-world data collection.

A custom software tool was developed using the C# programming language within the Visual Studio 2019 integrated development environment to perform precise anthropometric measurements on the AI-generated facial images. The application was designed to calculate the linear distance between any two manually selected reference points on the uploaded images. As illustrated in **Figure 1**, the measurement interface allows for user-defined selection of anthropometric landmarks, after which the pixel-based distance is computed and recorded. Each virtual face image in the dataset was individually uploaded to the software, and measurements were taken consistently by the same observer to ensure methodological standardization and reduce inter-observer variability. The resulting data from each measurement session were automatically exported and stored in Microsoft Excel file format, allowing for structured data management and subsequent statistical analysis.

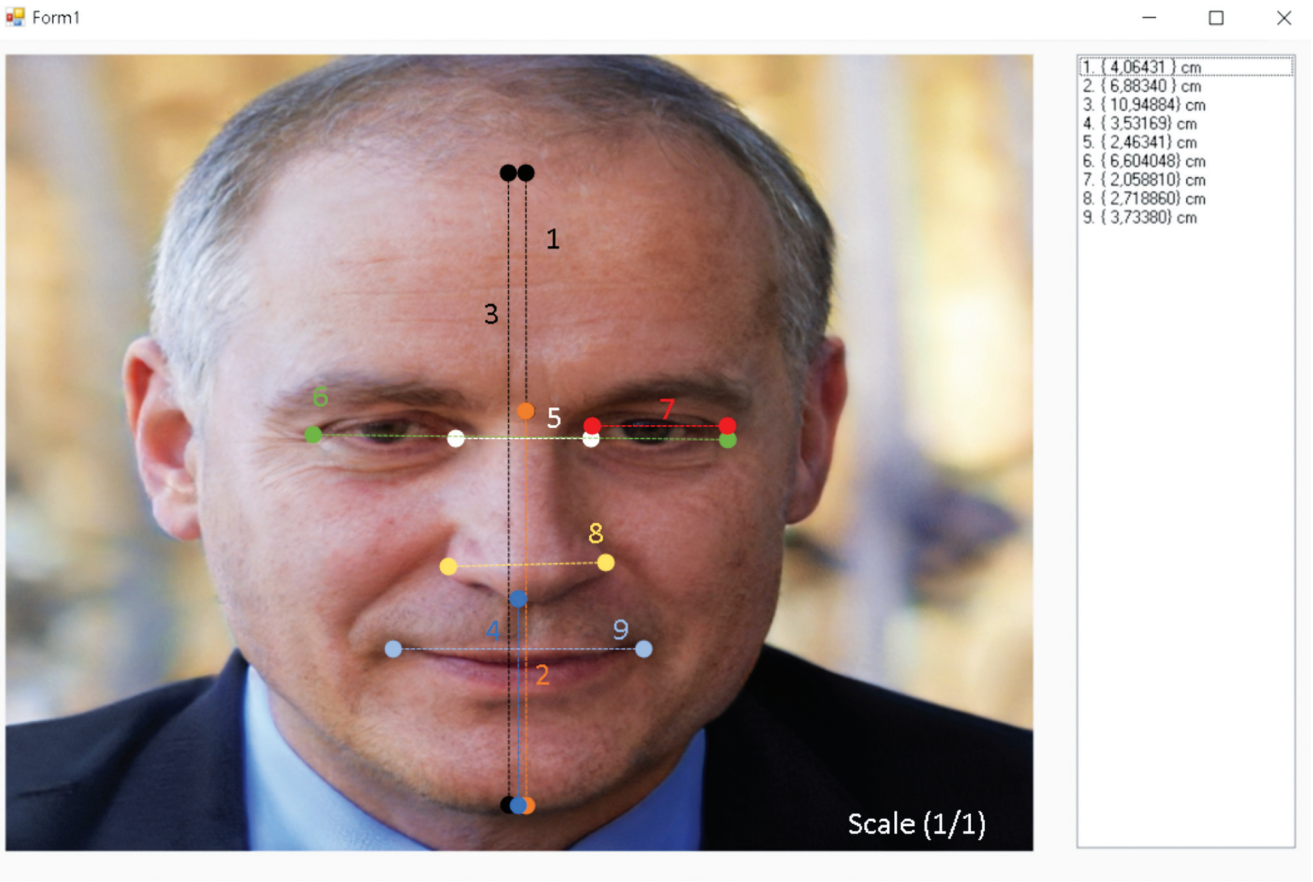

Figure 1. A sample analysis from the measurement software.

The dataset in this study was composed of non-realistic, artificially generated facial images obtained from the website "thispersondoesnotexist.com," which uses a Generative Adversarial Network (GAN) trained on a large-scale real image dataset (CelebAMask-HQ) to produce highly realistic, novel facial images.[19] Since each image generated by this platform is unique and disappears upon refresh, the number of images used in the study was carefully determined. A total of 150 virtual faces (75 male and 75 female) were selected based on predefined inclusion and exclusion criteria. The images selected did not represent any specific race or ethnic group, as the training data were drawn from a diverse population. Faces with overt emotional expressions (e.g., laughing, frowning, or grinning), those resembling children, or those with dark skin tones were excluded to maintain homogeneity in adult facial morphology and minimize potential measurement bias. As the images did not represent real individuals, ethical approval or informed consent was not required.

Each selected image was downloaded at full resolution and stored in a secure zip file archive. Since virtual faces have no medical background or variability due to physiological factors, they served as stable models for anthropometric analysis. The artificial intelligence system generates facial proportions at a 1:1 scale, simulating realistic human dimensions.

Standard anthropometric reference points were defined based on established literature (**Table 1**)[17–20] and 12 linear and ratio-based measurements were conducted between these points (**Table 2**). The measurement process was performed using custom-developed software, as previously described, which allowed researchers to mark two points on the image to calculate the real-world distance in millimeters. To reduce individual measurement bias, three independent researchers performed all measurements, and the mean values of their recordings were used in the final dataset. The anthropometric landmarks were applied uniformly to each image (**Figure 2**), ensuring methodological consistency throughout the analysis.

For each visual dataset, the average, minimum, and maximum values, as well as the standard deviation (SD),

Table 1
Reference points of the face.[17-20]

Anthopometric point	
Trichion (tr)	The point on the hairline in the midline of the forehead
Nasion (n)	The point in the midline of both the nasal root and the nasofrontal suture
Gnathion (gn)	The lowest median landmark on the lower border of the mandible
Subnasale (sn)	The midpoint of the columella base at the apex of the angle where the lower border of the nasal septum and the surface of the upper lip meet
Endocanthion (en)	The point at the inner commissure of the eye fissure.
Exocanthion (ex)	The point at the outer commissure of the eye fissure
Alare (al)	The most lateral point on each alar contour
Cheilion (ch)	The point located at each labial commissure

Table 2
Measurment points.[17-21]

Abbreviation	Description
tr-n	the extended forehead height
tr-gn	the physiognomical face height
n-gn	the morphologic face height
sn-gn	the lower face height
en-en	the intercanthal distance
ex-en	the palpebral fissure length
ex-ex	the biocular diameter
n-sn	the nose height
al-al	the nose width
ch-ch	the mouth width
en-en*100/ex-ex	canthal index
en-en*100/al-al	intercanthal–nasal width

were calculated separately for male and female virtual faces. The average anthropometric values from various racial groups documented in the literature[17,22–24] were also recorded for comparison. To assess the differences between the virtual faces and these established racial averages, a one sample T-test was performed using IBM SPSS Statistics Version 21 (Chicago, IL, USA). A p-value greater than 0.05 indicated no significant difference, suggesting that the anthropometric data of virtual faces were similar to those of the various racial groups.

In addition to this, the male and female data were analyzed separately and grouped according to their standard deviation (SD) relative to the North American White Young (NAW) data. The first group consisted of individuals whose measurements were within ±1 SD of the NAW mean, serving as the observed group. The second group included individuals with measurements greater than +1 SD, while the third group contained those whose measurements were smaller than -1 SD. These groups were considered the expected groups. A chi-square test was then conducted to compare the observed and expected group distributions. A p-value greater than 0.05 indicated no significant difference between the expected and observed groups, suggesting that the virtual faces did not significantly differ from the racial categories represented in the literature.

Results

The average data for anthropometric measurements of races was taken from a 2005 study by Farkas et al.[23] It has also been compared with anthropometric data from Evereklioğlu et al.,[24] Farkas et al.[23] and Yang et al.[25]

The descriptive statistical values of 75 artificial male faces are given in **Table 3**. With data from Farkas et al.,[23] n-gn data on artificial male faces showed similarities with NAW (p=0.45), Azeri (p=0.45), Bulgarian (p=0.15), Croatian (p=0.1), Greek (p=0.19), Hungarian (p=0.19), Vietnamese (p=0.55), Zulu (p=0.12) males. The

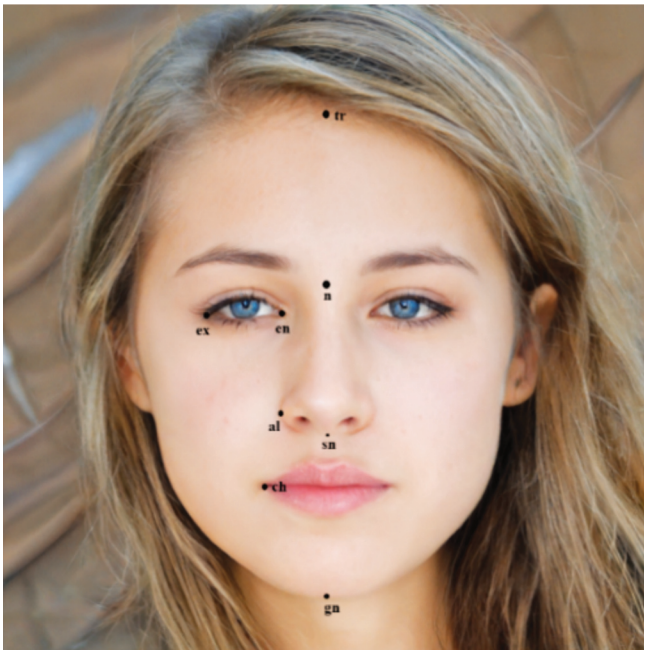

Figure 2. Showing the measurement points of the virtual face.

Table 3
Average, standard deviation, maximum and minimum values of male virtual faces.

Measurements (mm)	Min/Max	Mean±SD	SR	p-value
tr-n	5.69/9.58	8.09±0.87	noSR	<0.001
tr-gn	18.19/22.33	20.16±1.1	noSR	<0.001
n-gn	11.07/12.90	12.08±0.54	NAW	0.45
			Azeri	0.45
			Bulgarian	0.15
			Croatian	0.1
			Greek	0.19
			Hungarian	0.19
			Vietnamese	0.55
			Zulu	0.12
sn-gn	6.18/7.57	6.83±0.4	Azeri	0.16
			Bulgarian	0.16
			German	0.36
			Polish	0.62
en-en	3.30/4.11	3.70±0.25	Thai	0.55
			Japanese	0.11
			Zulu	0.08
ex-en	2.44/3.28	2.89±0.18	Czech	0.79
			Vietnamese	0.47
ex-ex	8.81/9.81	9.23±0.23	Croatian	0.59
			Angola	0.2
n-sn	4.49/5.98	5.13±0.32	German	0.09
			Russian	0.35
			Thai	0.68
			AfrAm	0.14
al-al	3.58/4.50	4.12±0.25	Thai	0.15
ch-ch	4.90/6.73	5.64±0.45	Zulu	0.27
			Hungarian	0.28
canthal indeks	34.45/46.69	40.15±3.4	noSR	<0.001
intercanthal–nasal width	75.15/102.52	90.03±7.05	noSR	<0.001

AfrAm: African American; **mm:** millimeter; **NAW:** North American white young; **noSR:** no similar data on races; **SD:** standart deviation; **SR:** similar data with races.

sn-gn data was similar in Azeri (p=0.16), Bulgarian (p=0.16), German (p=0.36), Polish (p=0.62) males. The en-en data is similar to Thai (p=0.55), Japanese (p=0.11) and Zulu (p=0.08) males. ex-en data; Czech (p=0.79) and Vietnamese (p=0.47), ex-ex data; Croatian (p=0.59) and Angola (p=0.2), n-sn data; show similarities with German (p=0.09), Russian (p=0.35), Thai (p=0.68) and African American (p=0.14) male. al-al data; Thai (p=0.15), ch-ch data are similar to Zulu (p=0.27), Hungarian (p=0.28) males (p>0.05). There was a significant difference between the generated groups with data of tr-n (p=0.000003) and n-GN (p= 0.0031) in the chi-square compatibility test. No significant differences were obtained between the other groups.

The descriptive statistical values of 75 virtual female faces are given in **Table 4**. With the data of Farkas et al.,[23] the n-gn data on artificial female faces showed similarities with Greek (p=0.07), Portuguese (p=0.18) and Turkish (p=0.07) female.[22] sn-gn data; NAW (p=0.03), Czech (p=0.92) and Iranian (p=0.77), ex-en data show similarities in Turkish (p=0.12) female. ex-ex data are similar to Portuguese (p=0.26), Turkish (p=0.21) and Japanese (p=0.36), n-sn data; German (p=0.33), Polish

Table 4
Average, standard deviation, maximum and minimum values of female virtual faces.

Measurements (mm)	Min/Max	Mean±SD	SR	p-value
tr-n	6.38/8.49	7.50±0.51	noSR	<0.001
tr-gn	19.08/20.60	19.28±0.41	noSR	<0.001
n-gn	10.72/12.70	11.74±0.49	Greek Portuguese Turkish	0.07 0.18 0.07
sn-gn	5.51/7.59	6.60±0.46	NAW Czech Iranian	0.03 0.92 0.77
en-en	3.23/4.29	3.83±0.19		
ex-en	2.62/3.47	2.94±0.2	Turkish	0.12
ex-ex	8.76/9.96	9.35±0.25	Portuguese Turkish Japanese	0.26 0.21 0.36
n-sn	4.36/5.66	5.10±0.31	German Polish Singapore Vietnamese	0.33 0.68 0.076 0.076
al-al	3.35/4.37	3.83±0.28	Zulu	0.24
ch-ch	4.17/6.71	5.33±0.55	Angolan and AfrAm	0.46 0.72
canthal indeks	32.73/47.47	40.99±2.68	noSR	<0.001
intercanthal–nasal width	82.17/114.18	100.27±8.26	noSR	<0.001

AfrAm: African American; **mm:** millimeter; **NAW:** North American white young; **noSR:** no similar data on races; **SD:** standart deviation; **SR:** similar data with races.

(p=0.68), Singapore (p=0.076), and Vietnamese (p=0.076) female. al-al data Zulu (p=0.24), ch-ch data; similar to Angolan (p=0.46) and African American (p=0.72) female (p>0.05). There was no significant difference in the chi-square compatibility test among the groups created.

Discussion

People distinguish other people from their faces and eyes.[22] The 2-D pictures are invaluable for facial surgeries, anthropology, delinquency and recognition of the individual. It can also provide research ease for forensic reconstructions.[17] The data obtained from these photographs are logged a system and provide a diagnosis of different sex and ethnic groups based on their face size. Artificial intelligence models are able to generate new faces by processing human faces in their substructures using image processing. These faces are very similar to real human faces.[18] In his work in 2019, Yang et al.[17] suggested that the face reference anthropometric ratios of one ethnic group were unsuitable for other groups of different ethnicities Artificial intelligence can be re-taught with a large number of 2D photographs of different ethnicities or of the same ethnicity.

In this study, 12 measurement data were obtained to calculate the anthropometric data of artificial faces. In the data obtained, some measurements of male and female showed similarities with races. It has been concluded that virtual faces do not seem a particular race, with all features. This dissimilarity suggested that data from virtual faces could be used in surgeries without racial discrimination.

Farkas et al.[23] investigated craniofacial similarities between different populations with anthropometric parameters of NAW male. They reported that certain ethnic groups exhibited significant anthropometric con-

vergence with NAW: Indian, Vietnamese, Thai, and Turkish male with consistent en-en distances; Thai, Vietnamese, Angolan, and Tongan male with parallel ex-ex distances; and Thai, Japanese, and African American male with parallel en-ex measurements. Farkas et al.[23] accepted values below $p<0.001$ representing the strictest threshold for anthropometric comparisons to determine statistical significance. We expected that the virtual data would not exactly match the data obtained from real human populations, as the virtual face generation site that formed the methodology of our study claimed that these faces were not real faces. Nevertheless, the similarity with some races in some anthropometric distances was detected. We believe this is due to the limitations of the training datasets used to train the artificial intelligence. The training data may have been limited because the dataset used was obtained from the faces of famous people who have general facial assumptions and are considered relatively beautiful. Evereklioğlu et al.[24] gave average distance values for en-en and en-ex data of Turks. When these data were compared with artificial intelligence face data, a significant difference was found between the averages. Yang et al.[17] gave canthal index and intercanthal-nasal mean data in Chinese. A significant difference was found when artificial intelligence faces were compared with these data. This shows that Turkish and Chinese face data and artificial faces are not similar. This made us think that the website from which we obtained the data in our study did not include the facial data of Turkish and Chinese celebrities while obtaining the data.

Although the virtual faces did not generally resemble the anthropometric facial data of a particular race, they showed some similarities. The measurements of the palpebral fissure length and the intercanthal distance around the eyes of our male virtual faces are more similar to those of the Far Eastern races. Measurements of nose height and width are more similar to those of Thais. The morphological face height and the lower face height are more similar to Azeri and Bulgarians. In female, the palpebral fissure length and the intercanthal distance measurements were similar to those of Turks. Although both sexes are similar to a particular race in the structure of the nose and eyes, artificial faces could not be completely likened to a race. The virtual faces did not represent the full profile of any race, suggesting that they were composed of partial characteristics of more than one group.

The main limitations of this study include the underestimation of the effect of the virtual face age factor on anthropometric measurements. Furthermore, the imbalance of ethnic representation in the training dataset of the artificial intelligence model (especially the lack of African and Middle Eastern populations) limited the morphological diversity. Another limitation is that only static facial parameters were analyzed in the study, and dynamic expressions and 3D morphometric variations were not included.

Conclusion

This study revealed that virtual faces generated with artificial intelligence exhibit similarities with the anthropometry characteristics of some ethnic groups in certain facial parameters. For example, eye circumference measurements (en-en, ex-ex) showed convergence with Asian populations, while nose height and facial proportions showed convergence with Eastern European and Western Asian groups. However, it was revealed that the virtual facial anthropometric data generated by artificial intelligence does not accurately reflect the profile of any race. AI algorithms were able to partially capture universal patterns in human facial anthropometry. It also supports the potential for modeling anthropometric relationships between races. AI-based virtual anthropometry data can provide an important basis for creating a race-neutral dataset and using it in multidisciplinary applications (aesthetic surgery prosthesis design, forensic anthropology). Future studies should train AI models with comprehensive datasets encompassing diverse age groups, extensive ethnic diversity, and dynamic facial parameters to enhance the validity of virtual anthropometry in clinical and anthropological applications.

Conflict of Interest

There are no conflict of interest.

Author Contributions

ZY: project development, data collection or management, data analysis, statistical analysis, manuscript writing/editing; AAS: data analysis, statistical analysis; OC: statistical analysis, manuscript writing/editing.

Ethics Approval

As the images did not represent real individuals, ethical approval or informed consent was not required.

Funding

No funding was received for this study.

References

1. Choi HI, Jung SK, Baek SH, Lim WH, Ahn SJ, Yang IH, Kim TW. Artificial intelligent model with neural network machine learning for the diagnosis of orthognathic surgery. J Craniofac Surg 2019;30:1986–9.
2. Lu H, Li Y, Chen M, Kim H, Serikawa S. Brain intelligence: go beyond artificial intelligence. Mobile Networks and Applications 2018;23:368–75.
3. Zhang L, Tan J, Han D, Zhu H. From machine learning to deep learning: progress in machine intelligence for rational drug discovery. Drug Discov Today 2017;22:1680–5.
4. Tan C, Sun F, Kong T, Zhang W, Yang C, Liu C. A survey on deep transfer learning. In International conference on artificial neural networks. Springer, Cham; 2018. pp. 270–9.
5. Dilsizian SE, Siegel EL. Artificial intelligence in medicine and cardiac imaging: harnessing big data and advanced computing to provide personalized medical diagnosis and treatment. Curr Cardiol Rep 2014;16:441.
6. Hamet P, Tremblay J. Artificial intelligence in medicine. Metabolism 2017;69S:36–40.
7. Ramesh AN, Kambhampati C, Monson JR, Drew PJ. Artificial intelligence in medicine. Ann Roy Coll Surg 2004;86:334–8.
8. Vegter F, Hage J. Facial anthropometry in cleft patients: a historical appraisal. Cleft Palate Craniofac J 2001;38:577–81.
9. Sforza C, Ferrario VF. Soft-tissue facial anthropometry in three dimensions: from anatomical landmarks to digital morphology in research, clinics and forensic anthropology. J Anthropol Sc 2006;84: 97–124.
10. Dere F, Oğuz Ö. Artistik anatomi. Adana: Nobel Tıp Kitabevi;1996. p. 110–4.
11. Yaşlı H, Bulut Ö. Morfolojik ve antropometrik yöntemlerin yüz karşılaştırma işlemlerinde uygulanması. Adli Bilimler Dergisi 2008; 7:7–16.
12. He ZJ, Jian XC, Wu XS, Gao X, Zhou SH, Zhong XH. Anthropometric measurement and analysis of the external nasal soft tissue in 119 young Han Chinese adults. J Craniofac Surg 2009;20:1347–51.
13. Husein OF, Sepehr A, Garg R, Sina-Khadiv M, Gattu S, Waltzman J, Edward CWu, Mason Shieh, Gregory MH, Galle SE. Anthropometric and aesthetic analysis of the Indian American woman's face. J Plast Reconstr Aesthet Surg 2010;63:1825–31.
14. Mishima K, Mori Y, Yamada T, Sugahara T. Anthropometric analysis of the nose in the Japanese. Cells Tissues Organs 2002; 170:198–206.
15. Gulsen A, Candan O, Aslan BI, Uner O, Yavuzer R. The relationship between craniofacial structures and the nose in Anatolian Turkish adults: a cephalometric evaluation. Am J Orthod Dentofacial Orthop 2006;130:131.e15–25.
16. Dalal AB, Phadke SR. Morphometric analysis of face in dysmorphology. Comput Methods Programs Biomed 2007;85:165–72.
17. Yang YH, Wang B, Ding Y, Shi YW, Wang XG. Facial anthropometric proportion of Chinese Han nationality. J Craniofac Surg 2019;30:1601–4.
18. Leong SC, Eccles R. Race and ethnicity in nasal plastic surgery: a need for science. Facial Plast Surg 2010;26:63–8.
19. This Person Does Not Exist Website. [Internet]. [Retrieved on January 01, 2020]. Available from: https://www.thispersondoesnotexist.com/
20. Karras T, Aila T, Laine S, Lehtinen J. Progressive growing of GANs for improved quality, stability, and variation. Neural and Evolutionary Computing 2017;arXiv:1710.10196v3.
21. Dawei W, Guozheng Q, Mingli Z, Farkas LG. Differences in horizontal, neoclassical facial canons in Chinese (Han) and North American Caucasian populations. Aesthetic Plast Surg 1997;21:265–29.
22. Kim YC, Kwon JG, Kim SC, Huh CH, Kim HJ, Oh TS, Koh KS, Choi JW, Jeong WS. Comparison of periorbital anthropometry between beauty pageant contestants and ordinary young women with Korean ethnicity: a three-dimensional photogrammetric analysis. Aesthetic Plast Surg 2018;42:479–90.
23. Farkas LG, Katic MJ, Forrest CR, Alt KW, Bagic I, Baltadjiev G, Cunha E, Cvicelová M, Davies S, Erasmus I, Gillett-Netting R, Hajnis K, Kemkes-Grottenthaler A, Khomyakova I, Kumi A, Kgamphe JS, Kayo-daigo N, Le T, Malinowski A, Negasheva M, Manolis S, Ogetürk M, Parvizrad R, Rösing F, Sahu P, Sforza C, Sivkov S, Sultanova N, Tomazo-Ravnik T, Tóth G, Uzun A, Yahia E. International anthropometric study of facial morphology in various ethnic groups/races. J Craniofac Surg 2005;16:615–46.
24. Everekliogluc C, Doganay S, Er H, Gunduz A, Tercan M, Balat A, Cumurcu T. Craniofacial antropometry in a Turkish population. Cleft Palate Craniofac J 2002;39:208–18.
25. Farkas LG, Katic MJ, Forrest CR. Comparison of craniofacial measurements of young adult African-American and North American white males and females. Ann Plast Surg 2007;59:692–8.

ORCID ID:
Z. Yıldız 0000-0001-6961-8202;
A. A. Süzen 0000-0002-5871-1652;
O. Ceylan 0000-0002-6060-0134

Correspondence to: Osman Ceylan, PhD
Department of Computer Technologies,
Isparta University of Applied Sciences, Isparta, Türkiye
Phone: +90 545 747 06 07
e-mail: osmanceylan@isparta.edu.tr

Conflict of interest statement: No conflicts declared.

 How to cite this article: Yıldız Z, Süzen AA, Ceylan O. Anthropometric measurements of human faces generated by artificial intelligence. Anatomy 2025;19(1):16–23.

anatomy
http://dergipark.org.tr/en/pub/anatomy
An International Journal of Experimental and Clinical Anatomy

Original Article

http://dergipark.org.tr/en/pub/anatomy
Received: November 21, 2024; Accepted: March 4, 2025
doi:10.2399/ana.25.1588809

Radiological evaluation of superior mesenteric artery syndrome: are aortomesenteric angle and distance measurements reliable?

Eren Çamur[1], Berkay Ersöz[2], Bilal Egemen Çifci[2], Mustafa Dağlı[2]

[1]*Department of Radiology, Ministry of Health Ankara 29 Mayıs State Hospital, Ankara, Türkiye*
[2]*Department of Radiology, Ankara Bilkent City Hospital, Health Sciences University, Ankara, Türkiye*

Abstract

Objectives: To evaluate the interobserver and intraobserver consistency of aortomesenteric angle (AMA) and aortomesenteric distance (AMD) measurements in diagnosing superior mesenteric artery syndrome (SMAS), and to assess their reliability as diagnostic parameters.

Methods: This retrospective study analyzed 200 abdominal CT scans of patients (124 females, 76 males; aged 17–42) with a preliminary diagnosis of SMAS between May 2021 and March 2024. AMA and AMD were measured on sagittal and oblique-sagittal images by three radiologists at two different times, independently and blinded to clinical data. Intraobserver and interobserver variability was evaluated using nonparametric statistical tests, with $p<0.05$ considered significant. Diagnostic thresholds were set at 22° for AMA and 8 mm for AMD.

Results: AMA measurements showed significant interobserver and intraobserver variability ($p<0.05$), while AMD measurements were reproducible and consistent ($p>0.05$). Variability in AMA led to diagnostic discrepancies in 9.1–10.4% of cases, compared to only 0.5–1.2% for AMD. These results indicate that AMA is less reliable and prone to user-dependent errors, whereas AMD offers greater diagnostic accuracy.

Conclusion: AMA measurements are influenced by factors such as patient positioning and respiratory phase, contributing to their inconsistency. AMD, in contrast, demonstrates low variability and high reliability, making it a more robust parameter in SMAS diagnosis. The study emphasizes the need to prioritize AMD over AMA in the diagnostic workflow for SMAS. AMD is a consistent and reliable parameter for SMAS diagnosis, while AMA demonstrates significant variability and potential for misdiagnosis.

Keywords: aortomesenteric angle; aortomesenteric distance; computed tomography; reliability; superior mesenteric artery; syndrome

Anatomy 2025;19(1):24–29

Introduction

Superior mesenteric artery syndrome (SMAS), a rare condition, is characterized by the obstruction of bowel transit due to the compression of the third portion of the duodenum. This compression occurs between the superior mesenteric artery, which lies anteriorly, and abdominal aorta or vertebrae, which are situated posteriorly.[1,2] The classic symptoms associated with this condition are often nonspecific and may include nausea, vomiting, abdominal pain, loss of appetite, abdominal distension, and weight loss. Recognizing superior mesenteric artery syndrome is crucial, as it can potentially lead to severe complications such as dehydration, metabolic imbalances, and in rare instances, even death.[3,4]

The diagnosis of SMAS relies on clinical presentation and imaging findings, with upper gastrointestinal contrast studies and computed tomography (CT) being a commonly used diagnostic tool. The characteristic signs

This study was presented as an oral presentation at TURKRAD congress, 12–16 November 2024, Antalya, Türkiye.

are the presence of an abrupt vertical or oblique compression of the duodenum, and decreased aortomesenteric angle (AMA) and distance (AMD).[5] However, interpreting these findings can be subject to interobserver variability. The lack of a standardized measurement technique due to variations especially in AMA and AMD measurements raises the question of how reliable these parameters are.

This study aimed to make interobserver and intraobserver comparisons of AMA and AMD measurements and thus demonstrate the reliability of these measurement parameters.

Materials and Methods

A retrospective analysis was conducted on clinical data and abdominal CT scans of patients aged 17 to 42 years who were prediagnosed with superior mesenteric artery syndrome (SMAS) between May 2021 and March 2024. A total of 242 scans from different patients were reviewed. Thirty-five scans were excluded due to significant bowel motion or respiratory artifacts, and seven were excluded because the superior mesenteric artery and aortic walls could not be clearly visualized on the same axis. Ultimately, 200 scans from 200 unique patients were included in the study. The flowchart of the study is presented in **Figure 1**.

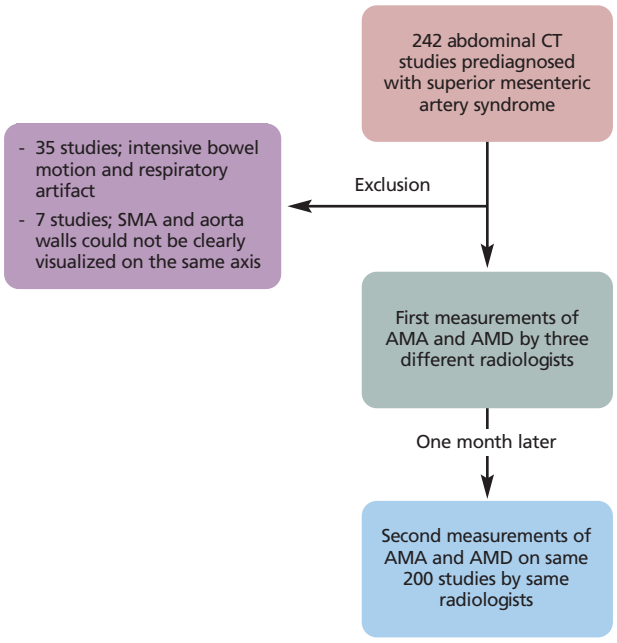

Figure 1. The flowchart of the study.

All CT scans were acquired on a 128-slice CT (GE Revolution EVO, GE Medical Systems, Milwaukee, WI, USA) with the patient in the supine position during inspiration and without an intravenous contrast agent. Image acquisition parameters included a tube voltage of 100 kV, a tube current of 180–300 mA, a spiral step factor of 0.98, a collimation thickness of 0.625 mm, a slice thickness of 1.3 mm and sharp kernel reconstruction with a 512×512–pixel image matrix. For image clarity. Also sagittal, axial, or oblique-sagittal multiplanar reconstruction (MPR) images were obtained to assess the branching configuration of SMA from abdominal aorta.

All images were sent electronically to a workstation (GE Medical Systems, Milwaukee, WI, USA) for evaluation. Images were evaluated blinded to patient information and clinical data by two radiology specialists (BEÇ: 10 years of abdominal radiology experience; EÇ: 7 years of general radiology experience) and one radiology resident (BE: 3 years of radiology residency). Radiologists performed the initial measurements on anonymized images independently and at different times, without knowledge of each other's assessments. Similarly, the order of the anonymized images was shuffled and the same measurements were performed again approximately one month later by all radiologists at different times without each other's knowledge.

The distance between SMA and abdominal aorta was measured as the maximum distance between the anterior margin of abdominal aorta and the posterior aspect of the superior mesenteric artery at the level where the duodenum crosses (**Figure 2**). The angle between these vessels was measured on reformatted sagittal or oblique sagittal images at the same level. To measure the angle, a line was drawn between the root of SMA and an imaginary point

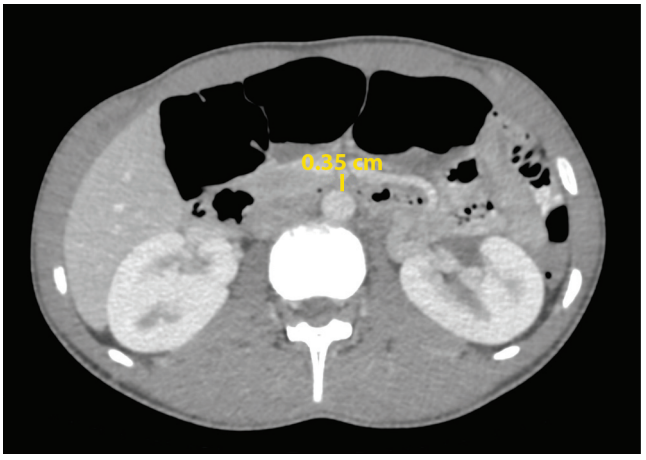

Figure 2. Measurement of aortomesenteric distance (AMD).

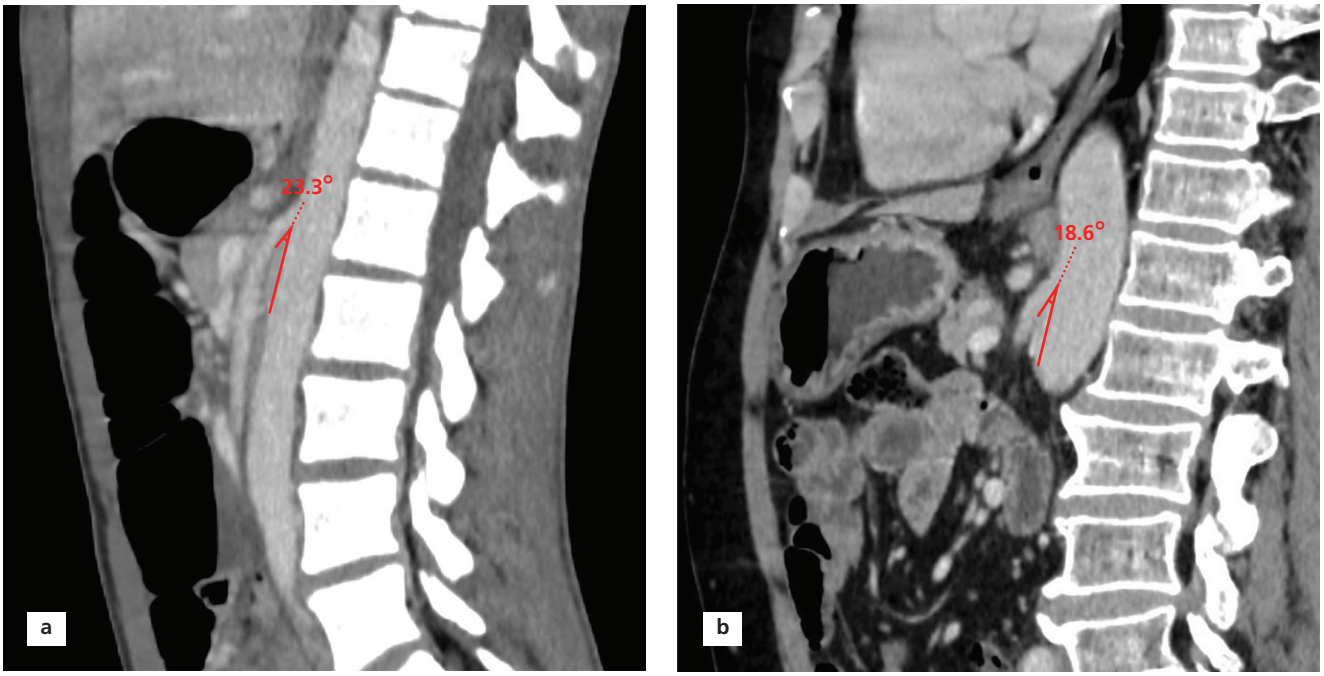

Figure 3a,b. Measurement of aortomesenteric angle (AMA).

on SMA where it begins to descend parallel to the abdominal aorta (**Figures 3a** and **b**). Measurements were taken using electronic calipers, and angles were obtained through manual tracing with automatic degree calculation. Cutoff values for the radiological diagnosis of SMAS were accepted as 22 degrees for AMA and 8 mm for AMD.[6]

Data were analyzed using SPSS version 26 (IBM Corp, Armonk, NY, USA). Descriptive statistics for continuous (quantitative) variables; were expressed as median, standard deviation, minimum, and maximum values, and categorical variables were expressed as numbers (n) and ratio (%). The normality of the variables was assessed using the Kolmogorov–Smirnov and Shapiro–Wilk tests. Since the data did not follow a normal distribution, nonparametric tests were applied. The Kruskal–Wallis test was used for comparisons among three or more dependent groups, while the Wilcoxon test was employed for subgroup analyses. A p-value of ≤0.05 was considered statistically significant, and Bonferroni correction was applied for multiple comparisons.

Results

A total of 200 patients were included in the study, comprising 124 females and 76 males. The descriptive characteristics of the study population are presented in **Table 1**.

There was a significant difference between the first and second AMA measurements of all three radiologists ($p<0.05$), but no significant difference was found in the first and second AMD measurements ($p>0.05$) (**Table 2**). Similarly, an interobserver significant difference was found in the statistical analyses performed for AMA measurements, whereas no interobserver significant dif-

Table 1
Descriptive data of the patients included in the study.

Age	Mean (interval)	26.37 (17–42)
	Median	20
Sex	Female	124 (63.3%)
	Male	76 (36.7%)

Table 2
Intraobserver consistency assessment of AMA and AMD measurements made by radiologists at different times.

	Asymp. Sig. (2-tailed) AMA	Asymp. Sig. (2-tailed) AMD
Radiologist 1	p<0.05	p=0.170
Radiologist 2	p<0.05	p=0.200
Radiologist 3	p=0.002	p=0.350

AMA: aortomesenteric angle; **AMD:** aortomesenteric distance.

ference was found in both measurements performed at different times for AMD measurements (Table 3).

The proportion of patients whose AMA and AMD measurements crossed the diagnostic cut-off values (22° for AMA and 8 mm for AMD) between the first and second assessments is presented in Table 4. While both intraobserver and interobserver variations in AMA measurements showed statistically significant differences at the 22° threshold, no significant variation was observed for AMD at the 8 mm cut-off. These findings indicate that AMA measurements lack reliability for diagnostic use, whereas AMD demonstrates high reproducibility, consistency, and diagnostic reliability.

Table 3
Interobserver consistency assessment of AMA and AMD measurements made by radiologists at different times.

	AMA	AMD
First measurement	p<0.001	p=0.170
Second measurement	p=0.021	p=0.238

AMA: aortomesenteric angle; **AMD:** aortomesenteric distance.

Discussion

SMAS is a rare but significant condition involving the compression of the third part of the duodenum between the superior mesenteric artery and the aorta, which leads to symptoms such as nausea, vomiting, and weight loss.[7,8] Diagnosis can be very challenging most of time.[3,4,9] Santer et al.[10] and Applegate et al.[11] pioneered the description of CT findings in SMAS and advocated dynamic thin-slice CT with sagittal reconstruction as an excellent imaging modality due to its safety, speed, and relatively non-invasive nature. Reduced AMA and AMD measurements are key CT diagnostic criteria for SMAS.[12–14] However, the reliability of these measurements has long been questioned, particularly in relation to interobserver and intraobserver variability. Although ranges for AMA and AMD have been reported in the literature for both the normal population and patients with SMAS ,to the best of our knowledge, there is no study in the literature that evaluates intraobserver and interobserver consistency to determine the reliability of these measurements.[13,15,16] This study is unique in terms of demonstrating intra- and interobserver consistency of these measurements.

The results of this study reveal critical insights into the variability of AMA and AMD measurements among experienced radiologists. AMA showed significant interobserver and intraobserver variability, suggesting it may not be a reliable diagnostic tool for SMAS. A major problem with the AMA is that the measurement varies depending on the patient's position, the tortuous course of the SMA, variations of the angle of exit from the its origin, or changes in respiration. In addition, the need for precise and user-dependent line generation for AMA measurement, where both the aorta and the SMA wall must be parallel, may also contribute to this discrepancy. Studies have also highlighted the technical difficulties of measuring AMA consistently, as it is very difficult to show the origin of the SMA on the same axis as the aorta, even on multiplanar reformatted images, and this is difficult to identify as a technical difficulty in measuring AMA.[17,18]

Conversely, AMD showed minimal variability, both between observers and within the same observer across different time points, making it a more consistent and reliable measure for diagnosing SMAS. The reproducibility of AMD makes it a more reliable parameter for SMAS, particularly when compared to AMA, which has demonstrated significant inconsistencies.

Another important result of our study is that in approximately %9.1–10.4 of the patients, measurement

Table 4
The percentage of patients in whom one radiologist found a different result according to the cut off value and the percentage of patients in whom the same radiologist found a different result in two measurements.

	AMA first and second measurement different results	AMA measurement interobserver different results	AMD first and second measurement different results	AMD measurement interobserver different results
Radiologist 1	9.1%	9.3%	1.1%	1.2%
Radiologist 2	9.7%	8.8%	0.5%	1%
Radiologist 3	10.4%	8.2%	0.9%	1.1%

AMA: aortomesenteric angle; **AMD:** aortomesenteric distance.

results were obtained on different sides of the cut-off value for radiological diagnosis of SMAS for two different AMA measurements performed by the same radiologist at different times. Similarly, for approximately %8.2–9.3 of patients, one radiologist measures different results for AMA measurement from three different radiologists, depending on the cut-off value. Beyond variability, this inconsistency shown by AMA may cause the patient to be misdiagnosed based on radiological evaluations. For AMD, these rates are only between %0.5–1.2 and are relatively acceptable. Therefore, this study underscores the need for more standardized imaging planes and radiological parameters for patients with prediagnosed SMAS to minimize variability in radiological measurements and to contribute to correct diagnosis.

The implications of these findings are significant for the clinical evaluation of patients suspected of having SMAS. Given the variability in AMA measurements, relying completely on this parameter may lead to unnecessary diagnostic errors, potentially affecting patient care. The consistency of AMD makes it a more robust radiological parameter. Clinicians must be careful to incorporate AMD as the primary measurement when evaluating potential SMAS cases, while remaining cautious about the inherent limitations of AMA.

This study has some limitations. The patients included in the study were not patients with a preliminary diagnosis of SMAS, whose diagnosis of SMAS was surgically confirmed. In addition, the patients were compared without subcategorizing them according to their body mass index (BMI). In patients with low BMI, the measurement consistency may be affected since the assessment of AMA and AMD will be more challenging, which is more evident in the measurement of AMA.

Conclusion

In conclusion, while repeated AMD measurements demonstrate clear intra- and interobserver consistency, the reliability of AMA measurements remains questionable. Future large-scale, multi-center studies incorporating both clinical and radiological correlations will be essential to standardize measurement techniques and establish robust diagnostic parameters for SMAS.

Conflict of Interest

The authors declare that there is no conflict of interest and this study was conducted without any commercial or financial relationships that could be construed as a potential conflict of interest.

Author Contributions

EÇ: design, data processing, materials, analysis and /or interpretation, literature review, writing, critical review; BE: data colletion and processing, literature review, writing; BEÇ: conception, data processing, supervision, critical review; MD: materials, analysis and /or interpretation, critical review.

Ethics Approval

The study was approved by Ankara City Hospital, Ethics Committee with approval number TABED-1-24-245.

Funding

No funding was received for this study.

References

1. Mathenge N, Osiro S, Rodriguez II, Salib C, Tubbs RS, Loukas M. Superior mesenteric artery syndrome and its associated gastrointestinal implications. Clin Anat 2014;27:1244–52.
2. Kingham TP, Shen R, Ren C. Laparoscopic treatment of superior mesenteric artery syndrome. JSLS 2004;8:376–9.
3. Mandarry MT, Zhao L, Zhang C, Wei ZQ. A comprehensive review of superior mesenteric artery syndrome. European Surgery 2010;42: 229–36.
4. Caterine S, Patil NS, Takrouri H, Issenman RM, Stein NR, Donnellan J, Yikilmaz A. Understanding the diagnosis of superior mesenteric artery syndrome: analysis of the location of duodenal impression on upper gastrointestinal studies. Pediatr Radiol 2023; 53:2633–41.
5. Lamba R, Tanner DT, Sekhon S, McGahan JP, Corwin MT, Lall CG. Multidetector CT of vascular compression syndromes in the abdomen and pelvis. Radiographics 2014;34:93–115.
6. Unal B, Aktaş A, Kemal G, Bilgili Y, Güliter S, Daphan C, Aydinuraz K. Superior mesenteric artery syndrome: CT and ultrasonography findings. Diagn Interv Radiol 2005;11:90–5.
7. Farina R, Foti PV, Cocuzza G, Costanzo V, Costanzo G, Conti A, Torcitto A, Pennisi M. Wilkie's syndrome. J Ultrasound 2017;20: 339–42.
8. Yale SH, Tekiner H, Yale ES. Historical terminology and superior mesenteric artery syndrome. Int J Surg Case Rep 2020;67:282–3.
9. Forte A, Santarpia L, Venetucci P, Barbato A. Aorto-mesenteric compass syndrome (Wilkie's syndrome) in the differential diagnosis of chronic abdominal pain. BMJ Case Rep 2023;16:e254157.
10. Applegate GR, Cohen AJ. Dynamic CT in superior mesenteric artery syndrome. J Comput Assist Tomogr 1988;12:976–80.
11. Santer R, Young C, Rossi T, Riddlesberger MM. Computed tomography in superior mesenteric artery syndrome. Pediatr Radiol 1991; 21:154–5.
12. Agrawal GA, Johnson PT, Fishman EK. Multidetector row CT of superior mesenteric artery syndrome. J Clin Gastroenterol 2007;41:62–5.

13. Ozkurt H, Cenker MM, Bas N, Erturk SM, Basak M. Measurement of the distance and angle between the aorta and superior mesenteric artery: normal values in different BMI categories. Surg Radiol Anat 2007;29:595–9.
14. Makary MS, Rajan A, Aquino AM, Chamarthi SK. Clinical and radiologic considerations for idiopathic superior mesenteric artery syndrome. Cureus 2017;9:e1822.
15. Arthurs OJ, Mehta U, Set PAK. Nutcracker and SMA syndromes: what is the normal SMA angle in children? Eur J Radiol 2012;81: e854–61.
16. Horton KM, Fishman EK. Volume-rendered 3D CT of the mesenteric vasculature: normal anatomy, anatomic variants, and pathologic conditions. Radiographics 2002;22:161–72.
17. Konen E, Amitai M, Apter S, Garniek A, Gayer G, Nass S, Itzchak Y, Konen E, Amitai M, Apter S, Garniek A, Gayer G, Nass S, Itzchak Y. CT angiography of superior mesenteric artery syndrome. AJR Am J Roentgenol 1998;171:1279–81.
18. Kane KE, Koons AL. The aortomesenteric angle as an aid in diagnosing superior mesenteric artery syndrome. Clin Pract Cases Emerg Med 2017;1:140.

ORCID ID:
E. Çamur 0000-0002-8774-5800;
B. Ersöz 0009-0000-3407-0822;
B. E. Çifci 0000-0002-1664-3241;
M. Dağlı 0000-0001-7794-0349

Correspondence to: Eren Çamur, MD
Department of Radiology, Ministry of Health Ankara 29 Mayıs State Hospital, Ankara, Türkiye
Phone: +90 541 632 84 72
e-mail: eren.camur@outlook.com

Conflict of interest statement: No conflicts declared.

 How to cite this article: Çamur E, Ersöz B, Çifci BE, Dağlı M. Radiological evaluation of superior mesenteric artery syndrome: are aortomesenteric angle and distance measurements reliable? Anatomy 2025;19(1):24–29.

anatomy
http://dergipark.org.tr/en/pub/anatomy
An International Journal of Experimental and Clinical Anatomy

Systematic Review

http://dergipark.org.tr/en/pub/anatomy
Received: November 30, 2024; Accepted: March 3, 2025
doi:10.2399/ana.25.1593366

Morphology, microstructure and biomechanical properties of tendinous cords of heart – a systematic review of cadaveric studies

Raman Ambiga, Suman Verma

Department of Anatomy, Jawaharlal Institute of Postgraduate Medical Education and Research, Dhanvantari Nagar, Puducherry, India

Abstract

Objectives: The rupture of tendinous cords (TC), affects the proper functioning of the atrioventricular (AV) valves and requires replacement by the prosthetic chordae. The morphology and ultrastructure of TC are vital to design prosthesis and to prevent the treatment failure.

Methods: The databases like PubMed, Google Scholar, Science direct and Scopus were searched till June 2024. The keywords used were TC, chordae, TC anatomy, TC morphology, TC morphometry, TC histology, TC ultrastructure, TC blood supply, TC development, TC embryology, TC biomechanical properties, strut chordae, false chordae, basal TC, and subvalvular apparatus. Out of 2545 articles collected, 43 were finally included.

Results: Majority of human studies were on the hearts from formalin-embalmed cadavers. There were more number of studies (28 studies) examining TC of left ventricle, than that of the right (8 studies). The number of chordae from anterior papillary muscle were greater in number than that from the posterior muscle in both the ventricles. In the left ventricle, anterior papillary muscle chordae were longer and broader. Maximum chordae inserted on the rough zone of mitral and tricuspid valves. Human chordae were structurally more rigid than the animal chordae. The arrangement of collagen bundles inside TC was orthogonal in human, but random and irregular in animal tissues.

Conclusion: This review outlines the details on the morphology, ultrastructure, and biomechanical properties of TC which would aid formulate appropriate reparative procedures to prevent postoperative complications and recurrence.

Keywords: chordae tendineae; heart ventricles; morphology; papillary muscle; review; tendinous cords

Anatomy 2025;19(1):30–40

Introduction

The tendinous cords (TC) or chordae tendineae are strong, filamentous collagenous cords connecting atrioventricular (AV) valve leaflets to papillary muscles (PM) of heart.[1,2] They transmit contraction of PM to AV valve, thereby preventing prolapse of leaflets into atria, during ventricular systole. Proper functioning of TC is vital for effective closure of AV valves.[3] In right ventricle (RV), the anterior and posterior leaflets of tricuspid valve (TV) are attached to corresponding PM via TC. Whereas, septal leaflet often directly attaches to ventricular wall via septal chordae.[4] In left ventricle (LV), both anterior and posterior mitral leaflets are attached to PM via TC. The AV valve receives TC with various branching patterns.[2]

Histologically, chordae are composed of collagen and elastic fibers. They possess high degree of elasticity and endurance to perform efficiently.[3] Comparison of the ultrastructure and mechanical properties of human and porcine TC, provides possible replacement of chordal prosthetics by porcine chordae.[5–7] In both, TC configuration is essentially the bundles of collagen fibers forming the core structure. There are, however, differences in the arrangement of collagen tissue at TC and PM juncture where bundles are more organized in human tissue than that in porcine.[6] The junction of chordae with valve may comprise diminished collagen content in its thin outline and the higher load of cardiac muscle contraction on the left side increases the risk of rupture of left ventricle TC. Rupture of TC leads to displacement

of AV valves, resulting in regurgitation of blood into atria, during ventricular systole.[2] Standard treatment for chordal rupture is substitution with expanded polytetrafluoroethylene (ePTFE) sutures. Here, ruptured chordae are replaced by synthetic ones. Bioprosthetic, which may replace mechanical valves, reduce thromboembolic occurrences. Recurrent mitral regurgitation in chordal replacement patients is reported in the literature. The possible causes of treatment failure are placement of less sutures, increased length and inappropriate thickness of suture materials. Thus, understanding of normal measurements, mechanics and microstructure of TC is essential for improved success rate of chordal repair and replacement procedures.[8]

Various authors have described the morphology of TC in human cadaveric and animal hearts. Cadaveric studies mainly focus on gross appearance of chordae which includes origin, insertion, and branching pattern.[2,9–12] Studies providing morphometric data of TC such as their length and thickness, in both ventricles are restricted as only few have examined these parameters.[3,10,13–16] Based on branching pattern and insertion of TC on to valvular leaflet, several classifications have been proposed, that are useful for academic purpose and their clinical applicability needs to be reviewed further.[2,11,12,15,17,18] Existing literature also describes the histology, biomechanical properties, and developmental aspects of TC.[3,6,13,19–22] Most available studies are on TC of LV than RV, as area where TC merge and fix to the valve tissue is thin and more likely to get disrupted on the left due to higher systolic load, thus maximum reparative procedures are done on mitral valve (MV) apparatus. The data on morphology and morphometry of TC of RV are comparatively less in the literature.[2,9,10,12,17,23,24]

Surgeons need comprehensive knowledge on TC morphology and morphometry, to repair AV valves and subvalvular apparatus. Awareness on variations in position and structure of TC is vital to visualize them intraoperatively and during echocardiography.[2] TC could pose difficulties with transcatheter MV prosthesis placement, expansion, and fixation.[24] Data on length and thickness of TC are crucial for surgeons to decide on measurements of chordal prosthetic sutures.[25] Existing studies on histology and biomechanical properties of TC improve the understanding of their structure and function.[3] This review further outlines the morphology, ultrastructure, and biomechanical properties of TC which would aid in designing prosthesis and preventing treatment failure.

Materials and Methods

Literature search was carried out till June 2024. Search engine used was Google and databases were PubMed, Google Scholar, Science direct and Scopus. Plan for search was adapted according to abovementioned databases. Search strategy was formulated as per PRISMA guidelines (**Figure 1**). Keywords used were tendinous cords, chordae tendineae, chordae, tendinous cords/chordae tendineae anatomy, tendinous cords/chordae tendineae morphology, tendinous cords/chordae tendineae morphometry, tendinous cords/chordae tendineae histology, tendinous cords/chordae tendineae ultrastructure, tendinous cords/chordae tendineae blood supply, tendinous cords/chordae tendineae development, tendinous cords/chordae tendineae embryology, biomechanical properties, strut chordae, false chordae, basal chordae, basal, and subvalvular apparatus. Initially 2545 articles were found. Articles without full text, unpublished data, case reports, pathological studies, imaging studies, and publications written in language other than English were not considered. We included studies involving only cadaveric and fresh autopsied hearts which comprised data on normal parameters of heart. Since case reports, pathological studies and imaging studies of heart dealt with abnor-

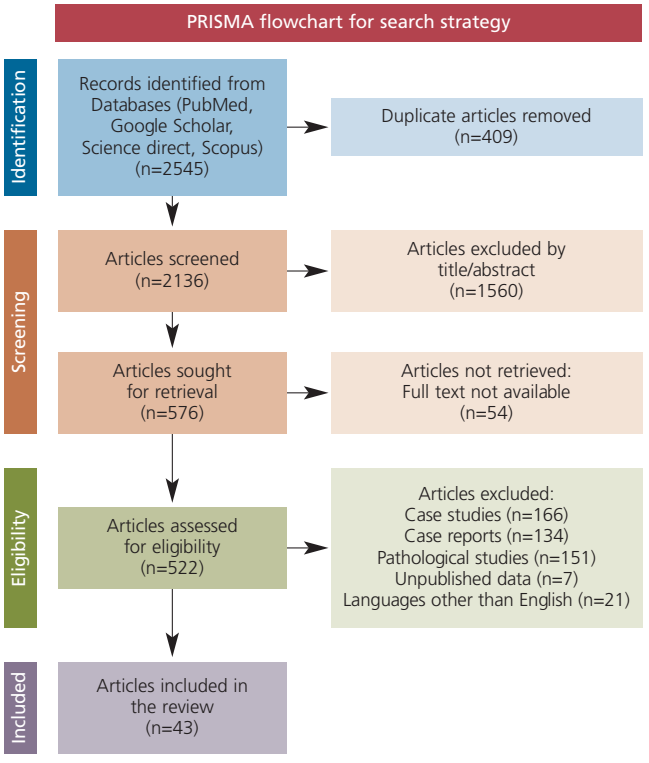

Figure 1. PRISMA flowchart for search strategy.

mal parameters we excluded them. Lastly, 43 studies were included. LV cords were examined in 28 studies, RV in eight studies, four studies examined TC in both ventricles and three did not specify sample source. Based on study material used, 25 studies were human and 14 were animal and four studies compared both. In 25 human studies, 16 were carried out in formalin-embalmed hearts, seven in autopsied specimens and two studies compared both. TC of RV were studied in eight and LV in 17 of human studies. None of the studies observed TC of both ventricles in same sample. Number of studies on each parameter of TC are summarized in **Table 1**. Sample size of the studies included in the review ranged from 8 to 116 in number. A higher sample size is desirable as it is more likely to reflect the population variability, generates ample data for statistical analysis and thus making it appropriate to apply the study outcomes to the general population, however, many factors like availability of specimens, feasibility may limit the sample size. Morphology of TC was systematically reviewed and their features in both ventricles were reexamined. Also, salient ultrastructure and biomechanical properties of TC in human and animals were outlined.

Table 1
Number of studies on various parameters of tendinous cords.

Parameters studied	Human and animal studies	Human studies
A	16	12
B	1	1
C	6	1
D	5	2
A+B	5	5
A+C	1	0
C+D	1	0
A+B+C	1	1
A+B+D	1	0
Development	2	0
Blood supply	2	2
Lymphatics	2	1
Total	43	25

A: morphology (includes origin, insertion, branching pattern); **B:** morphometry (includes length, thickness); **C:** histology (includes connective tissue, neurovasculature); **D:** biomechanical properties.

Results

Development

TC are derived from endothelial cells of endocardial cushions.[26] Chordal development is a programmed cellular and hemodynamic event which occurs between 6 to 13 days of development. PM develop as primitive elevations from ventricular wall. These elevations later bifurcate into thin, web-like folds which are attached to AV valve leaflets. These folds are the primordial chordae. Alternate linear ridges and depressions develop on primordial chordal folds. The depressions later perforate to form individual chordae from linear ridges. Some interchordal connecting tissues can persist.[21] Morphological variations of TC are a result of various aberrations occurring in delamination of ventricular musculature.[23] Muscular chordae are formed because of abnormal delamination of endocardium during development, which leads to persistence of myocardial fibers within the endocardium lined cords.[27] Muscular cords are prone to fibrosis and hence their presence become undesirable.[28]

Number of tendinous cords at origin

TC arise either from PM or directly from ventricular wall and insert onto AV valve.[12] In RV, there are anterior PM (APM), posterior PM (PPM) and septal PM (SPM). PM give origin to one or more cords which insert to TV.[1] Average number of chordae arising from APM is 3.88±0.45, PPM is 3.71±0.31 and SPM is 3.15±0.7.[29] Maximum chordae arise from APM.[11,29] In RV, TC originate from SPM or when SPM are absent, they directly originate from RV septal wall. When only one prominent SPM exists (Lancisi's muscle), its small head with single apex attaches to TC which head to septal and anterior TV leaflets.[30–32] The Lancisi's muscle, other nearby SPM and isolated TC that directly originate from septal wall are together termed as medial papillary complex.[31]

LV comprises APM and PPM (**Table 2**). Each PM gives rise to TC which insert to the MV.[1] Average number of chordae present in LV are 17.31±3.28.[13] Number of cords originating from one PM is 9.09± 4.29 (range: 2–18).[2,33] APM gives rise to more chordae than PPM.[12] Most chordae arise from lateral sides of PM belly (73.22%) and apex gives rise to 19.06%.[10] Chen et al.[13] discovered that more chordae originated from APM (11.23±2.24) than PPM (8.23±2.05). In MV replacement surgeries, preservation of PM and TC improves LV function post-operatively. Hence, clear knowledge about number of chordae at origin becomes important.[2]

Table 2
Number of tendinous cords originating from left ventricular papillary muscle.

Studies	Sample size	Number of cords originating from anterior papillary muscle	Number of cords originating from posterior papillary muscle
Victor et al.[23]	100	4–22	2–18
Kavitha et al.[10]	50	7–16 (10.42)	6–17 (9.72)
Mundra et al.[12]	98	12.45±3.16 6–1 (12)	9.67±3.85 3–22 (10)
Ozog et al.[17]	100	11.5±4 (1–14)	13.1±4.1 (2–13)

Number of tendinous cords at insertion

Each TC after emerging often divides into multiple thin secondary branches and attach to AV valve.[1,3] Each leaflet can receive chordae from one or more PM.[34] Chordae can also insert to adjacent PM or ventricular wall.[2,11] In RV, chordae either arise from PM belly or directly from ventricular septal wall and insert to TV. Average number of chordae inserting to TV are 19.25 and most insert on its rough zone.[11,18] Number of marginal chordae is more in posterior, than anterior and septal leaflets. Anterior leaflet has TC from APM (86.19±11.66%) and PPM (13.09±1.74%). Posterior leaflet receives TC from PPM (85.67±11.48%) and SPM (14.33±1.83%). Septal cusp receives cords from SPM (19.0±2.55%) and APM (80.99±10.85%).[29]

In MV, TC attach to anterior/aortic leaflet and posterior/mural leaflet (**Table 3**). Each leaflet can receive chordae from APM and PPM.[34] From a surgeon's perspective, chordae arising from APM insert to left halves of both MV leaflets and chordae arising from PPM insert to right halves.[35] Ozan et al.[33] noted that 9 to 60 chordae inserted to corresponding half of MV. Leaflet coverage ratio of APM chordae (51.58±3.35) is significantly greater than that of PPM chordae (48.42±3.35).[13] There is no gender difference in number of chordae at the valve.[15] In chordal repair procedures, ePTFE are used to construct artificial chordae.[25,36] A single suture material is successively passed from tip of PM to free margin of AV valve, to create multiple pairs of artificial cords.[25] Thus, a wide information about origin and insertion of TC to AV valve is mandatory.

Branching pattern and types of tendinous cords

Several branching patterns have been documented in literature so far (**Figure 2**). Most common branching pattern of chordae is fan-shaped (100%) and spiral/dichotomous (34.48%).[2,12] Fan-shaped chordae are frequently found at commissures. This fanning out of chordae at commissures is essential to open and close the leaflets during ventricular diastole and systole respectively.[15,23] Least common patterns are irregular/ web-shaped (15.51%) and unbranched chordae (19.82%).[2] There can be anastomosis between adjacent chordae (52%).[12]

TC can originate from different sites on a PM such as its apex, base, or lateral margins.[10] Chordae which arise from apex of PM are termed as apical pillar chordae. Basal

Table 3
Number of tendinous cords inserting to mitral valve leaflets.

Studies	Sample size	Number of cords inserting to anterior valve leaflet	Number of cords inserting to posterior valve leaflet
Victor et al.[23]	100	14–72	12–80
Mundra et al.[12]	98	28–91 (50)	33–84 (56)
Ozog et al.[17]	100	30.3±7.8 (14–55)	40.6±13 (6–40)
Lam et al.[15]	50	9	14

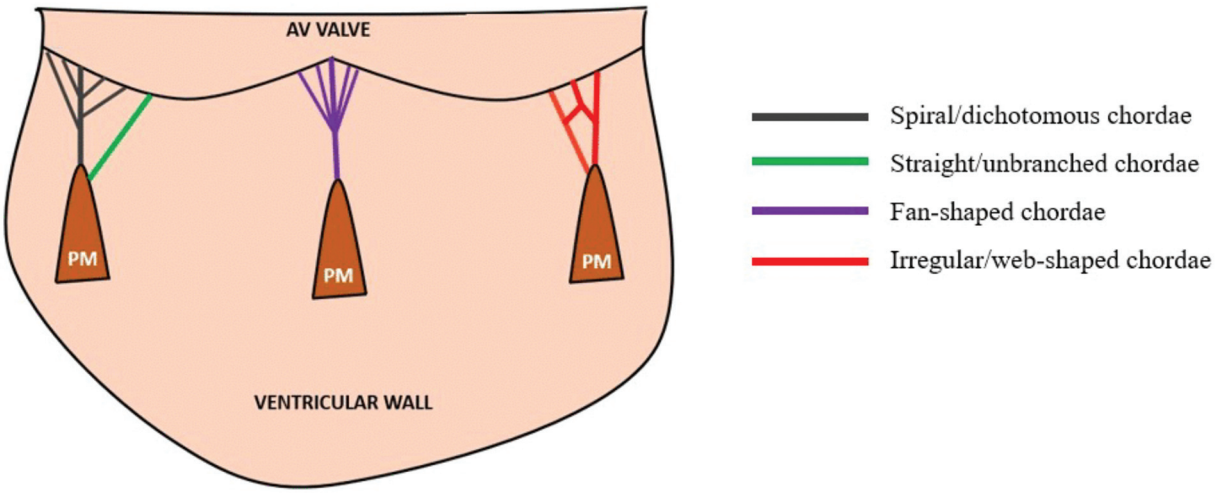

Figure 2. Branching pattern of tendinous cords. **AV:** atrioventricular; **PM:** papillary muscle.

pillar chordae arise from base of PM.[2] On AV valve, chordae can attach to various regions on the leaflet. Ventricular surface of each leaflet has free margin, rough zone, clear zone, and basal zone.[12,17] Clear zone is present between rough and basal zones.[18] Based on their shape and site of insertion onto valve, chordae in RV are mostly divided into five types such as rough zone, fan shaped, free edge, deep and basal. Rough zone chordae are the most observed type and always found in anterior and septal leaflets of TV.[11,18] Fan shaped chordae are found in antero-posterior and postero-septal commissures. Free edge chordae branch before inserting to leaflet margin and form a delta shaped expansion at insertion site.[11]

Gunnal et al.[2] have classified TC of MV into various types based on their attachment to different parts of MV complex. True chordae or cusp-pillar chordae arise from PM and insert into cusp of MV. These are further classified based on their site of insertion onto mitral leaflet as cusp chordae, cleft chordae, and commissural chordae. Commissural chordae play an important role in approximation of two adjacent cusps during ventricular contraction to bring about valve closure. Based on area of insertion and distribution of chordae on the cusps, TC are divided into different types. First order chordae are attached to free margins of valve leaflet and hence they are also called Marginal chordae or Free zone chordae or primary chordae Chordae inserted to free edges of AV valve, prevent marginal prolapse and align their zones of coaptation.[24]

Secondary chordae include cords which insert to ventricular surface of valve leaflet in general. These chordae are attached to rough zone of the valve and hence also termed as rough zone chordae.[2] Rough zone chordae are more common in posterior mitral leaflet (4–14), than anterior (3–10).[9] Among these rough zone chordae few are strong and tough and named as strut chordae, which often insert to cusp with broad aponeurosis.[2] Strut chordae are responsible for normal and non-homogenous movement of anterior mitral leaflet, and their absence can predispose to mitral regurgitation due to abnormal motion of leaflet.[17] Also, strut cords inhibit ballooning and allow leaflet's load to be distributed evenly and responsible for the tunnel-shaped configuration of MV.[15,17,24] Thus, primary or first order chordae are responsible for valve competence and secondary chordae are involved in maintenance of ventricular geometry and function.[37] Atypical rough zone chordae are those which have less than three chords. Lam et al.[15] examined 50 human hearts and found that 17% of rough zone chordae of anterior leaflet and 16% of those of posterior leaflet are atypical. In such regions of valve with atypical chords, adjacent chordae send branches to overcome chordal deficiency.

The chordae which arise from ventricular wall and insert to basal zone of ventricular surface of valve leaflet close to hinge line are termed as basal or tertiary or third order chordae.[15,17] Degandt et al.[5] compared the number of basal chordae of LV in three different species. They found 24.6±4.21 basal chordae in porcine hearts, 19.7±2.90 in ovine hearts, and 18.81±3.54 in human hearts. They also found that basal chordae always inserted to leaflet close to mitral annulus, except in anterior

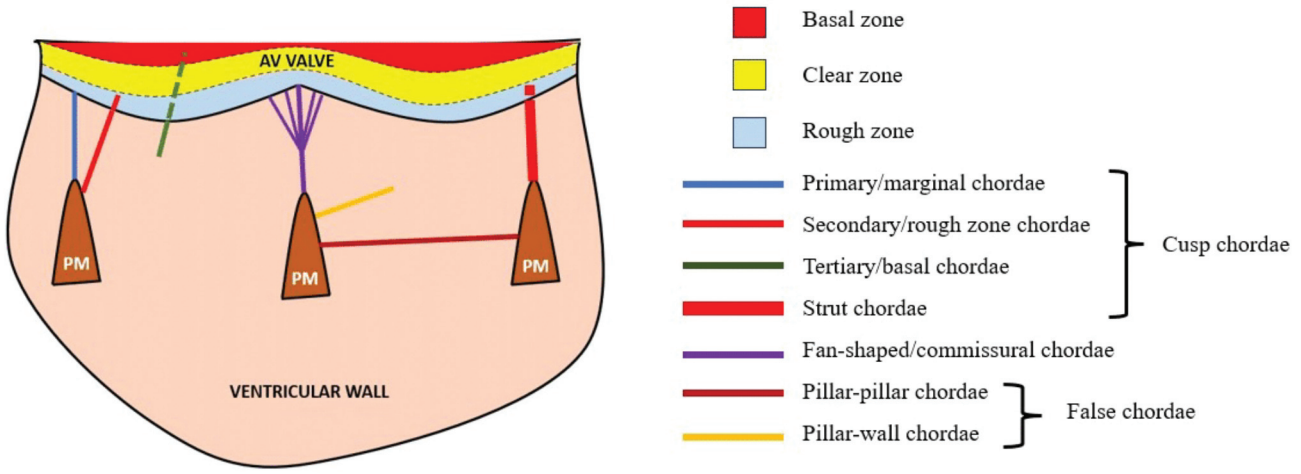

Figure 3. Zones of atrioventricular valve and types of tendinous cords attached. **AV:** atrioventricular; **PM:** papillary muscle.

mitral leaflet where it inserted between smooth and rough zones. Basal cords strengthen the ventricular component of AV junction and aid in maintaining proper ventricular shape.[24] Based on the site of attachment of chordae to leaflet they can also be divided into main, paramedian and paracommissural chordae. Commissural chordae can be anterior or posterior commissural chordae.[16] Nomenclature of cords often used clinically are marginal/primary, rough zone/secondary, basal/tertiary and strut chordae. The zones of AV valve and types of TC attached to them are shown in **Figure 3**.

Based on the gross appearance, TC are termed as tendinous, muscular, and membranous chordae.[2,12] Majority chordae in a ventricle are tendinous (100%) and next common type is muscular (14.65%). Membranous chords are least common type (6.03%).[2] Mundra et al.[12] found muscular chordae or chordae muscularis in 6.1% of heart specimens. The possibility of conduction of cardiac impulses through muscular cords, predisposes the heart for arrhythmias. Muscular cords are also often encountered in cases of hypertrophic cardiomyopathy and premature ventricular contraction.[27]

False chordae

TC which arises from PM or ventricular wall but not inserting to valve leaflet are termed as false chordae (**Figure 3**). False chordae may connect a PM to another PM, to ventricular wall or pass from one point to other on ventricular wall.[11,17,38] Sometimes a muscular band can connect two adjacent PM.[17] False chordae are classified as interpillar chordae (50%) and pillar wall chordae (6.03%). Interpillar chordae connect two PM and pillar wall chordae connect a PM to ventricular wall.[2] Ozog et al.[17] examined the LV and noted average number of false chordae arising from anterior PM as 3.5±2.2 and from posterior PM as 5.4±2.7. thus, a greater number of false chordae arose from posterior PM. Kosinski et al.[38] studied false chordae of RV and classified them into six groups, based on their pattern of attachment. Type I attach a PM to ventricular wall; type II chordae connect two individual segments of PM; type III connect a PM to interventricular septum; type IV connect various PM. False chordae attaching to ventricular wall around the apex are classified as type V. Type VI chordae connect the septomarginal trabeculae to other structures in RV.

False cords protect the ventricles from over dilatation. They are worth to note as they predispose to thromboembolic and arrhythmogenic events. Literature reports that they significantly influence the electromechanical functions of heart.[38] They are also found in LV outflow tract and significantly impair the transcatheter procedures related to aortic valve. Usually, these false chords cannot be visualized using imaging techniques as they are too thin, but thick false cords may lead to diagnostic errors in echocardiography.[17,38]

Morphometry of tendinous cords

In valve replacement and chordal repair surgeries, length of TC plays a vital role in deciding effective postoperative ventricular functioning and thus the outcome.[10] In LV, TC are 15–22 mm long and 0.45–0.66 mm broad on an average.[3,13] The average length of anterior PM chordae is 12.77±4.03 mm and its average breadth is

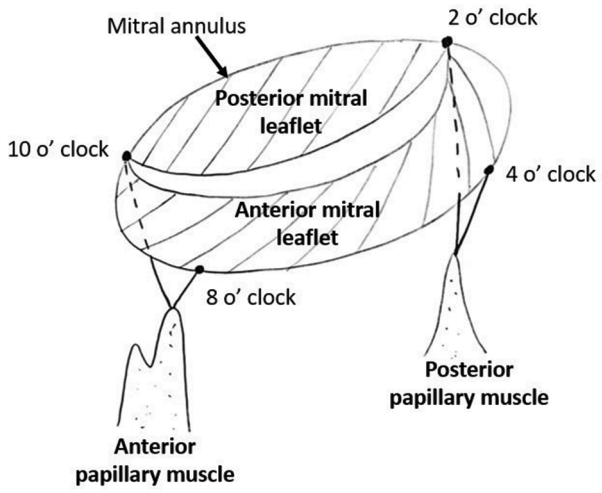

Figure 4. Schematic picture representing measurement of annulo-papillary distance in the mitral valve. The 2-o'clock and 10-o'clock positions are placed at the valvular commissures, and 4-o'clock and 8-o'clock positions are placed at the anterior margin of mitral annulus. For the papillary muscle with two heads, highest point is taken for the measurement.

0.28±0.20 mm. Whereas, on an average posterior PM chordae are 12.33±3.89 cm long and 0.25±0.14 mm broad. Thus, the length and breadth of anterior PM chordae is more than that of posterior PM chordae.[10] Rough zone chordae of anterior mitral leaflet are 1.75±0.25 cm long and 0.84±0.28 mm thick on an average. Similarly, in posterior mitral leaflet, rough zone chordae measure about 1.40±0.08 cm in length and 0.65±0.24 mm in thickness. Length of anterolateral and posteromedial commissural chordae is 1.2±0.31 cm and 1.4±0.40 cm, respectively. Posteromedial commissural chordae are thicker (1.0±0.30 mm) than anterolateral commissural chordae (0.70±0.20 mm).[15]

Kumar et al.[14] compared the length of TC in LV, in both cadaveric and autopsied heart specimens. Chordae attached to anterior mitral leaflet of both specimens were nearly same in length from 1.6 to 1.8 cm. In posterior and commissural mitral leaflets, a slight difference of 2–3 mm was observed, where chordae were longer in autopsied hearts. TC are thinnest near their insertion to MV leaflets. Hence chordal ruptures are most encountered at that site.[24]

Chordae attaching to anterior mitral cusp and MV commissures are lengthier in male, when compared to female but their average thickness is same (0.05 cm). Average length of chordae attaching to anterolateral and posteromedial commissures of MV in male are 1.4 cm and 1.7 cm respectively, whereas in female are 1 cm and 1.3 cm respectively. The average length of TC arising from anterolateral and posteromedial PM to the apex of anterior mitral leaflet in male are 2.1 cm and 2.2 cm respectively, whereas in female are 1.6 cm and 1.8 cm respectively.[16]

Annulo-papillary distance

Annulo-papillary distance is measured between the tip of PM to the annulus of AV valve of corresponding ventricle as shown in **Figure 4**.[14,39] In MV replacement and repair surgeries, annulo-papillary continuity is vital. Hence, a normal annulo-papillary distance should be maintained during repair for a proper resuspension. In LV, the distance from tip of anterior PM to left trigone (10-o'clock position) and to the point between anterior and middle scallops of mural leaflet (8-o'clock position) is 23.5±3.7 mm and 23.2±3.6 mm, respectively. Distance from the tip of posterior PM to right trigone (2-o'clock position) and to the point between middle and posterior scallops of mural leaflet (4-o'clock position) is 23.5±4.0 mm and 23.5±3.9 mm, respectively. Annulo-papillary distances of mitral apparatus are alike in various locations such as 2-, 4-, 8- and 10-o'clock positions. Mitral annular diameter correlates with annulo-papillary distance.[39] Kumar et al.[14] observed that the annulo-papillary distance in LV of both cadaveric and autopsied hearts was equal (2 cm). Kavitha et al.[40] examined 50 human cadaveric hearts and found that the mean vertical annulo-papillary distance was 16.56 mm.

Microstructure and histochemical properties

The human chordae are made of collagen and elastic fibers.[3,10] Scanning electron microscopic and light microscopic examination of human TC shows undulated planar wavy pattern of collagen fibrils arranged in longitudinal bundles along their entire circumference which forms the dense core.[3] These wavy crimp like collagen fibrils are intertwined with each other like a helix, which are heterogenous throughout the length of a chordae.[41] These collagen fibrils are of types I and III.[3,22] In human heart, the bundles of collagen fibrils are wavy when relaxed and become straight when stretched which helps in sustaining the peak stress developed during ventricular contractions.[20] Core connective tissue is loose in proximal parts of chordae, dense regular in middle parts and dense irregular in distal ends where they insert on AV valve.[42] The collagen fibril core is covered by endocardium which is simple squamous epithelium which is

continuous with other regions of heart. A dense layer of elastic fibers is present underneath the endocardium. Immunofluorescence studies show presence of thin irregular and longitudinal tenascin fibers in inner fibroblast coat of elastic fiber layer. Collagen fibrils are wavy in younger population but becomes less wavy or straight in adults.[20] Tenascin concentration in the elastic matrix surrounding collagen core increases with aging.[22] Wavy collagen fibrils elongate and reduce in cross sectional area as age advances in human which can lead to stretching and eventual rupture of chordae.[3]

Gupta et al. studied the histology of chordae in goat hearts and found that in a 32 days old goat embryo, the central core of TC was made up of myocardial cells with reticular fibers surrounded by single layer of endothelial cells. Chordae were mainly collagenous in mid and late prenatal periods. They also found few fibroblast, reticular and elastic fibers, and endothelial cells surrounding collagen core. Histochemical reaction exhibited the activity for existence of polysaccharides, lipids, DNA, and alkaline phosphatase in TC which increased with advancing age.[43] DNA and collagen content was more in anterior and posterior marginal chordae when compared to other types of chordae. Thus, microstructure of TC varies based on their type.[44]

The junctional area between PM and TC is histologically different in human and porcine hearts. In human hearts, collagen bundles are more organized forming a meshwork with fibers disposed in orthogonal angles whereas, in porcine hearts they are arranged randomly.[6] In avian hearts, papillary myotendinous junctions resemble skeletal myotendinous junctions in their protein composition, but their ultrastructure more closely resembles sites of thin filament-membrane association in smooth muscle. They exhibit minimal folding of the junctional membrane, resembling smooth muscle more than the highly folded junctions in humans. Avian papillary myotendinous junctions lack certain proteins found in human cardiac fasciae adherentes, such as alpha-actinin and zeugmatin.[45] Various current therapies available for repair of chordal failure, face issues of recurrence of disease and poor therapy outcome.[8] Thus, extensive data on microstructure of TC is imperative.

Microstructure and neurovascular components

Discrepancies exist among studies on vascularity of human TC and the literature lacks clarity. TC are traditionally referred to as avascular structures.[1,3] Few reports have described presence of blood vessels in them.[44,46,47] Ritchie et al.[44] examined porcine chordae in LV by performing special staining and immunohistochemistry. They observed that the blood vessels from PM, ascended longitudinally and in circumferential manner, encircling the chordae and supplied MV leaflets. Vascularization was observed more often in strut chordae of anterior mitral leaflet. Human fetuses and calves possess blood vessels in free margins of AV valve which anastomose with vessels in PM via chordae.[47] Blood vessels ranging from arterioles to capillaries are observed in human and porcine chordae.[46] In human chordae, lymphatic capillaries are also found within superficial layers of endocardial lining, especially near their origin from PM. There are no lymphatics in deep connective tissue layers of chordae.[48] Ichikawa et al.[49] examined TC in canine hearts and found the presence of lymphatic capillaries in junctional area between TC and PM, under electron microscope.

AV valves contain plexuses of nerves which are acetylcholine esterase positive, and are denser at their free margins where TC attach. These dense nerve plexuses extend into PM via TC attached to them. Such extension of nerve fibers into chordae is detected in porcine and canine hearts. AV valve and TC of rodents like mice, lack acetylcholine esterase positive nerve fibers.[50] In human, only few chordae contain nerve plexuses in them which are adrenergic or cholinergic in nature. The pattern of distribution of nerve fibers in chordae is however similar among human and porcine hearts. Most nerve fibers are located around blood vessels. Presence of nerve fibers in chordae suggests that AV valvular function is under neuronal control, through regulation of TC and PM.[46]

Biomechanical properties

In LV, posterior PM chordae are stiffer than anterior PM chordae due to increased collagen core ratio and dense collagen fibrils.[13] Thicker chordae are more extensible and less stiff when compared to thinner chordae. Thus, strut chordae are most extensible in nature. Marginal chordae are least extensible as they are the thinnest. Thin chordae have lower average fibril diameter, but greater average fibril density when compared to thicker chordae. Hence, they have a greater number of fibril-to-fibril interactions, and therefore a greater modulus.[51] Smaller chordae are less extensible and stiffer when compared with larger chordae. This inverse relationship between size and

Table 4
Comparison of human and animal tendinous cords.

Features	Human chordae	Animal chordae
Collagen bundles	Arranged orthogonally	Randomly arranged (porcine)
Stiffness	Stiffer	Less stiff (avian chordae)
Arrangement of blood vessels	Longitudinal	Longitudinal and circumferential (porcine)
Nerve fibres	Present in few chordae	Present in most chordae (porcine, canine, rodent)

stiffness of chordae maintains even surface of the valve leaflets during closure.[19] Chordae of younger population are more extensible when compared to adults, as collagen fibrils are wavier.[20] Human chordae are significantly stiffer than corresponding ovine chordae.[52] Paskaleva et al.[53] examined the porcine hearts and found that MV chordae were stiffer than TV chordae. They also noted that chordae attaching to septal leaflets were more extensible. It is necessary to know about the biomechanical properties of chordae to formulate different modalities of therapy for chordal repair and to improve treatment outcomes.[8] The features of human and animal TC are summarized in Table 4.

Conclusion

Most true chordae originate from apex of PM and insert onto rough zone of AV valve leaflet. Fan-shaped chordae are often present in commissures of the AV valves. In LV, APM chordae are longer and thicker than PPM chordae. The males have longer chordae compared to the females but there is no difference in TC thickness between two genders. Histologically, human and porcine TC are similar but collagen bundles in human chordae are more regularly arranged leading to higher tensile strength. LV chordae are stiffer than chordae of RV in both human and porcine hearts.

Compared to the related articles in literature, this review has provided the detailed overview of number, morphological types, neurovascular components, development of TC and its biomechanical properties in human and other different species. However, imaging studies and studies involving pathological hearts or symptomatic patients were not included. Meta-analysis could not be done due to limited data about morphology and morphometry of TC in both ventricles.

In future, data on morphometry of chordae from a large sample would help to formulate appropriate reparative procedures. Studies need to further explore the morphology of RV chordae and their insertion to TV, to compare the features of TC in RV and LV. It would aid in prevention of postoperative complications and recurrence. Understanding the ultrastructure and biomechanical properties of human and animal chordae would be useful to produce biological prosthesis for chordal replacement procedures.

Conflict of Interest

No potential conflict of interest relevant to this article was reported.

Author Contributions

SV: protocol development, literature search, search strategy, manuscript editing; RA: protocol development, literature search, search strategy, manuscript writing.

Ethics Approval

No ethical approval was necessary for this systematic review article.

Funding

This research did not receive any specific grant from funding agencies in the public, commercial, or not-for-profit sectors.

References

1. Tunstall R (ed). Thorax. In: Standring S (ed). Gray's anatomy - the anatomical basis of clinical practice. 42nd ed. Edinburgh (Scotland): Elsevier Churchill Livingstone; 2020. p. 1075–84.
2. Gunnal SA, Wabale RN, Farooqui MS. Morphological study of chordae tendinae in human cadaveric hearts. Heart Views 2015;16:1–12.
3. Millington-Sanders C, Meir A, Lawrence L, Stolinski C. Structure of chordae tendineae in the left ventricle of the human heart. J Anat 1998;192:573–81.
4. Chaudhary K, Roy M, Shinde M. Cadaveric study on papillary muscles of human tricuspid valve. International Journal of Anatomy 2017;6:71–4.
5. Degandt AA, Weber PA, Saber HA, Duran CMG. Mitral valve basal chordae: comparative anatomy and terminology. Ann Thorac Surg 2007;84:1250–5.
6. Gusukuma LW, Prates JC, Smith RL. Chordae tendineae architecture in the papillary muscle insertion. Int J Morphol 2004;22:267–72.
7. Wang K, McGlinn EP, Chung KC. A biomechanical and evolutionary perspective on the function of the lumbrical muscle. J Hand Surg Am 2014;39:149–55.
8. Ross CJ, Zheng J, Ma L, Wu Y, Lee CH. Mechanics and microstructure of the atrioventricular heart valve chordae tendineae: a review. Bioengineering (Basel) 2020;7:E25.

9. Aulakh K K, Aneja P S, Garg S. A study of morphology of the chordae tendineae of the left ventricle in human cadaveric hearts of North West Indian population. National Journal of Clinical Anatomy 2020;9:115–20.
10. Kavitha S, Anand A, Manjunath KY. Morphometric analysis of chorda tendinae of mitral valve in human hearts. International Journal of Current Research and Review 2014;6:1–6.
11. Kujur B, Thakur N, Prasad R. Morphological study of chordae tendineae of right ventricle in embalmed human cadavers. IOSR Journal of Dental and Medical Sciences 2016;15:72–6.
12. Mundra P. Morphology of chordae tendinae of mitral valve in adult Indian cadavers. Journal of Advanced Medical and Dental Sciences Research 2018;6:66–70.
13. Chen S, Sari CR, Gao H, Lei Y, Segers P, De Beule M, Wang G, Ma X. Mechanical and morphometric study of mitral valve chordae tendineae and related papillary muscle. J Mech Behav Biomed Mater 2020;111:104011.
14. Kumar BS, Selvi PG, Rekha G, Rajitha V, Anitha MR. Morphometry of chordae tendineae of mitral valves and annulopapillary distance for mitral allografts. International Journal of Medical Science and Public Health 2013;2:967–71.
15. Lam JH, Ranganathan N, Wigle ED, Silver MD. Morphology of the human mitral valve. I. Chordae tendineae: a new classification. Circulation 1970;41:449–58.
16. Rusted IE, Scheifley CH, Edwards JE. Studies of the mitral valve. I. Anatomic features of the normal mitral valve and associated structures. Circulation 1952;6:825–31.
17. Ożóg AK, Hołda MK, Bolechała F, Siudak Z, Sorysz D, Dudek D, Klimek-Piotrowska W. Anatomy of the mitral subvalvular apparatus. J Thorac Cardiovasc Surg 2018;155:2002–10.
18. Silver MD, Lam JHC, Ranganathan N, Wigle ED. Morphology of the human tricuspid valve. Circulation 1971;43:333–48.
19. Lim KO, Boughner DR. Mechanical properties of human mitral valve chordae tendineae: variation with size and strain rate. Can J Physiol Pharmacol 1975;53:330–9.
20. Lim KO, Boughner DR. Morphology and relationship to extensibility curves of human mitral valve chordae tendineae. Circ Res 1976;39:580–5.
21. Morse DE, Hamlett WC, Noble Jr. CW. Morphogenesis of chordae tendineae. I: scanning electron microscopy. Anat Rec 1984; 210:629–38.
22. Sato I, Shimada K. Quantitative analysis of tenascin in chordae tendineae of human left ventricular papillary muscle with aging. Ann Anat 2001;183:443–8.
23. Victor S, Nayak VM. Variations in the papillary muscles of the normal mitral valve and their surgical relevance. J Card Surg 1995; 10:597–607.
24. Van Mieghem NM, Piazza N, Anderson RH, Tzikas A, Nieman K, De Laat LE, McGhie JS, Geleijnse ML, Feldman T, Serruys PW, de Jaegere PP. Anatomy of the mitral valvular complex and its implications for transcatheter interventions for mitral regurgitation. J Am Coll Cardiol 2010;56:617–26.
25. David TE. Artificial chordae. Semin Thorac Cardiovasc Surg 2004;16:161–8.
26. Lincoln J, Alfieri CM, Yutzey KE. Development of heart valve leaflets and supporting apparatus in chicken and mouse embryos. Dev Dyn 2004;230:239–50.
27. Nakagawa Y, Furusho H, Miwa K, Yasuda T. A case of premature ventricular contraction originating at the aortomitral fibrous continuity and exiting from the anterolateral papillary muscle due to muscular chordae tendineae. HeartRhythm Case Rep 2023;9:38–42.
28. Layman TE, Edwards JE. Anomalous mitral arcade. A type of congenital mitral insufficiency. Circulation 1967;35:389–95.
29. Skwarek M, Hreczecha J, Dudziak M, Jerzemowski J, Grzybiak M. The morphology and distribution of the tendinous chords and their relation to the papillary muscles in the tricuspid valve of the human heart. Folia Morphol (Warsz) 2007;66:314–22.
30. Aktas EO, Govsa F, Kocak A, Boydak B, Yavuz IC. Variations in the papillary muscles of normal tricuspid valve and their clinical relevance in medicolegal autopsies. Saudi Med J 2004;25:1176–85.
31. Restivo A, Smith A, Wilkinson JL, Anderson RH. The medial papillary muscle complex and its related septomarginal trabeculation. A normal anatomical study on human hearts. J Anat 1989;163:231–42.
32. Wenink ACG. The medial papillary complex. Br Heart J 1977;39:1012–8.
33. Ozan H, Kocabiyik N, Demirel B, Yalcin B, Comert A. Pattern of connection between papillary muscle and chordae tendineae of left ventricle. Gulhane Medical Journal 2012;54:275.
34. Saha A, Roy S. Papillary muscles of left ventricle-morphological variations and its clinical relevance. Indian Heart J 2018;70:894–900.
35. Mestres CA, Bernal JM. Mitral valve repair: the chordae tendineae. J Tehran Heart Cent 2012;7:92–9.
36. Vendramin I, Milano AD, Pucci A, Lechiancole A, Sponga S, Bortolotti U, Livi U. Artificial chordae for mitral valve repair. J Card Surg 2022;37:3722–8.
37. Obadia JF, Casali C, Chassignolle JF, Janier M. Mitral subvalvular apparatus: different functions of primary and secondary chordae. Circulation 1997;96:3124–8.
38. Kosiński A, Grzybiak M, Dubaniewicz A, Kędziora K, Makarewicz W, Kozłowski D. False chordae tendineae in right ventricle of adult human hearts – morphological aspects. Arch Med Sci 2012;8: 834–40.
39. Sakai T, Okita Y, Ueda Y, Tahata T, Ogino H, Matsuyama K, Miki S. Distance between mitral anulus and papillary muscles: anatomic study in normal human hearts. J Thorac Cardiovasc Surg 1999;118:636–41.
40. Kavitha S, Selvam V, Anand A, Manjunath KY. Morphometric analysis of annulo-papillary distances in left ventricle of human hearts. International Journal of Health Sciences and Research 2014;4:25–30.
41. Vidal Bde C, Mello ML. Structural organization of collagen fibers in chordae tendineae as assessed by optical anisotropic properties and Fast Fourier transform. J Struct Biol 2009;167:166–75.
42. Parto P, Tadjalli M, Ghazi SR. Light and ultrastructural study of the chordae tendineae in the heart of the ostrich (Struthio camelus). World Journal of Medical Sciences 2009;4:93–7.
43. Gupta S, Pathak A, Farooqui M, Prakash A. Histochemical study on the ventricles of heart in prenatal goat (Capra hircus). Indian Journal of Veterinary Anatomy 2020;32:32–4.
44. Ritchie J, Warnock JN, Yoganathan AP. Structural characterization of the chordae tendineae in native porcine mitral valves. Ann Thorac Surg 2005;80:189–97.

45. Tidball JG, Andolina KL. Structure and protein composition of sites of papillary muscle attachment to chordae tendineae in avian hearts. Cell Tissue Res 1992;270:527–33.
46. De Biasi S, Vitellaro-Zuccarello L, Blum I. Histochemical and ultrastructural study on the innervation of human and porcine atrio-ventricular valves. Anat Embryol (Berl) 1984;169:159–65.
47. Duran CM, Gunning AJ. The vascularization of the heart valves: a comparative study. Cardiovasc Res 1968;2:290–6.
48. Eliskova M, Oldrich E. How lymph is drained away from the human papillary muscle: anatomical conditions. Cardiolology 2008;81:371–7.
49. Ichikawa S, Uchino S, Hirata Y. Lymphatics of the cardiac chordae tendineae with particular consideration of their origin. Lymphology 1989;22:123–31.
50. Williams TH, Folan JC, Jew JY, Wang YF. Variations in atrioventricular valve innervation in four species of mammals. Am J Anat 1990;187:193–200.
51. Liao J, Vesely I. A structural basis for the size-related mechanical properties of mitral valve chordae tendineae. J Biomech 2003;36:1125–33.
52. Zuo K, Pham T, Li K, Martin C, He Z, Sun W. Characterization of biomechanical properties of aged human and ovine mitral valve chordae tendineae. J Mech Behav Biomed Mater 2016;62:607–18.
53. Pokutta-Paskaleva A, Sulejmani F, DelRocini M, Sun W. Comparative mechanical, morphological, and microstructural characterization of porcine mitral and tricuspid leaflets and chordae tendineae. Acta Biomater 2019;85:241–52.

ORCID ID:
R. Ambiga 0000-0001-5473-8746;
S. Verma 0000-0001-7266-9318

Correspondence to: Suman Verma, Professor
Department of Anatomy, Jawaharlal Institute of Postgraduate Medical Education and Research, Dhanvantari Nagar, Gorimedu, Puducherry, India
Phone: +91 413 229 84 63
e-mail: suman2v@gmail.com

Conflict of interest statement: No conflicts declared.

 How to cite this article: Ambiga R, Verma S. Morphology, microstructure and biomechanical properties of tendinous cords of heart – a systematic review of cadaveric studies. Anatomy 2025;19(1):30–40.

Review

http://dergipark.org.tr/en/pub/anatomy
Received: November 28, 2024; Accepted: February 12, 2025
doi:10.2399/ana.25.1592350

anatomy
An International Journal of Experimental and Clinical Anatomy

Neurodevelopmental challenges following preterm birth: effects on brain structure and function with a focus on visual perception

Fatma Hilal Çimen[1], **Zahide Pamir**[1,2]

[1]*Department of Neuroscience, Aysel Sabuncu Brain Research Center and National Magnetic Resonance Imaging Center (UMRAM), Bilkent University, Ankara, Türkiye*
[2]*Department of Psychology, Bilkent University, Ankara, Türkiye*

Abstract

Preterm birth is prevalent globally, with approximately 15 million babies born preterm annually. The number of surviving preterm babies has been increasing in recent years due to advancements in medical interventions. This highlights the urgent need to understand the long-term effects of preterm birth, especially on brain development, to minimize the potential negative impacts and to develop effective rehabilitative strategies. Preterm birth disrupts brain development, leaves the infant exposed to environmental stimuli that they are not ready to process, and often leads to brain damage. Two crucial stages of structural and functional brain development are thought to be significantly disrupted due to preterm birth: myelination and synaptic pruning. As a result, preterm birth often coexists with neurodevelopmental disorders affecting motor and cognitive, perceptual systems. The impairments in visual abilities, especially in perceptual domain, are of particular interest, as these issues often go unnoticed and negatively impact academic performance. Notably, these effects can be observed even in the absence of significant brain damage and frequently persist into adulthood. Therefore, this review aims to emphasize the urgent need to address this critical public health concern by comprehensively characterizing the effects of preterm birth on visual functioning and investigating the underlying neural mechanisms. Two hypotheses have been proposed in the literature to explain the neural basis of visual deficits associated with preterm birth. The first posits that preterm birth mainly disrupts the functioning of the dorsal visual pathway, resulting in poorer performance on visuospatial tasks. The second hypothesis suggests that compensatory mechanisms may be involved, where non-visual brain areas compensate for impairments in visual information processing by eliciting higher activations than usual. In this review, inspired by findings from the recent literature on impaired visuospatial processing abilities in early brain-based visual impairments, we propose an alternative hypothesis that preterm birth may be associated with global visual impairment, likely resulting from impaired top-down information processing.

Keywords: brain development; dorsal stream dysfunction; preterm birth; prematurity; top-down processing; visual impairment; visual perception

Anatomy 2025;19(1):41–51

Introduction

Preterm birth is widespread around the world. Approximately 15 million babies, which is 11% of all babies born alive, are born preterm (before the 37th week of the standard 40-week gestation period) each year. About 15% of these babies are born extremely preterm (before 32 weeks).[1] The survival rate of preterm babies has significantly increased in recent years due to the advancements in medical intervention.[2] Therefore, there is an urgent need to understand the long-term effects of preterm birth on individuals to minimize the potential negative impacts and develop effective rehabilitative strategies.

A common consequence of preterm birth is brain damage, with its severity varying based on both the timing and underlying cause. Typically, the conditions that lead to preterm birth or complications during delivery contribute to brain damage. However, even if no visible brain damage occurs during preterm birth, brain development can still be significantly disrupted due to the

removal of the infant from an ideal environment for growth and protection, and premature exposure to environmental stimuli and stressors they are not yet equipped to handle.[3,4] Such disruptions or damage during this critical developmental period can lead to lasting cognitive and motor impairments.

This review article explores the effects of preterm birth on brain structure and function. The first section examines how leaving the womb and exposure to environmental stimuli before the brain is fully prepared can impact structural and functional brain development. The second section summarizes current knowledge on the motor and cognitive deficits associated with preterm birth. Following sections focus on the impact of preterm birth on perception, with a particular emphasis on visual perception and visual information processing in the brain.

Impaired visuoperceptual abilities in individuals born preterm suggest that the effects of preterm birth extend beyond obvious motor or cognitive impairments. Even adults born preterm, without evident brain damage or complications, may face perceptual visual challenges. This issue warrants attention for two key reasons. First, it highlights that preterm birth is not solely associated with developmental delays but can have long-lasting perceptual effects into adulthood. Second, in the absence of other noticeable complications, these perceptual difficulties often go unrecognized, despite their significant impact on individuals' abilities, particularly in academic performance. Therefore, understanding how preterm birth affects brain function is crucial for addressing these challenges and developing effective rehabilitative strategies. With this motivation, this article emphasizes findings from studies examining the impact of preterm birth on visuoperceptual abilities, focusing on complications in visual information processing rather than ocular issues.

Two hypotheses have been proposed in the literature to explain the neural basis of visual deficits associated with preterm birth. One emphasizes the role of dorsal pathway dysfunction, while the other highlights compensatory mechanisms. In the final section, inspired by research on early brain-based visual impairments, we propose an alternative hypothesis regarding the effect of preterm birth on visual information processing. Specifically, we suggest that preterm birth may be associated with a global impairment in top-down visual information processing, rather than an isolated dysfunction of the dorsal pathway. To date, existing hypotheses lack strong behavioral and neural evidence. Additionally, no studies have yet explored the concept of global visual impairment in preterm individuals. Therefore, the behavioral and neural correlates of preterm birth on visual perception require further investigation.

The Effect of Preterm Birth on Structural and Functional Brain Development

Healthy fetal brain maturation is completed by several complex processes that unfold in overlapping times, such as proliferation, neuronal migration, and differentiation. Preterm birth may disrupt any one of these processes and cause damage at both structural and functional levels, resulting in neurodevelopmental disorders.[5]

Two crucial stages of brain development are thought to be significantly disrupted as a result of preterm birth. The first is myelination, a process in which the myelin membrane wraps around the axons of neurons, speeding up communication between neurons. Myelination begins around the 13th week of pregnancy and continues after birth into adulthood.[4,6] This process and the resulting changes in white matter are critical for numerous brain functions, including information processing and learning.

White matter damage is a common outcome in individuals born preterm and is often associated with disruptions in the myelination process.[7] At 11 years old, preterm children show persistent white matter disturbances and smaller brain size.[8] More subtle forms of white matter damage, such as punctate white matter lesions and diffuse white matter abnormalities are observed more frequently in the preterm population compared to severe forms of brain injuries like periventricular leukomalacia; and pose a neurodevelopmental threat to the infant.[9] Specifically, diffused white matter abnormalities are a predictor of poor motor development and are associated with diminished brain network efficiency; while punctate white matter lesions are predictive of neurodevelopmental deficits such as motor and cognitive delays.[10–13] Abnormalities and reduction in white matter volume are observed even in low-risk preterm groups without a clinical white matter impairment, and this reduction is correlated with poorer performance in processing speed.[14]

The second mechanism that might be affected by preterm birth is synaptic pruning, which begins in the second half of pregnancy and typically continues after

birth. During brain development, neurons form connections known as synapses, and this process is crucial for shaping functional neural circuits. In the early stages of brain development, neurons make as many synaptic connections as possible, but not all are necessary. Synaptic pruning is the process of removing extra, unused connections, thereby organizing brain regions so that only essential synapses remain. The removal of unused connections optimizes brain connectivity by reallocating resources to the more frequently used connections, making them stronger and more stable. This process is essential for healthy brain development.[15,16]

A recent study utilizing connectomic analysis found that preterm infants exhibit different brain network connectivity compared to full-term infants. In particular, reduced connectivity strength, and impaired global efficiency have been reported.[17] Additionally, cortical thinning with age, a process driven by synaptic pruning, has been found to be deficient in preterm children.[18] The negative impact of preterm birth on myelination and synaptic pruning persists into adulthood. This suggests that preterm birth not only delays brain development but also causes permanent structural damage.[7,19–21] Consistently, preterm birth has been linked to lifelong neurodevelopmental disorders.[1] Moreover, a recent study exploring resting neural activity in the visual cortex of healthy preterm infants revealed an accelerated functional maturation of the sensory visual cortex.[22] As the authors discussed, this finding may pose a risk to healthy cortical maturation. The earlier maturation of sensory areas, compared to executive functioning and association areas such as the frontal brain areas, could disrupt the typical sequence of functional maturation, potentially leading to life-long changes in brain function.

Motor and Cognitive Deficits Associated with Preterm Birth

In a study that monitored more than 4000 babies born between 22 and 24 weeks, 43% of surviving infants were reported to have a neurodevelopmental deficit.[2] Neurodevelopmental damage in preterm infants often affects the motor system. For example, preterm birth is the most common known cause of cerebral palsy.[1] Mild motor dysfunction and lack of coordination are also highly prevalent in this population. As these infants grow into childhood and adulthood, they often exhibit motor deficits characterized as developmental coordination disorders including problems with balance, coordination, gross and fine motor control, and visual-motor integration.[23]

Previous studies have reported that preterm birth is also associated with cognitive difficulties.[24] Both preterm and extremely preterm children show lower performance in cognitive skills such as perception, attention, memory, and information processing speed compared to their term peers.[18,25,26] Some studies have also reported lower IQ levels in preterm children compared to their term peers.[25,27] Additionally, children born preterm are more likely to have neurodevelopmental disorders such as attention deficit hyperactivity disorder (ADHD), and autism than their peers born at term.[1,28,29] Moreover, as gestational age decreases, a linear decline is observed in IQ scores and the risk of ADHD increases.[30,31]

Consistent with the persistent structural changes mentioned earlier, studies with preterm adolescents and adults indicate that cognitive deficits and neurobehavioral problems observed in childhood persist into adulthood as well, and lower gestational age is associated with poorer academic and cognitive performance.[32–35] However, these results primarily reflect the impact of extreme preterm birth on cognitive functions, as cognitive outcomes for late preterm births (i.e., between 32 and 37 weeks) are rarely studied. Limited research comparing individuals born extremely and late preterm suggests that cognitive deficits associated with preterm birth persist into adulthood primarily in extremely preterm individuals or those with very low birth weight, while late preterm adults tend to catch up to their peers.[36] However, others argue that while the detrimental effects of preterm birth on cognitive tasks are less pronounced in late preterm individuals, they still perform significantly worse compared to their term-born peers and are more likely to face academic challenges.[37–39] Despite these findings, late preterm infants typically do not receive specialized healthcare, as they are considered low-risk, resulting in very limited studies involving this group.[40] Given that late preterm births constitute a substantial portion of the preterm population, greater attention should be directed toward this group.

Perceptual Deficits Associated with Preterm Birth

Preterm birth is associated with various deficits in the perceptual domain, and preterm children are at higher risk for sensory processing disorder.[41] Deficits in the

auditory domain include hearing disabilities, language and speech delays, and atypical speech sound discrimination patterns compared to full-term peers.[42–44] Also, unlike their term peers, preterm infants show no indication of maternal voice recognition.[44] Temporal auditory processing is also affected, as preterm children demonstrate reduced performance in temporal ordering and resolution tasks, as well as atypical neural signaling during these activities.[45] Furthermore, while full-term infants exhibit significantly greater neural responses to forward speech compared to backward speech, preterm infants show no such difference, indicating a deficit in speech discrimination.[46]

Preterm birth is also a risk factor for somatosensory deficits. Preterm infants show heightened tactile sensitivity and a lower threshold for cutaneous withdrawal reflex, suggesting an immature inhibitory system.[47,48]

Multisensory processing is affected by preterm birth as well. Sensory integration problems such as motor coordination and visual-motor integration difficulties are frequently observed in preterm children.[49–51] A neuroimaging study investigating the development of multisensory process with auditory, somatosensory, and combined auditory-somatosensory multisensory stimuli showed atypical patterns of event-related potential (ERP) topographies for multisensory and summed unisensory processes in preterm infants.[52] Another study, using a simple detection task with auditory, visual, and simultaneous auditory-visual stimuli, reported slower and more variable responses in general regardless of the sensory modality, and altered multisensory processes in school-age preterm children compared to full-term peers. This result indicates the long-lasting effects of pre-term birth on various sensory and multisensory processes.[53]

Despite the limited studies in other sensory modalities, vision and visual perception performance accompanying preterm birth has been extensively studied. Challenges in visual perception have been reported to be among the most common neuropsychological deficits in this group.[54,55] Preterm infants are at a higher risk of developing various visual ocular impairments, such as retinopathy of prematurity (retinal damage), nearsightedness or farsightedness due to light refraction defects, strabismus, abnormal ocular motility, nystagmus, decreased contrast sensitivity, visual acuity and visual fields compared to full-term infants.[54,56,57] In addition to these ocular issues, they often perform poorly on visuospatial tasks, suggesting brain-related complications.[58] Consistent with this, preterm birth is one of the most common causes of cerebral visual impairment,[59] a brain-based perceptual impairment that primarily occurs due to perinatal neurological damage and significantly affects visual abilities.[60–65] However, even individuals born preterm without any neurodevelopmental deficit or brain damage have been reported to experience visual problems.[33] Therefore, in this review article, we aim to highlight difficulties in visual perception caused by brain-related issues, as opposed to ophthalmological problems associated with preterm birth because while ophthalmological problems are well-documented in the literature and relatively easier to detect (see Robitaille[59] for a comprehensive review of ophthalmological issues linked to preterm birth), brain-related perceptual difficulties are often overlooked and go unrecognized.

In a psychophysical experiment, MacKay et al.[66] measured motion coherence thresholds in preterm children between the ages of 5 to 8 years old, to assess their local and global motion perception. In this experiment, participants were shown a group of dots, some moving in the same direction and some moving in different directions completely randomly, and were asked to report the direction in which the dots moved. This task measures the proportion of dots that need to move in the same direction for participants to perceive a global motion. This study showed that the preterm group had a higher motion coherence threshold, meaning that they needed more dots to move in the same direction to perceive global motion. According to the results, 41% of preterm children performed significantly worse on a local or global motion detection task compared to their term peers, and performance was particularly affected when global motion tasks were used. These results were supported by subsequent studies.[67,68] Similarly, Jakobson et al.[69] showed that 49% of preterm children failed the motion-defined form recognition test. Sensitivity to biological motion is also impaired in extremely preterm children.[68] In addition to poor performance in different types of motion perception, impairments in visuospatial working memory, depth perception, and visual attention have also been reported in this group.[69–73] Even after controlling for the effect of low IQ and ocular impairments, preterm children perform worse on visuospatial tasks than their term peers.[74] Additionally, studies have found that preterm infants demonstrated reduced abilities in recognizing faces and did not show a preference for intact faces over distorted ones.[75,76]

Performance on a limited number of visual tasks has been reported to be comparable between preterm and term groups. For instance, behavioral studies with preterm infants have reported no impairment in shape perception, in contrast to motion perception,[77] or that the degree of impairment in shape perception is significantly less severe than that in motion perception.[68] Similarly, preterm children performed poorly on motion and form coherence tests; however, the deficit in form perception disappeared after controlling for IQ and visual acuity.[78] Furthermore, studies investigating visual discrimination, visual closure, and visual working memory have reported similar performance between preterm and term groups.[50,79–80]

It should also be noted that the literature presents mixed findings regarding performance on various visual tasks. For instance, one study found no significant differences in form constancy, visual closure, or figure-ground discrimination performance between 5-year-old preterm children and their term-born peers.[81] However, another study indicated that preterm children perform significantly worse on figure-ground discrimination tasks, and lower birth weight is associated with poorer results in form constancy, visual closure, and figure-ground discrimination.[82] Furthermore, contrary to numerous studies mentioned above, one study reported comparable results in ophthalmological and visual cognitive performance including visual acuity, colour vision, stereopsis, stereoacuity, visual fields, ocular motility, motor fusion, visual-motor, and visual-spatial skills and pattern-reversal visual evoked potentials between preterm children without major neuromotor impairment and their full-term peers.[83] The discrepancy between the findings may be related to the heterogeneity of the preterm group in terms of the timing and cause, and accompanying motor and cognitive conditions.

In addition to lifelong, permanent impairments in brain structure (as discussed in the section "the effect of preterm birth on brain development"), cognitive performance, and motor functioning, adults born preterm have also been shown to perform worse on various visual tasks.[23,33,84] Importantly, structural brain damage is not always necessary for these perceptual impairments to manifest. Visual deficits are often observed in preterm individuals who display no obvious structural brain damage detectable through standard brain imaging,[85,86] suggesting the presence of lasting functional impairments in the brain. Therefore, to gain a deeper understanding of poor behavioral performance, it is crucial to investigate how preterm birth affects the brain's information-processing mechanisms.

Effect of Preterm Birth on Visual Information Processing

There is limited information on how preterm birth affects visual information processing. Two explanations have been proposed in the literature so far to account for how visual information processing might be affected by preterm birth. Some researchers suggest that preterm birth may exclusively impair information processing along the dorsal pathway. In the classical two-stream organization of visual information processing,[87,88] spatial features of visual information such as location, direction, and motion are processed in the dorsal pathway, while stimulus-related features like color, shape, and size are processed in the ventral pathway. Previous studies have shown that the dorsal pathway is more vulnerable to damage than the ventral pathway due to physiological reasons during brain development.[89,90] As a result, it has been suggested that brain damage in the early stages of life more frequently affects the dorsal pathway. This view is supported by clinical reports indicating that tasks associated with the dorsal pathway are more commonly impaired in individuals with brain damage. Consistently, visual impairments in preterm individuals are also often linked to dysfunctions in the dorsal pathway, suggesting that preterm birth may lead to dorsal stream dysfunction. Furthermore, studies showing comparable shape and form perception,[68,77,78] in contrast to motion perception, support the view that preterm birth leads to a specific deficit in the dorsal stream. Consistently, a meta-analysis[50] has shown that while preterm individuals exhibit poorer visuospatial perceptual abilities, their performance on visual closure tasks is comparable to that of term groups. However, despite behavioral evidence supporting this hypothesis, neural evidence remains lacking.

Another line of research suggests the existence of compensatory neural mechanisms, where activations in both visual and non-visual brain areas may compensate for impairments in visual processing regions in preterm individuals. In one of the few functional brain imaging studies on visual processing in preterm children, researchers first tested nonverbal skills at age five on preterm children without visual or other neurodevelopmental impairments using standard intelligence tests for preschool children. At age twelve, the same children's

brain activity was assessed using functional magnetic resonance imaging (fMRI) during visual discrimination and visual closure tasks from the Motor-Free Visual Perception Test.[91] Five-year-old preterm children performed significantly worse than their term peers on nonverbal intelligence tests. However, while no differences in visual performance were observed between the two groups at age twelve (notably, visual functions were not assessed at age five), preterm children who outperformed their preterm peers at age five on nonverbal intelligence tests demonstrated stronger neural activation in various regions of the posterior cortex, a critical area for visual tasks and cognitive functions. Also, there was no such association in the control group.[79] The same research group found similar results in a study involving adolescents on visual closure, deviating figure and figure-ground discrimination tasks. Their results demonstrated an increased neural activity in brain regions not directly associated with visual tasks (e.g., frontal, anterior cingulate, temporal, and posterior medial parietal/cingulate cortices, as well as parts of the cerebellum, thalamus, and caudate nucleus) in the extremely preterm group.[80] In the first study, the visual tasks primarily required ventral stream processing, yet increased activity was observed in the dorsal stream areas.[79] In the second study, increased neural activity was mainly observed in non-visual areas.[80] Therefore, the researchers suggested that the similar perceptual performance between preterm and full-term groups, alongside increased neural activity in either non-critical visual areas for the executed visual task or non-visual regions, may indicate a compensatory mechanism in the preterm group.

The compensation hypothesis has been explored by other studies. For example, Narberhaus et al.[92] found that while behavioral performance in a visuo-spatial memory task was similar, a distinct neural network emerged in the very preterm group during visuo-perceptual learning processing. Specifically, during encoding, increased fMRI signals were observed in the occipital and parietal cortex, along with certain subcortical regions, while the frontal cortex showed decreased signal. During recognition, very preterm adults exhibited increased signals in the right cerebellum and bilateral anterior cingulate gyrus. These findings were interpreted as evidence of neural compensation. In support of these findings, other studies also demonstrated altered fMRI activity in multiple brain regions, including the frontal and parietal cortices, in very preterm groups compared to their term peers during visual memory or learning tasks involving encoding and recognition.[93,94] In another study on visuospatial working memory in very preterm and term children, researchers found that younger and low-performing preterm children exhibited an atypical working memory network, particularly within the frontal brain areas. In contrast, older and high-performing preterm children displayed a typical neural network, similar to that of controls, again, suggesting a compensatory mechanism.[95]

A New Proposal for the Effect of Preterm Birth on Visual Information Processing

So far, two hypotheses have been proposed in the literature regarding the neural basis of visual problems associated with preterm birth. The first hypothesis suggests that preterm birth disrupts information processing in the dorsal pathway, leading to impaired behavioral performance on tasks linked to this pathway. The second hypothesis posits that, in cases where visual performance is unaffected, regions of the brain not directly involved in visual information processing may take over during visual tasks, serving as a compensatory mechanism for the damage caused by preterm birth.

A recent functional brain imaging study on patients with cerebral visual impairment suggested that increased activation in visual areas that are not directly related to task demands may be linked to difficulty in suppressing irrelevant visual information, rather than serving as a compensatory mechanism. This finding points to a more global impairment in the visual system, specifically in top-down information processing, through which limited neuronal resources are allocated based on task demands or the observer's expectations and goals.[62] Furthermore, before this discovery, the prevailing view in the literature was that cerebral visual impairment was primarily associated with dorsal pathway dysfunction based on the behavioral results and clinical reports.

Although the visual problems associated with preterm birth are not as severe as those seen in cerebral visual impairment, the underlying causes and consequences of both conditions are quite similar. In fact, for a considerable number of individuals with cerebral visual impairment, preterm birth is the primary factor in the medical history related to impaired vision.[65] Therefore, underlying neural mechanisms may be similar in both conditions. If this is the case, increased neural activity in either visual areas that are not directly related to task demands

or non-visual brain areas may not be directly related to compensatory neural mechanisms, and preterm birth may not cause only dorsal pathway dysfunction, but a global impairment in the top-down visual information processing as in the case of cerebral visual impairment. This impairment may hinder the system's ability to effectively prioritize relevant visual information while suppressing the irrelevant information, due to an inefficient allocation of limited neural resources. Supporting this view, a recent behavioral study reported that preterm children had more difficulty than full-term children in suppressing distractors in a visual search task especially when visual distractors were increased.[96] Additionally, Morcom and Henson[97] investigated compensatory mechanisms through increased frontal activity in healthy aging. They suggested that the increased prefrontal activity is associated with reduced efficiency or specificity rather than compensation. Considering the altered neural networks, particularly in the frontal areas, observed in the very preterm group in the studies mentioned in the previous section,[93,94] the compensation hypothesis alone may not fully explain the changes in brain functioning in this group, and altered neural activity in frontal brain regions may be associated with impairments in top-down processing.

Concluding Remarks

Preterm birth is a neurodevelopmental risk factor with lasting negative effects into adulthood. Disruption of normal brain development due to preterm birth can result in varying degrees of brain damage.[7,19,20] Even without significant brain damage, preterm birth is linked to a range of persistent developmental disorders. Behavioral studies have identified notable differences in motor, cognitive, and visual-perceptual functions, though the neural basis for these differences remains unclear. Beyond current hypotheses on potential neural mechanisms affecting visual perception, this review proposes that a global impairment in top-down information processing may underlie the visual processing deficits associated with preterm birth. Comprehensive behavioral and neuroimaging studies are needed to investigate these potential mechanisms.

In this review, we aim to highlight the potential neural mechanisms affected by preterm birth, including the two already identified in the preterm literature, as well as recent findings on early brain-based visual impairments in cerebral visual impairment, to emphasize the need for further research. Understanding the visual perception deficits associated with preterm birth, along with their underlying neural mechanisms, is crucial, as these deficits are also linked to impaired academic performance, including challenges in math and reading.[82] Identifying both the behavioral and neural effects of preterm birth could enable early intervention through targeted neuropsychological rehabilitation or occupational therapy for preterm children. As Lind et al.[79] pointed out that while programs exist to support the cognitive and motor development of preterm infants, no programs specifically aim to improve their visual abilities. To bridge this gap, it is critical to investigate preterm birth-related visual impairments and their neural underpinnings. In particular, long-term studies on healthy adults born preterm, without known neurodevelopmental disorders or brain pathology, are necessary. Focusing on this population would help distinguish the effects of preterm birth on information processing mechanisms from those caused by brain damage or other complications, providing a clearer understanding of the behavioral and neural challenges linked specifically to preterm birth.

Conflict of Interest

We declare no conflict of interest related to this work.

Author Contributions

FHÇ: investigation, writing: original draft, writing: reviewing and editing; ZP: conceptualization, methodology, investigation, writing: original draft, writing: reviewing and editing.

Ethics Approval

Not applicable.

Funding

No financial support was received for this article; however, the author ZP holds a TÜBİTAK grant (1001, Project Number: 124K976) to investigate neural mechanisms affected by preterm birth.

References

1. Crump C. An overview of adult health outcomes after preterm birth. Early Hum Dev 2020;150.
2. Younge N, Goldstein RF, Bann CM, Hintz SR, Patel RM, Smith PB, Bell EF, Rysavy MA, Duncan AF, Vohr BR, Das A, Goldberg RN, Higgins RD, Cotten CM; Eunice Kennedy Shriver National Institute of Child Health and Human Development Neonatal Research Network. Survival and neurodevelopmental outcomes among periviable infants. N Engl J Med 2017;376:617–28.

3. Peterson BS. Brain imaging studies of the anatomical and functional consequences of preterm birth for human brain development. Ann N Y Acad Sci 2003;1008:219–37.
4. Nelson CA, de Haan M, Thomas KM. Brain development and neural plasticity: a precis to brain development. In: Nelson CA, de Haan M, Thomas KM, editors. Neuroscience of cognitive development: the role of experience and the developing brain. Hoboken (NJ): John Wiley & Sons, Inc.; 2015. p. 4–29.
5. Wallois F, Routier L, Bourel-Ponchel E. Impact of prematurity on neurodevelopment. Handb Clin Neurol 2020:173:341–75.
6. Volpe JJ. Overview: normal and abnormal human brain development. Ment Retard Dev Disabil Res Rev 2000;6:1–5.
7. Back SA. White matter injury in the preterm infant: pathology and mechanisms. Acta Neuropathol 2017;134:331–49.
8. Nagy Z, Westerberg H, Skare S, Andersson JL, Lilja A, Flodmark O, Fernell E, Holmberg K, Bohm B, Forssberg H, Lagercrantz H, Klingberg T. Preterm children have disturbances of white matter at 11 years of age as shown by diffusion tensor imaging. Pediatr Res 2003;54:672–9.
9. Rutherford MA, Supramaniam V, Ederies A, Chew A, Bassi L, Groppo M, Anjari M, Counsell S, Ramenghi LA. Magnetic resonance imaging of white matter diseases of prematurity. Neuroradiology 2010;52:505–21.
10. Parikh NA, Sharma P, He L, Li H, Altaye M, Illapani VS, Cincinnati Infant Neurodevelopment Early Prediction Study (CINEPS) Investigators. Perinatal risk and protective factors in the development of diffuse white matter abnormality on term-equivalent age magnetic resonance imaging in infants born very preterm. J Pediatr 2021;233:58–65.
11. Kline JE, Illapani VS, Li H, He L, Yuan W, Parikh NA. Diffuse white matter abnormality in very preterm infants at term reflects reduced brain network efficiency. Neuroimage Clin 2021;31: 102739.
12. de Bruïne FT, van den Berg-Huysmans AA, Leijser LM, Rijken M, Steggerda SJ, van der Grond J, van Wezel-Meijler G. Clinical implications of MR imaging findings in the white matter in very preterm infants: a 2-year follow-up study. Radiology 2011;261: 899–906.
13. de Bruijn CAM, Di Michele S, Tataranno ML, Ramenghi LA, Rossi A, Malova M, Benders M, van den Hoogen A, Dudink J. Neurodevelopmental consequences of preterm punctate white matter lesions: a systematic review. Pediatr Res 2022;93:1480–90.
14. Soria-Pastor S, Gimenez M, Narberhaus A, Falcon C, Botet F, Bargallo N, Mercader JM, Junque C. Patterns of cerebral white matter damage and cognitive impairment in adolescents born very preterm. Int J Dev Neurosci 2008;26:647–54.
15. Paolicelli RC, Bolasco G, Pagani F, Maggi L, Scianni M, Panzanelli P, Giustetto M, Ferreira TA, Guiducci E, Dumas L, Ragozzino D, Gross CT. Synaptic pruning by microglia is necessary for normal brain development. Science 2011;333:1456–8.
16. Sakai J. How synaptic pruning shapes neural wiring during development and, possibly, in disease. Proc Natl Acad Sci U S A 2020;117:16096–9.
17. Sa de Almeida J, Meskaldji DE, Loukas S, Lordier L, Gui L, Lazeyras F, Hüppi PS. Preterm birth leads to impaired rich-club organization and fronto-paralimbic/limbic structural connectivity in newborns. Neuroimage 2021;225:117440.
18. Brumbaugh JE, Conrad AL, Lee JK, DeVolder IJ, Zimmerman MB, Magnotta VA, Axelson ED, Nopoulos PC. Altered brain function, structure, and developmental trajectory in children born late preterm. Pediatr Res 2016;80:197–203.
19. Laureano B, Irzan H, O'Reilly H, Ourselin S, Marlow N, Melbourne A. Myelination of preterm brain networks at adolescence. Magn Reson Imaging 2024;105:114–24.
20. Allin MP, Kontis D, Walshe M, Wyatt J, Barker GJ, Kanaan RA, McGuire P, Rifkin L, Murray RM, Nosarti C. White matter and cognition in adults who were born preterm. PLoS One 2011;6: e24525.
21. Sripada K, Løhaugen GC, Eikenes L, Bjørlykke KM, Håberg AK, Skranes J, Rimol LM. Visual-motor deficits relate to altered gray and white matter in young adults born preterm with very low birth weight. Neuroimage 2015;109:493–504.
22. Witteveen IF, McCoy E, Holsworth TD, Shen CZ, Chang W, Nance MG, Belkowitz AR, Dougald A, Puglia MH, Ribic A. Preterm birth accelerates the maturation of spontaneous and resting activity in the visual cortex. Front Integr Neurosci 2023;17: 1149159.
23. Ream MA, Lehwald L. Neurologic consequences of preterm birth. Curr Neurol Neurosci Rep 2018;18:48.
24. Bhutta AT, Cleves MA, Casey PH, Cradock MM, Anand KJ. Cognitive and behavioral outcomes of school-aged children who were born preterm. JAMA 2002;288:728–37.
25. Geldof CJA, de Kieviet JF, Dik M, Kok JH, van Wassenaer-Leemhuis AG, Oosterlaan J. Visual search and attention in five-year-old very preterm/very low birth weight children. Early Hum Dev 2013;89:983–8.
26. Rose SA, Feldman JF. Memory and processing speed in preterm children at eleven years: a comparison with full-terms. Child Dev 1996;67:2005–21.
27. Talge NM, Holzman C, Wang J, Lucia V, Gardiner J, Breslau N. Late-preterm birth and its association with cognitive and socioemotional outcomes at 6 years of age. Pediatrics 2010;126:1124–31.
28. Delobel-Ayoub M, Arnaud C, White-Koning M, Casper C, Pierrat V, Garel M, Burguet A, Roze JC, Matis J, Picaud JC, Kaminski M, Larroque B, EPIPAGE Study Group. Behavioral problems and cognitive performance at 5 years of age after very preterm birth: the EPIPAGE study. Pediatrics 2009;123:1485–92.
29. Polic B, Bubic A, Meštrovic J, Markic J, Kovacevic T, Antoncic Furlan I, Utrobicic I, Kolcic I. Emotional and behavioral outcomes and quality of life in school-age children born as late preterm: retrospective cohort study. Croat Med J 2017;58:332–41.
30. Kerr-Wilson CO, Mackay DF, Smith GC, Pell JP. Meta-analysis of the association between preterm delivery and intelligence. J Public Health (Oxf) 2012;34:209–16.
31. Lindström K, Lindblad F, Hjern A. Preterm birth and attention-deficit/hyperactivity disorder in schoolchildren. Pediatrics 2011; 127:858–65.

32. Kajantie E, Strang-Karlsson S, Evensen KA, Haaramo P. Adult outcomes of being born late preterm or early term – what do we know? Semin Fetal Neonatal Med 2019;24:66–83.
33. Woodward LJ, Horwood LJ, Darlow BA, Bora S. Visuospatial working memory of children and adults born very preterm and/or very low birth weight. Pediatr Res 2022;91:1436–44.
34. Robinson R, Girchenko P, Pulakka A, Heinonen K, Lähdepuro A, Lahti-Pulkkinen M, Hovi P, Tikanmäki M, Bartmann P, Lano A, Doyle LW, Anderson PJ, Cheong JLY, Darlow BA, Woodward LJ, Horwood LJ, Indredavik MS, Evensen KAI, Marlow N, Johnson S, de Mendonca MG, Kajantie E, Wolke D, Räikkönen K. ADHD symptoms and diagnosis in adult preterms: systematic review, IPD meta-analysis, and register-linkage study. Pediatr Res 2023;93:1399–409.
35. Ma Q, Wang H, Rolls ET, Xiang S, Li J, Li Y, Zhou Q, Cheng W, Li F. Lower gestational age is associated with lower cortical volume and cognitive and educational performance in adolescence. BMC Med 2022;20:424.
36. Suikkanen J, Miettola S, Heinonen K, Vääräsmäki M, Tikanmäki M, Sipola M, Matinolli HM, Järvelin MR, Räikkönen K, Hovi P, Kajantie E. Reaction times, learning, and executive functioning in adults born preterm. Pediatr Res 2020;89:198–204.
37. Cheong JL, Doyle LW. Long term outcomes in moderate and late preterm infants. In: Boyle EM, Cusack J, editors. Emerging topics and controversies in neonatology. Cham (Switzerland): Springer; 2020. p. 403–13.
38. Heinonen K, Eriksson JG, Lahti J, Kajantie E, Pesonen AK, Tuovinen S, Osmond C, Raikkonen K. Late preterm birth and neurocognitive performance in late adulthood: a birth cohort study. Pediatrics 2015;135:e818–25.
39. Jin JH, Yoon SW, Song J, Kim SW, Chung HJ. Long-term cognitive, executive, and behavioral outcomes of moderate and late preterm at school age. Clin Exp Pediatr 2020;63:219–25.
40. Martínez-Nadal S, Bosch L. Cognitive and learning outcomes in late preterm infants at school age: a systematic review. Int J Environ Res Public Health 2020;18:74.
41. Niutanen U, Harra T, Lano A, Metsäranta M. Systematic review of sensory processing in preterm children reveals abnormal sensory modulation, somatosensory processing and sensory-based motor processing. Acta Paediatr 2020;109:45–55.
42. Barre N, Morgan A, Doyle LW, Anderson PJ. Language abilities in children who were very preterm and/or very low birth weight: a meta-analysis. J Pediatr 2011;158:766–74.
43. Vohr BR. Language and hearing outcomes of preterm infants. Semin Perinatol 2016;40:510–9.
44. Therien JM, Worwa CT, Mattia FR, deRegnier RA. Altered pathways for auditory discrimination and recognition memory in preterm infants. Dev Med Child Neurol 2004;46:816–24.
45. Durante AS, Mariano S, Pachi PR. Auditory processing abilities in prematurely born children. Early Hum Dev 2018;120:26–30.
46. Bartha-Doering L, Alexopoulos J, Giordano V, Stelzer L, Kainz T, Benavides-Varela S, Wartenburger I, Klebermass-Schrehof K, Olischar M, Seidl R, Berger A. Absence of neural speech discrimination in preterm infants at term-equivalent age. Dev Cogn Neurosci 2019;39:100679.
47. André V, Durier V, Beuchée A, Roué JM, Lemasson A, Hausberger M, Sizun J, Henry S. Higher tactile sensitivity in preterm infants at term-equivalent age: a pilot study. PLoS One 2020;15:e0229270.
48. Andrews K, Fitzgerald M. The cutaneous withdrawal reflex in human neonates: sensitization, receptive fields, and the effects of contralateral stimulation. Pain 1994;56:95–101.
49. Bröring T, Oostrom KJ, Lafeber HN, Jansma EP, Oosterlaan J. Sensory modulation in preterm children: Theoretical perspective and systematic review. PLoS One 2017;12:e0170828.
50. Geldof CJ, van Wassenaer AG, de Kieviet JF, Kok JH, Oosterlaan J. Visual perception and visual-motor integration in very preterm and/or very low birth weight children: a meta-analysis. Res Dev Disabil 2012;33:726–36.
51. Pinheiro RC, Martinez CMS, Fontaine AMGV. Visual motor integration and overall development of preterm and at term children at the beginning of schooling. Journal of Human Growth and Development 2014;24:181–7.
52. Maitre NL, Key AP, Slaughter JC, Yoder PJ, Neel ML, Richard C, Wallace MT, Murray MM. Neonatal multisensory processing in preterm and term infants predicts sensory reactivity and internalizing tendencies in early childhood. Brain Topogr 2020;33:586–99.
53. Décaillet M, Denervaud S, Huguenin-Virchaux C, Besuchet L, Fischer Fumeaux CJ, Murray MM, Schneider J. The impact of premature birth on auditory-visual processes in very preterm schoolchildren. NPJ Sci Learn 2024;9:42.
54. Leung MP, Thompson B, Black J, Dai S, Alsweiler JM. The effects of preterm birth on visual development. Clin Exp Optom 2018;101:4–12.
55. Lind A, Nyman A, Lehtonen L, Haataja L. Predictive value of psychological assessment at five years of age in the long-term follow-up of very preterm children. Child Neuropsychol 2020;26:312–23.
56. O'Connor AR, Wilson CM, Fielder AR. Ophthalmological problems associated with preterm birth. Eye (Lond) 2007;21:1254–60.
57. Jain S, Sim PY, Beckmann J, Ni Y, Uddin N, Unwin B, Marlow N. Functional ophthalmic factors associated with extreme prematurity in young adults. JAMA Netw Open 2022;5:e2145702.
58. van Gils MM, Dudink J, Reiss IK, Swarte RMC, van der Steen J, Pel JJM, Kooiker MJG. Brain damage and visuospatial impairments: exploring early structure-function associations in children born very preterm. Pediatr Neurol 2020;109:63–71.
59. Robitaille JM. Long-term visual outcomes in prematurely born children. J Binocul Vis Ocul Motil 2024;74:1–8.
60. Fazzi E, Galli J, Micheletti S. Visual impairment: a common sequela of preterm birth. NeoReviews 2012;13:e542–50.
61. Pamir Z, Bauer CM, Bailin ES, Bex PJ, Somers DC, Merabet LB. Neural correlates associated with impaired global motion perception in cerebral visual impairment (CVI). NeuroImage Clin 2021;32:102821.
62. Pamir Z, Manley CE, Bauer CM, Bex PJ, Dilks DD, Merabet LB. Visuospatial processing in early brain-based visual impairment is associated with differential recruitment of dorsal and ventral visual streams. Cereb Cortex 2024;34:bhae203.

63. Good WV. Cortical visual impairment: new directions. Optom Vis Sci 2009;86:663–5.
64. Kozeis N. Brain visual impairment in childhood: mini review. Hippokratia 2010;14:249–51.
65. Dutton GN. The spectrum of cerebral visual impairment as a sequel to premature birth: an overview. Doc Ophthalmol 2013; 127:69–78.
66. MacKay TL, Jakobson LS, Ellemberg D, Lewis TL, Maurer D, Casiro O. Deficits in the processing of local and global motion in very low birthweight children. Neuropsychologia 2005;43:1738–48.
67. Atkinson J, Braddick O. Visual and visuocognitive development in children born very prematurely. Prog Brain Res 2007;164:123–49.
68. Taylor NM, Jakobson LS, Maurer D, Lewis TL. Differential vulnerability of global motion, global form, and biological motion processing in full-term and preterm children. Neuropsychologia 2009;47:2766–78.
69. Jakobson LS, Frisk V, Downie ALS. Motion-defined form processing in extremely premature children. Neuropsychologia 2006;44:1777–86.
70. Caravale B. Cognitive development in low risk preterm infants at 3–4 years of life. Arch Dis Child Fetal Neonatal Ed 2005;90:F474–9.
71. Luciana M, Lindeke L, Georgieff M, Mills M, Nelson CA. Neurobehavioral evidence for working-memory deficits in school-aged children with histories of prematurity. Dev Med Child Neurol 1999;41:521–33.
72. O'Connor AR, Stephenson T, Johnson A, Tobin MJ, Moseley MJ, Ratib S, Ng Y, Fielder AR. Long-term ophthalmic outcome of low birth weight children with and without retinopathy of prematurity. Pediatrics 2002;109:12–8.
73. Foreman N, Fielder A, Minshell C, Hurrion E, Sergienko E. Visual search, perception, and visual-motor skill in "healthy" children born at 27–32 weeks' gestation. J Exp Child Psychol 1997;64: 27–41.
74. Butcher PR, Bouma A, Stremmelaar EF, Bos AF, Smithson M, Van Braeckel KN. Visuospatial perception in children born preterm with no major neurological disorders. Neuropsychology 2012;26:723–34.
75. Perez-Roche T, Altemir I, Giménez G, Prieto E, González I, López Pisón J, Pueyo V. Face recognition impairment in small for gestational age and preterm children. Res Dev Disabil 2017;62: 166–73.
76. Pereira SA, Pereira Junior A, Costa MF, Monteiro MV, Almeida VA, Fonseca Filho GG, Arrais N, Simion F. A comparison between preterm and full-term infants' preference for faces. J Pediatr (Rio J) 2017;93:35–9.
77. Geldof CJ, Oosterlaan J, Vuijk PJ, de Vries MJ, Kok JH, van Wassenaer-Leemhuis AG. Visual sensory and perceptive functioning in 5-year-old very preterm/very-low-birthweight children. Dev Med Child Neurol 2014;56:862–8.
78. Benassi M, Bolzani R, Forsman L, Ådén U, Jacobson L, Giovagnoli S, Hellgren K. Motion perception and form discrimination in extremely preterm school-aged children. Child Dev 2018;89:e494–e506.
79. Lind A, Parkkola R, Laasonen M, Vorobyev V, Haataja L; PIPARI Study Group. Visual perceptual skills in very preterm children: developmental course and associations with neural activation. Pediatr Neurol 2020;109:72–8.
80. Lind A, Haataja L, Laasonen M, Saunavaara V, Railo H, Lehtonen T, Vorobyev V, Uusitalo K, Lahti K, Parkkola R; PIPARI Study Group. Functional magnetic resonance imaging during visual perception tasks in adolescents born prematurely. J Int Neuropsychol Soc 2021;27:270–81.
81. Geldof CJ, Oosterlaan J, Vuijk PJ, de Vries MJ, Kok JH, van Wassenaer-Leemhuis AG. Visual sensory and perceptive functioning in 5-year-old very preterm/very-low-birthweight children. Dev Med Child Neurol 2014;56:862–8.
82. Perez-Roche T, Altemir I, Giménez G, Prieto E, González I, Peña-Segura JL, Castillo O, Pueyo V. Effect of prematurity and low birth weight in visual abilities and school performance. Res Dev Disabil 2016;59:451–7.
83. O'Reilly M, Vollmer B, Vargha-Khadem F, Neville B, Connelly A, Wyatt J, Timms C, de Haan M. Ophthalmological, cognitive, electrophysiological and MRI assessment of visual processing in preterm children without major neuromotor impairment. Dev Sci 2010;13:692–705.
84. Pétursdóttir D, Holmström G, Larsson E. Visual function is reduced in young adults formerly born prematurely: a population-based study. Br J Ophthalmol 2020;104:541–6.
85. Birtles DB, Braddick OJ, Wattam-Bell J, Wilkinson AR, Atkinson J. Orientation and motion-specific visual cortex responses in infants born preterm. Neuroreport 2007;18:1975–9.
86. Guzzetta A, Cioni G, Cowan F, Mercuri E. Visual disorders in children with brain lesions: 1. Maturation of visual function in infants with neonatal brain lesions: correlation with neuroimaging. Eur J Paediatr Neurol 2001;5:107–14.
87. Haxby JV, Grady CL, Horwitz B, Ungerleider LG, Mishkin M, Carson RE, Herscovitch P, Schapiro MB, Rapoport SI. Dissociation of object and spatial visual processing pathways in human extrastriate cortex. Proc Natl Acad Sci U S A 1991;88: 1621–5.
88. Goodale MA. Separate visual systems for perception and action: a framework for understanding cortical visual impairment. Dev Med Child Neurol 2013;55:9–12.
89. Braddick O, Atkinson J, Wattam-Bell J. Normal and anomalous development of visual motion processing: motion coherence and 'dorsal-stream vulnerability'. Neuropsychologia 2003;41:1769–84.
90. Grinter EJ, Maybery MT, Badcock DR. Vision in developmental disorders: is there a dorsal stream deficit? Brain Res Bull 2010;82: 147–60.
91. Colarusso RP, Hammill DD. MVPT-3: motor-free visual perception test. 3rd ed. Novata (CA): Academic Therapy Publications; 2003.
92. Narberhaus A, Lawrence E, Allin MP, Walshe M, McGuire P, Rifkin L, Murray R, Nosarti C. Neural substrates of visual paired associates in young adults with a history of very preterm birth:

alterations in fronto-parieto-occipital networks and caudate nucleus. Neuroimage 2009;47:1884–93.

93. Tseng CJ, Froudist-Walsh S, Brittain PJ, Karolis V, Caldinelli C, Kroll J, Counsell SJ, Williams SC, Murray RM, Nosarti C. A multimodal imaging study of recognition memory in very preterm born adults. Hum Brain Mapp 2017;38:644–55.
94. Brittain PJ, Froudist Walsh S, Nam KW, Giampietro V, Karolis V, Murray RM, Bhattacharyya S, Kalpakidou A, Nosarti C. Neural compensation in adulthood following very preterm birth demonstrated during a visual paired associates learning task. Neuroimage Clin 2014;6:54–63.
95. Mürner-Lavanchy I, Ritter BC, Spencer-Smith MM, Perrig WJ, Schroth G, Steinlin M, Everts R. Visuospatial working memory in very preterm and term born children – impact of age and performance. Dev Cogn Neurosci 2014;9:106–16.
96. Datin-Dorrière V, Borst G, Guillois B, Cachia A, Poirel N. The forest, the trees, and the leaves in preterm children: the impact of prematurity on a visual search task containing three-level hierarchical stimuli. Eur Child Adolesc Psychiatry 2020;30:253–60.
97. Morcom AM, Henson RNA. Increased prefrontal activity with aging reflects nonspecific neural responses rather than compensation. J Neurosci 2018;38:7303–13.

ORCID ID:
F. H. Çimen 0000-0002-0583-4886;
Z. Pamir 0000-0003-1813-400X

Correspondence to: Zahide Pamir, PhD, Assist. Prof. of Psychology & Neuroscience
Departments of Psychology & Neuroscience, Bilkent University,
Ankara, Türkiye
Phone: +90 312 290 10 67
e-mail: zahide.pamir@bilkent.edu.tr

Conflict of interest statement: No conflicts declared.

 How to cite this article: Çimen FH, Pamir Z. Neurodevelopmental challenges following preterm birth: effects on brain structure and function with a focus on visual perception. Anatomy 2025;19(1):41–51.

anatomy
http://dergipark.org.tr/en/pub/anatomy
An International Journal of Experimental and Clinical Anatomy

Review

http://dergipark.org.tr/en/pub/anatomy
Received: January 13, 2025; Accepted: March 4, 2025
doi:10.2399/ana.25.1619001

The importance of World Anatomy Day and a few examples of activities

Ozan Turamanlar

Department of Anatomy, Faculty of Medicine, Izmir Kâtip Çelebi University, Izmir, Türkiye

Abstract

At the General Assembly of the 19th International Federation of Associations of Anatomists Congress held in London in 2019, a decision was made to declare October 15th of each year as World Anatomy Day. Recognizing the significance of Andreas Vesalius's contributions, the IFAA designated his death (October 15) anniversary as World Anatomy Day, ensuring that the legacy of this foundational science continues to be celebrated worldwide through various events. The preservation and transmission of valuable traditions are crucial for ensuring that future generations can gain a deeper understanding of the past and present. Consequently, the organization and dissemination of World Anatomy Day activities should be considered a fundamental responsibility for all anatomists.

Keywords: Andreas Vesalius; October 15; World Anatomy Day

Anatomy 2025;19(1):52–54

What is World Anatomy Day?

At the General Assembly of the 19th International Federation of Associations of Anatomists (IFAA) Congress held in London in 2019, a decision was made to declare October 15th of each year as World Anatomy Day (WAD). This proposal was initiated by the Turkish Society of Anatomy and Clinical Anatomy, with Prof. Erdogan Sendemir playing a pivotal role. As the president of the society at that time, Prof. Sendemir advocated for a global recognition day to highlight the importance of body donation, which ultimately led to the establishment of WAD.[1] Of particular note, the WAD logo, employed by the IFAA in all its publications and announcements, was created by Professor Ahmet Sınav, a Turkish anatomist and medical illustrator.

Why October 15?

Andreas Vesalius was a prominent scientist of the 16th century. As a Renaissance physician who believed that the best way to understand human anatomy was through the dissection of human cadavers, Vesalius is renowned as the "father of modern anatomy" due to his groundbreaking work, "De humani corporis Fabrica", published in 1543. Vesalius passed away on October 15, 1564, at 50.[2,3] Recognizing the significance of his contributions, the IFAA designated his death anniversary as World Anatomy Day, ensuring that the legacy of this foundational science continues to be celebrated worldwide through various events.

What Actions Have Been Taken, and What Future Actions Are Possible?

In a 2019 reminder statement, the IFAA outlined recommendations for WAD events. These recommendations included enhancing public awareness of anatomy, promoting the diversity of professions within the discipline, transforming public perception of anatomy, acknowledging donors, potentially addressing the current shortage of donors, and attracting young scientists to the field of anatomical sciences.[4] Despite being a relatively new initiative, World Anatomy Day is increasingly celebrated yearly through various events held at universities and institutions. National anatomy associations under the IFAA umbrella, anatomy departments, volunteer anatomists, physicians, medical students, and healthcare professionals promote their WAD activities through official and private websites, local and national news outlets, and social media platforms. A case in point is the "Biomedical Visualization" webinar held in India on October 15, 2023, which over 700 participants attended.[5]

Media coverage of cadavers and body donation during WAD can significantly enhance public awareness of this critical issue. For instance, in Türkiye, during WAD and body donation awareness week, a "Corner of Respect for Silent Teachers of Medicine" was established. This initiative involved gathering the opinions of medical students, academic staff, and administrative personnel regarding cadavers and body donation, answering their questions, conducting a survey, and introducing the body donation form.[6] In a parallel event at universities in China, medical students commenced their inaugural class with a tribute to their "silent teachers". Adorned in white coats, they honored the memory of body donors by placing flowers on the memorial wall and observing a moment of silent reflection.[7] Additionally, during WAD and National Anatomy Week, a social media campaign organized jointly by a student community and the anatomy department of a university addressed questions related to the importance of cadavers in anatomy education, legal and religious aspects of body donation, and cadaver donation practices. An academic from the law faculty provided insights into the legal implications of body donation, while an academic from the theology faculty addressed religious perspectives. Medical students and faculty members from the anatomy department also answered frequently asked questions about body donation.[8]

A comprehensive overview of World Anatomy Day activities conducted in Malaysia was compiled into an article, with detailed explanations supported by figures. Notable events held in 2019 and 2021 included crossword puzzles, Kahoot! sessions, a "dream wheel" activity, model assembly, an "amazing race" competition, an anatomy clinic exhibition and museum tour, "anatomy fun" activities, and a "quiz let's play dough" game. In China, on October 15, 2019, the oath ceremony for university students and the official opening of the Anatomy course coincided with World Anatomy Day. To foster greater interest in anatomy, various events were organized, such as anatomy-related exhibitions, conferences, museum visits, and body donation ceremonies. These diverse activities can serve as valuable inspiration for individuals and organizations planning their own World Anatomy Day celebrations.[9,10]

Efforts should be made to foster participation from both students and the general public. As an example, a museum successfully engaged visitors by providing medical information and organizing entertaining activities centered around anatomical models and skeletal remains.[11] As part of the World Anatomy Day celebrations in Germany in 2021, opened an exhibition featuring a carefully curated collection of historical anatomical models and contemporary specimens. This exhibition also included a rare first edition of Andreas Vesalius's influential work, "Fabrica."[12]

To broaden the appeal of these events, organizers should consider incorporating sports and arts activities in outdoor settings. As an illustration, a poetry and prose writing competition focused on anatomy was organized, with prizes awarded to the winners.[13] A "Salute to Netter" drawing competition was organized in 2022 by several universities across China.[14] Additionally, an international anatomy arts and crafts competition was held during WAD.[15] Other initiatives included an anatomy quiz, an anatomy exhibition, and a donor appreciation event centered around the theme "Exploring the Human Body: A Journey Through Anatomy".[16] Moreover, a university organized a celebration to recognize the achievements of senior anatomists.[17]

By creating and distributing posters and brochures, various activities are organized to commemorate World Anatomy Day in both academic settings and public spaces. The primary goals of these activities are to raise awareness about anatomy, particularly regarding cadaver and body donation, and to share this information with a wider audience. Additionally, events are organized with the participation of families of donors who have donated their bodies for anatomical study. WAD can serve as a platform for discussing various topics, including the history of anatomy, anatomical terminology, and advancements in anatomical research. A South African university organized a lecture series in 2019 to celebrate World Anatomy Day. The series included a presentation by an emeritus professor on the history of the School of Anatomical Sciences, and talks by junior faculty members exploring the future of anatomy education. In a conference held in Sri Lanka, a faculty member discussed the integration of innovative technologies into anatomy education while emphasizing the continued importance of cadaver dissection.[1] A virtual symposium held in South Africa to mark World Anatomy Day included a special session focusing on "Women in Anatomy". Female anatomists discussed the challenges and opportunities they have faced in their field.[7]

A multidisciplinary approach to anatomical studies can be fostered by collaborating with other medical disciplines. As an example, a medical school in Pakistan hosted a World Anatomy Day event in 2024, which included presentations on "Innovations in Anatomy" and "Surgical Integrations in Anatomy", organized by the Department of Anatomy and Histology.[18] For instance, athletes and their coaches from a sports university in a Chinese province participated in World Anatomy Day commemo-

rations by visiting the Life Science Museum.[14] By providing information to school-aged children, anatomy can be introduced as a fundamental science underlying medicine. Addressing students' questions about the human body, diseases, and the medical profession can inspire them to consider careers in healthcare.

Conclusion

Upholding certain traditions is imperative to ensure that future generations can appreciate the historical and contemporary significance of anatomy. Consequently, the organization and dissemination of WAD activities should be considered a fundamental responsibility of every anatomist. All events must be widely publicized, and announcements on the official websites of the hosting institutions are particularly effective. Furthermore, by aligning academic events such as scientific congresses, symposia, and panels with this date, we can maximize the reach and impact of these activities on a global scale.

Conflict of Interest

No potential conflict of interest relevant to this article was reported.

Ethics Approval

No ethical approval was necessary for this review article.

Funding

None.

References

1. PLEXUS. The Newsletter of International Federation of Associations of Anatomists. 2020;1.
2. Dziedzic M, Ostrowski P, Ghosh SK, Balawender K, Koziej M, Bonczar M. Exploring the evolution of anatomy: from historical foundations to modern insights. Translational Research in Anatomy 2024;35:100286.
3. Bendiner E. Andreas Vesalius: man of mystery in life and death. Hosp Pract (Off Ed) 1986;21:199–234.
4. October 15th World Anatomy Day Reminder. [Internet]. [Retrieved on December 21, 2024]. Available from: https://www.ifaa.net/wp-content/uploads/2019/10/WAD-Reminder.pdf
5. PLEXUS. The Newsletter of International Federation of Associations of Anatomists. 2024;1.
6. Örs AB, Olgunus ZK. Mersin Üniversitesi'nde "Tıbbın Sessiz Öğreticilerine Teşekkür" Etkinlikleri. Mersin Üniversitesi Tıp Fakültesi Lokman Hekim Tıp Tarihi ve Folklorik Tıp Dergisi 2023;13:4–7.
7. PLEXUS. The Newsletter of International Federation of Associations of Anatomists. 2020;2.
8. Ulusal Anatomi Haftasi "Beden Bagisi" [Internet]. [Retrieved on December 21, 2024]. Available from: https://youtu.be/Ktxx65f8ldg?si=RR0yXA1WsxcKnN8j
9. Simok AA, Hadie SNH, Mohd Ismail ZI, Asari MA, Kasim F, Mohd Yusof NA, Shamsuddin SA, Mohd Amin MSI, Mukhtar SF. Anatomy outreach through the world anatomy day celebration in Universiti Sains Malaysia. Education in Medicine Journal 2022;14:113–20.
10. Nicholson H, Pather N. International Federation of Associations of Anatomists Newsletter PLEXUS Newsletter 2019;2:13–7.
11. World Anatomy Day - 15 October 2024 - Amazing Anatomy event held at the Grant Museum [Internet]. [Retrieved on December 21, 2024]. Available from: https://www.ucl.ac.uk/biosciences/news/2024/sep/world-anatomy-day-15-october-2024-amazing-anatomy-event-held-grant-museum
12. PLEXUS. The Newsletter of International Federation of Associations of Anatomists. 2022;1.
13. World Anatomy Day 2024: writing competition. [Internet]. [Retrieved on December 21, 2024]. Available from: https://oldoperatingtheatre.com/world-anatomy-day-2024-writing-competition/
14. PLEXUS. The Newsletter of International Federation of Associations of Anatomists. 2023;1.
15. https://www.anatsoc.org.uk/news/all-news/2024/10/15/world-anatomy-day-15-october-2024-anatomical-society-international-undergraduate-anatomy-arts-crafts-competition
16. World Anatomy Day 15 October 2024 Anatomical Society International undergraduate anatomy arts & crafts competition. [Internet]. [Retrieved on December 21, 2024]. Available from: https://college.rrmch.org/wp-content/uploads/sites/3/2024/10/World-Anatomy-Day.pdf
17. World Anatomy day 2024 was celebrated on 15th October 2024. [Internet]. [Retrieved on December 21, 2024]. Available from: https://kvv.edu.in/news/world-anatomy-day-2024-was-celebrated-on-15th-october-2024/
18. PLEXUS. The Newsletter of International Federation of Associations of Anatomists. 2024;2.

ORCID ID:
O. Turamanlar 0000-0002-0785-483X

Correspondence to: Ozan Turamanlar, Prof, PhD, MD
Department of Anatomy, Faculty of Medicine,
Izmir Kâtip Çelebi University, Izmir, Türkiye
Phone: +90 232 386 08 88
e-mail: ozanturamanlar@hotmail.com

Conflict of interest statement: No conflicts declared.

 How to cite this article: Turamanlar O. The importance of World Anatomy Day and a few examples of activities. Anatomy 2025;19(1):52–54.

Letter to the Editor

http://dergipark.org.tr/en/pub/anatomy
Received: April 1, 2025; Accepted: April 23, 2025
doi:10.2399/ana.25.1668894

anatomy
An International Journal of Experimental and Clinical Anatomy

Letter: Wind-shield wiper effect of the ligamentum teres femoris: is it for real?

Vivek Perumal[1], **Bhoobalan Baskaran**[2]

[1]*Department of Anatomy, Lee Kong Chian School of Medicine, Nanyang Technological University, Novena, Singapore*
[2]*Madurai Medical College, Madurai, India*

Anatomy 2025;19(1):55–57

Dear Editor,

Through this letter, we try to clarify the long-contested function of the ligament of the ligamentum teres femoris (LTF); or the ligament of the head of femur (LHF), as it is known by anatomists. The LTF is an intra-articular ligament of the hip joint.[1] In adults, there is evidence that the ligament has a vascular and mechanical function at the hip joint.[2-4] It is often mentioned that the LTF aids joint lubrication by spreading synovial fluid over the head of femur.[5-10] These works refer back to Gray and Villar,[11] who are said to have hypothesized a 'wind-shield wiper' action of the ligament that helped joint lubrication. However, this original reference[11] does not mention any specific wiper action in its text, and the concept remains theoretical. Reviewing the literature on the LTF anatomy, and from our previous dissection findings, we propose that the anatomical features of the LTF in situ limit its intra-articular mechanics, and that it might not contribute to a wind-shield wiper action.[12]

The only mention of the lubrication functions of the LTF identified in the historical literature is by Cheselden[13] and Welcker.[14] It is stated that the LTF could press the synovial tissue at the bottom of the acetabular fossa[13] and that the LTF could provide a 'brushing action' to distribute the synovial fluid.[14] An absence of this brushing mechanism could render the articular surfaces dry during walking due to inadequate flow of synovial fluid.[14] However, from our current understanding of the LTF anatomy, this brushing action appears to be limited for the following reasons: the LTF always stays within the acetabular fossa and does not have contact with the weight bearing surfaces of the hip joint during any range of movement. This anatomical arrangement aids the ligament and the indwelling vessels to be protected throughout the joint range of motion.

Our previous dissections have shown that the mean length of the LTF is 22.3±4 mm and does not exceed the dimensions of the acetabular fossa (26.1±7×33.9±7 mm).[12] The shorter length, and its fixed proximal attachments at the inferior aspect of the fossa restricts the ligament from exiting the acetabular fossa during any movement; the LTF could travel over the head of femur but only a little more than a quarter of its surface area.[14,15] This extent of the LTF's travel over the head of femur could be visualised by exposing the medial aspect of the acetabulum and applying a contrast such as Indian ink around the ligament (**Figure 1**).

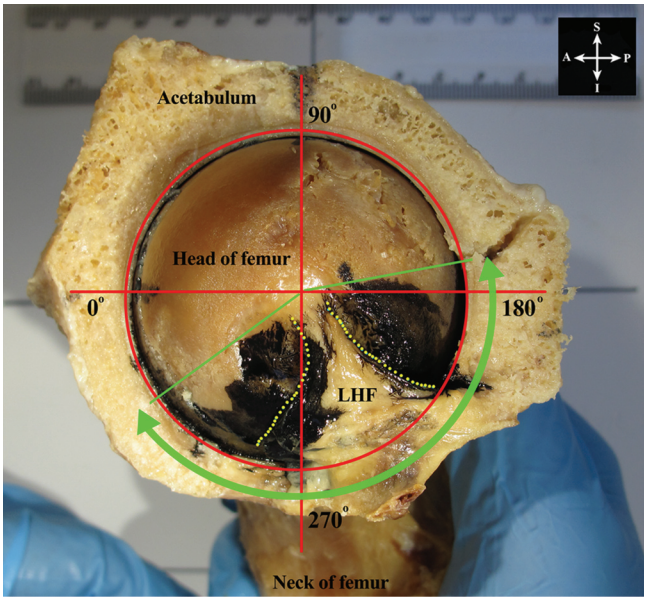

Figure 1. Left hip joint opened from the medial aspect showing the ligament of head of femur (**LHF**) in situ (dotted outline). Indian ink was injected around the ligament and the joint was moved in its full range in all orthogonal planes. The extent of Indian ink distribution on the head of femur is marked in green.

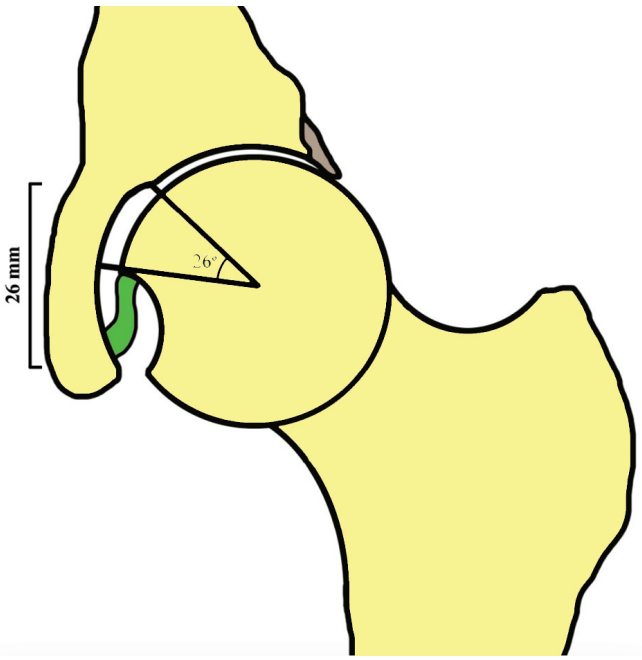

Figure 2. Schematic representation of the hip joint showing the relative positions of the acetabular margins, fovea capitis and the ligamentum teres femoris (ligament of head of femur). The ligament (**green**) is slack in neutral hip position.

Our hypothesis also draws further evidence from clinical studies. Radiological investigations of the hip joint show that in neutral position, there is a distance of up to 26° from the superior foveal margin to the central acetabular margin.[16–18] (**Figure 2**). Even during full adduction, where the ligament might potentially tense,[12] the fovea capitis resides within the acetabular fossa.[15] Thus, the LTF could not reach the superior weight bearing surface of the hip where the need for joint lubrication would be higher. Any inadvertent contact to the articular surface would either immediately injure the ligament or compress the blood vessels traveling through it.[2,19,20]

These observations suggest that the LTF at no point could contact the articular cartilage surface of the hip joint, could not travel throughout the articular surfaces, and it is evident that the LTF could not perform a brushing or 'wind-shield wiper' action to aid joint lubrication. While our works did not explore the effect of negative pressure and potential capillary action of the synovial fluid within the hip joint in situ, any contribution from these factors would still fail to justify the brushing action of the LTF.

Acknowledgment

The cadaveric photograph used in this article was obtained from the first author's PhD thesis entitled "*Clinical and Surgical Anatomy of the Ligament of the Head of Femur*". This thesis was conducted in accordance with the Declaration of Helsinki and was approved by the University of Otago Human Ethics Committee. The overview of the PhD thesis is available online: https://ourarchive.otago.ac.nz/esploro/outputs/doctoral/Clinical-and-Surgical-Anatomy-of-the/9926481871401891. The authors would like to acknowledge the body donors from whom the tissues were utilized for the study and the photograph used in the publication.

References

1. Standring S. Gray's anatomy: the anatomical basis of clinical practice. 41st ed. Edinburgh (Scotland): Elsevier Churchill Livingstone; 2016. p. 1378–9.
2. Perumal V, Woodley SJ, Nicholson HD. Neurovascular structures of the ligament of the head of femur. J Anat 2019;234:778–86.
3. Perumal V, Scholze M, Hammer N, Woodley SJ, Nicholson HD. Load-deformation properties of the ligament of the head of femur in situ. Clin Anat 2020;33:705–13.
4. Philippon MJ, Rasmussen M, Turnbull T, Trindade CA, Hamming MG, Ellman MB, Harris M, LaPrade RF, Wijdicks CA. Structural properties of the native ligamentum teres. Orthop J Sports Med 2014;2:2325967114561962.
5. Bardakos NV, Villar RN. The ligamentum teres of the adult hip. J Bone Joint Surg Br 2009,91:8–15.
6. Cerezal L, Kassarjian A, Canga A, Dobado MC, Montero JA, Llopis E, Rolón A, Pérez-Carro L. Anatomy, biomechanics, imaging, and management of ligamentum teres injuries. Radiographics 2010,30:1637–51.
7. Cerezal L, Arnaiz J, Canga A, Piedra T, Altónaga JR, Munafo R, Pérez-Carro L. Emerging topics on the hip: ligamentum teres and hip microinstability. Eur J Radiol 2012;81:3745–54.
8. Mei-Dan O, McConkey MO. A novel technique for ligamentum teres reconstruction with all-suture anchors in the medial acetabular wall. Arthrosc Tech 2014;3:217–21.
9. Byrd JWT, Jones KS. Traumatic rupture of the ligamentum teres as a source of hip pain. Arthroscopy 2004;20:385–91.
10. Botser IB, Martin DE, Stout CE, Domb BG. Tears of the ligamentum teres: prevalence in hip arthroscopy using 2 classification systems. Am J Sports Med 2011;39:117S–25S.
11. Gray AJ, Villar RN. The ligamentum teres of the hip: an arthroscopic classificationof its pathology. Arthroscopy 1997;13:575–8.
12. Perumal V, Techataweewan N, Woodley SJ, Nicholson HD. Clinical anatomy of the ligament of the head of femur. Clin Anat 2019;32:90–8.

13. Cheselden W. The anatomy of the human body. 7th ed. London: Hitch & R Dodsley; 1750. p. 1–334.
14. Welcker H. Über das Hüftgelenk, nebst einigen Bemerkungen über Gelenke überhaupt, insbesondere über das Schultergelenk. Z Anat Entwicklungsgesch 1875;41–79.
15. Kapandji IA. Physiology of joints. Vol. 2. Lower limb. 6th ed. London: Churchill Livingstone; 2007. p. 24.
16. Beltran LS, Mayo JD, Rosenberg ZS De Tuesta MD, Martin O, Neto LP Sr, Bencardino JT. Fovea alta on MR images: is it a marker of hip dysplasia in young adults? Am J Roentgenol 2012;199: 879–83.
17. Nötzli HP, Muller SM, Ganz R. The relationship between fovea capitis femoris and weight bearing area in the normal and dysplastic hip in adults: a radiologic study. Z Orthop Ihre Grenzgeb 2001; 319:502–6.
18. Siebenrock KA, Steppacher SD, Albers CE, Haefeli PC, Tannast M. Diagnosis and management of developmental dysplasia of the hip from triradiate closure through young adulthood. J Bone Joint Surg 2013;95:748–55.
19. Cruveilhier J. Anatomy of the human body. New York (NY): Harper & Brothers; 1844. p. 944.
20. Byrd JWT. Operative hip arthroscopy. 3rd ed. New York (NY): Springer-Verlag; 2012. p. 100–9.

ORCID ID:
V. Perumal 0000-0002-9610-5813;
B. Baskaran 0009-0005-1594-8368

Correspondence to: Vivek Perumal, MD
Department of Anatomy, Lee Kong Chian School of Medicine,
Nanyang Technological University, Novena, Singapore
Phone: +65 93743930
e-mail: vivek.perumal@ntu.edu.sg

Conflict of interest statement: No conflicts declared.

 How to cite this article: Perumal V, Baskaran B. Letter: Wind-shield wiper effect of the ligamentum teres femoris: is it for real? Anatomy 2025;19(1):55–57.

Table of Contents

Volume **19** / Issue **1** / April **2025**

(Continued from back cover)

Reviews

Letter to the Editor

On the Front Cover:
Measurement of aortomesenteric distance (AMD). From Çamur E, Ersöz B, Çifci BE, Dağlı M. Radiological evaluation of superior mesenteric artery syndrome: are aortomesenteric angle and distance measurements reliable? *Anatomy* 2025;19(1):24–29.

http://dergipark.org.tr/en/pub/anatomy

anatomy

An International Journal of Experimental and Clinical Anatomy

Table of Contents

Volume **19** / Issue **1** / April **2025**

Original Articles

Systematic Review

(Contents continued on inside back cover)

deomed®